DEVELOPMENT AND CHARACTERIZATION OF BAOBAB POD FIBRE NANOCELLULOSE REINFORCED LOW DENSITY POLYETHYLENE POLYMER COMPOSITES

BY

IBRAHIM Aliyu Isah

MEng/SEET/2017/7164

DEPARTMENT OF CHEMICAL ENGINEERING

FEDERAL UNIVERSITY OF TECHNOLOGY

MINNA

OCTOBER/2021

DEVELOPMENT AND CHARACTERIZATION OF BAOBAB POD FIBRE NANOCELLULOSE REINFORCED LOW DENSITY POLYETHYLENE COMPOSITES

BY

ALIYU IBRAHIM ISAH

MEng/SEET/2017/7164

A THESIS SUBMITTED TO THE POSTGRADUATE SCHOOL FEDERAL UNIVERSITY OF TECHNOLOGY, MINNA, NIGERIA IN PARTIAL FULFILLMENT OF THE REQUIREMENTS FOR THE AWARD OF MASTER OF ENGINEERING IN CHEMICAL ENGINEERING

OCTOBER/2021

ABSTRACT

This study focused on the use of Baobab pod fibres as a potential reinforcement material for polymer nanocomposites. The physical, chemical and mechanical properties of the fibres were investigated in order to fully comprehend its behaviour. Box-Behnken module of response surface methodology (RSM) available in "Design Expert® Version V10" was used to establish design matrix, optimize treatment conditions and analyze experimental data. The optimization of chemical treatment of fibre predicts solution for NaOH concentration at 6.963, soaking time of 359.9. Fibres were chemically treated in order to remove lignin, pectin and other impurities and also to improve the adhesive tendency with the reinforcement material. Acid hydrolysis was then used to produce cellulose nanocrystals (CNC) from the treated fibres. An increase in the cellulose content of 17.9 % was recorded after NaOH treatment and a further increase of 25.3 % was recorded after acid hydrolysis. The effect of NaOH treatment and acid hydrolysis on surface morphology, crystallinity, and thermal properties of fibres were investigated using Fourier Transform Infrared (FTIR), Scanning electron microscopy/Energy dispersive X-ray spectroscopy (SEM/EDS), X-ray Diffraction (XRD) and Thermogravimetric analysis (TGA/DTA). The fibre reinforced composites were produced using compression moulding at a temperature of 150 ^{0}C for 30 min and a formulation of nanocellulose (CNC) to low density polyethylene (LDPE) ratios of 10-90 wt%, 20-80 wt%, 30-70 wt% and 40-60 wt% were used respectively. The mechanical properties of the fibre and that of the composites produced were then investigated. Single fibre length was obtained to be 50.42 mm; density was 0.65 g/cm^3, tensile strength of 40.15 MPa, water absorption of 9.40 % and cellulose content of 53.2%. The composite with 10-90 wt% CNC/LDPE ratios was found to have a good water absorption property of 0.212 % and the best mechanical properties with tensile property of 75.72 MPa, Impact strength of 4.46 J/mm^2, flexural strength of 17.24 MPa and hardness of 26.7 HV. Based on the results obtained, it shows that Nanocellulose hydrolyzed from Baobab pod fibres has excellent properties for use as polymer reinforcement.

TABLE OF CONTENTS

LIST OF TABLES

LIST OF FIGURES

LIST OF PLATES

LIST OF ABBREVIATIONS

ADF	Acid Detergent Fibre
ADL	Acid Detergent Lignin
ANOVA	Analysis of Variance
ASTM	American Society for Testing and Materials
BBD	Box-Behnken Design
BPFs	Baobab Pod Fibres
CNC	Cellulose Nanocrystals
CrI	Crystallinity Index
CS	Crystallite size
EDX	Energy Dispersive X-ray Analysis
FTIR	Fourier Transform Infrared Spectroscopy
HDPE	High Density Polyethylene
LDPE	Low Density polyethylene
MOE	Modulus of Elasticity
NF	Natural Fibres
PE	Polyethylene
PET	Polyethylene Terephthalate
PP	Polypropylene
PVC	Poly Vinyl Chloride
SEM	Scanning Electron Microscope
TGA	Thermogravimetric Analysis
TS	Tensile Strength
XRD	X-ray Diffraction
YM	Young Modulus

CHAPTER ONE

1.0 INTRODUCTION

1.1 Background of the Study

Natural fibres are readily available in nature, and are found all over the globe. Natural fibre-based composites are becoming popular day-by-day and are replacing petroleum based fibre-oriented composites due to their outstanding, renewability, biodegradability, decomposability, stiffness, higher length to weight ratio, and low cost (Jeyapragash *et al.*, 2020, Balla *et al.*, 2019).

Natural fibre reinforced polymer composites present an opportunity to partially minimize environmental impacts by integrating biodegradable fibre such as Baobab in place of synthetic fibres in composite materials production. Hazards of synthetic fibre, recycling issues, and toxic by-products are the main driving factors in the research and development of bio-composites (Mohammed, 2021). The combination of organic, natural fibres and inorganic or organic polymers and nanoparticles has a high potential for improving mechanical performances, and thus expanding the areas of application (Farid *et al.*, 2020). Although, composites reinforced with synthetic fibres possess superior mechanical properties, they have some severe drawbacks that include high cost, poor recyclability and non-biodegradability (Mohammed *et al.*, 2015).

However, natural fibre itself has some limitation when related to manmade fibre due to hydrophilic nature of the natural fibre which caused weak interfacial interaction between the polymer matrix and the fibre. In order to improve the fibre surface morphology different chemical treatment techniques have been used. Also the methods are used to improve surface morphology of the fibre ensuring that unwanted materials are kept removed from its surface (Anteneh *et al.*, 2021).

Nano-based reinforced polymeric composites are also generating dramatic revolutions in this sector for sophisticated applications, especially to water repellency, corrosion, and antibacterial properties. Nanomaterials could be applied as filler materials, along with biofibres and matrix polymer, in composites for acquiring better performances (Chen *et al.*, 2019).

Numerous researches have been carried out using different forms of natural fibre reinforcement agent for polymers, this include; jute, hemp, sugarcane bagasse, sisal, coir, bamboo and cotton. Baobab (adansonia digitata) is a native of the Sahelian region and belongs to the Malvaceae family (De Caluwé *et al*., 2010). Popularly called Kuka among the Hausa speaking populace of northern Nigeria is widely distributed and is found in all parts of the region.

The plant is mostly found in the hot and drier region of the African continent. It has multi-purpose uses and all part of the plant is reported to be useful. Fibre from the bark is strong and is used for making ropes, snares, basket nets, fishing lines and it is even used for weaving. The fibres are also available from disintegrated wood and have been used for packing. Other fibres used for making rope are obtained from root bark (Leja, 2010). Baobab has seeds (pods) which contains natural fibres and pulp. The pulp is either consumed or made into a drink while the bark is used in making ropes (Igboeli *et al*., 1997).

Even though Baobab pod fibres are available locally, they are presently underutilized in Nigeria due to lack of good marketing system and poor processing (Sidibe and Williams, 2009). Fibres are the most important class of reinforcements, as they satisfy the desired conditions and transfer strength to the matrix constituent influencing and enhancing their properties as desired. Lot of factors makes Natural fibres fall short of their effective utilization. These factors include; shrinkage due to aggressive washing, low degree of resiliency, availability and price fluctuation. The performance of a fibre composite is judged

by its length, shape, orientation, composition and the mechanical properties of the matrix (Nissen and Stutz, 1985).

Natural fibre`s availability, renewability, low density, and price as well as satisfactory mechanical properties make them an attractive ecological alternative to man-made fibres. They are more environmental friendly, and are used in transportation, military applications, building and construction industries, packaging and consumer products. A lot of studies have carried on chemical composition, mechanical, thermal, and morphological characteristics of natural fibres (Bouasker *et al.*, 2014;Yusriah *et al.*, 2014). Natural fibres are categorized into four main classes: seed fibres; Baobab, cotton, coir, and kapok, leaf fibres; sisal, agave, pineapple, and abaca, bast fibres; kenaf, ramie, hemp, jute, and flax, and stalk fibres; wood, straw, and bamboo (Al-Oqla *et al.*, 2015).

There have been global researches by scientist to develop biodegradable polymers as a waste management option to curtail plastic pollution which is amongst the biggest environmental disasters of modern era (Saba *et al*., 2014). This study on Baobab fibres is expected to harness the use of a novel fibre that has been scantly reported in literature to enhance local content development and contribute to cur tailing the problem of non-biodegradability of synthetic plastic.

1.2 Statement of the Research Problem

Productions of reinforced composites from natural fibres have been reported in the literature. However, experimental work is very rare involving Baobab pod fibre (Shehu *et al.,* 2017). This project is different from existing effort due to the fact that it used natural Baobab pod fibre to replace the synthetic polymers, like Polyethylene, to become biodegradable materials that can be use as an alternative material for several engineering applications.

To further evaluate the optimal condition for the chemical treatment process of the raw Baobab pod fibre, response surface methodology (RSM) is adopted for this purpose. It is an excellent technique use in optimization (Zwawi, 2021). Currently, no such studies have been reported in the literature. Generally, natural fibres have poor mechanical properties but that can be enhanced via chemical treatment at optimal condtions.

1.3 Aim and Objectives of the Study

The aim of this research is to develop and characterize Baobab pod fibre nanocellulose reinforced polymer composites, using low density polyethylene (LDPE) matrix. The aim was achieved through the following objectives:

i. Extraction and optimization of Baobab fibre treatment method using Box-Behken module of response surface Methodology (RSM) available in "Design Expert® Version X software".
ii. Isolation of cellulose nanocellulose (CNC) from Baobab pod fibres using acid hydrolysis and its characterization.
iii. To produce and characterize Baobab nanocellulose reinforced low density polyethylene (LDPE) nanocomposites.

1.4 Justification of the Study

Even though Baobab pod fibre is readily available and environmental friendly, its potential for use as polymer reinforcement has not been fully harnessed when used in nano form it is possible to obtain composite of improved properties to micro form. This study harnesses the

potential opportunities of the use of nanocellulose in reinforcing low density polyethylene composites of improved mechanical strength and performance.

1.5 Scope of the Study

In this research, natural fibres from a locally grown Baobab plant was characterized and chemically treated. Cellulose nanocrystals were isolated from the treated fibres which were used as a reinforcement material with low density polyethylene to produce a nanocomposite. The nanocomposites produced were evaluated and characterised for their physical, chemical and thermal properties. The physical, chemical and thermal properties of fibres, reinforcing materials (LDPE) and composites produced were evaluated using analytical instruments.

CHAPTER TWO

2.0 LITRATURE REVIEW

2.1 Concept of Composites

Composites are formed by adding multiple phase components in a material in such a way that the properties of the resultant material are different and not otherwise reached. Composites have been found to be the most discerning and promising material available in this century (Dipen *et al.*, 2019). Composite materials are engineering materials made from two or more constituent materials that remain distinct and separate on a macroscopic level while forming a uniform component (Layth *et al*., 2015). Composites are formed when two (2) or more different materials are laminated together. These laminate were found to have lots of applications due their high strength to weight ratio, corrosion resistance and surface degradation (Randbaran *et al.*, 2020).

For composites that are fibre reinforced, the matrix material sticks to the fibres together and acts as the medium through which an externally applied stress is transmitted and distributed to the fibres through the interface while only a very little proportion of the applied load is taken by the matrix material (Brigante, 2014). Polymers are the most common matrix for composite materials (Matthews and Rawlings, 1999), they are used because the overall features of the composites are superior to those of the individual components for example polymer/ceramic. Composites have a greater modulus than the polymer component but aren't as brittle as ceramics.

2.2 Advantages of Composites Materials

With interests growing towards composite materials recently, and their augmentation as part of integrated business from medical applications to aerospace engineering and others, which are getting increasing attention on composite materials in recent operations (Randbaran *et al.*, 2020). Also, mechanical properties of reinforced fibre composite materials closely depend

upon the properties of the component materials such as void content, orientation, type, quantity and fibre distribution. Moreover, the main concept of the interfacial bonds and the mechanism of load transfer at inter lamina also plays an important role (Narin *et al*., 2019).

Inherent damping, tailorable properties, ease of formability, increased electric or thermal conductivity, and redundant load paths, these make them useful in manufacture of bearings and linkages, building and automobile structures such as sliding panels (Shehu e*t al.*, 2017). Composites provide the fabricator, designer, equipment manufacturer, and consumer with adequate flexibility to meet the demands presented by different environments as well as any other special requirements. Material selection and proper design can avoid many of the disadvantages (Schwartz, 1997)

2.3 Classification of Composites Materials

Different kinds of polymers and polymer matrix composites reinforced with ceramic particles have a wide range of industrial applications such as electrodes, heaters; composite materials are commonly classified at following two distinct levels (Omrani *et al*., 2016).

a. The first level of classification is made with respect to matrix constituents. The main composite classes include metal matrix composites, organic matrix composite, and ceramic matrix composites.
b. The second level of classification refers to the reinforcement form – laminar reinforced composites, particulate composites and fibre reinforced composites. Fibre reinforced composites can be further divided into containing discontinuous and continuous fibres.

The matrix also prevents the individual fibres from surface damage due to chemical attack from the environment or mechanical abrasion. The strength of the interface between the matrix and reinforcing component generally controls the mechanical properties of a

composite (Pickering, 2011). Figure 2.1 represents a commonly accepted classification scheme for composite materials.

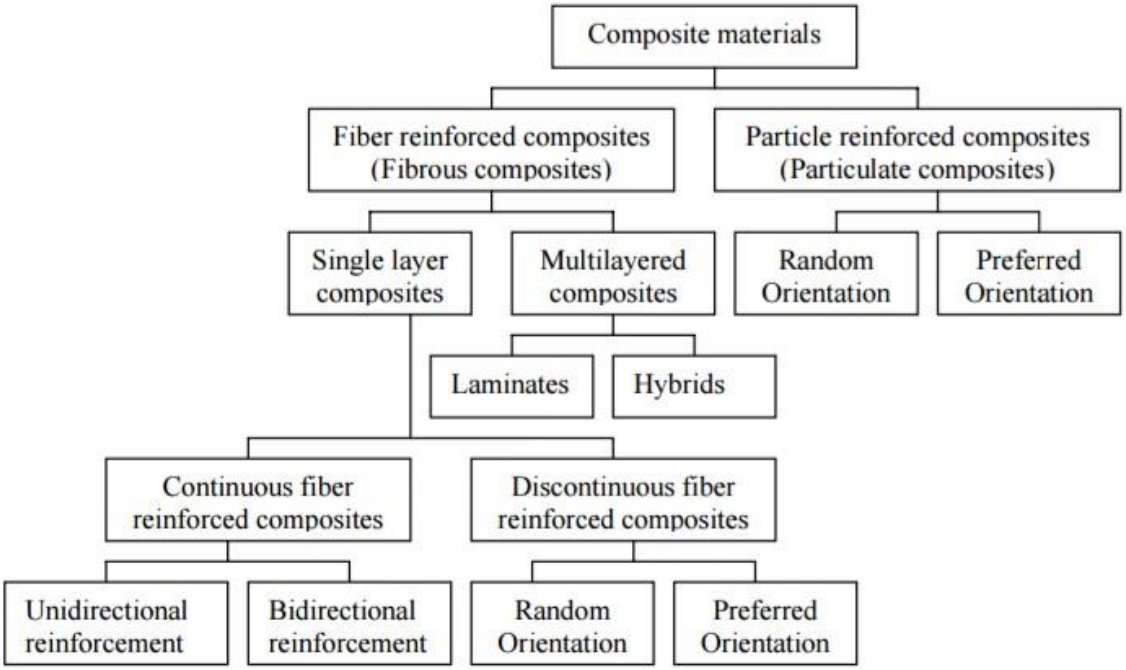

Figure 2.1: Basic Classification of composites (Paulo *et al*., 2018)

2.3.1 Fibre reinforced composite

Fibres or particles embedded in matrix of another material are the best example of modern-day composite materials, which are mostly structural. The driving force behind the development of most existing composites is their capability to be designed to provide the targeted material behaviour (Harrigan, 1998). A fibre is characterized by its length being much greater compared to its cross-sectional dimensions. The dimensions of the reinforcement determine its capability of contributing its properties to the composite. Synthetic fibres are man-made fibres such as carbon fibres, aramid fibres and glass fibres. They have been used in reinforcing polymers and metals producing high performance materials for structural applications (Saba *et al*., 2014).

2.3.2 Particle reinforced composites

Particle-reinforced composite (PRC) is not that effective by means of material strength and fracture resistance property. However, ceramic, metal, or inorganic particles restrict the deformation and provide good material stiffness (Dipen *et al.*, 2019). Particle fillers are widely used to improve the properties of matrix materials such as to modify the thermal and electrical conductivities, improve performance at elevated temperatures, reduce friction, increase wear and abrasion resistance, improve machinability, increase surface hardness and reduce shrinkage. Moreover, these composites are manufactured using similar techniques used for monolithic material (Chawla & Shen, 2001). Research findings from many researchers have indicated the need for improvement in the mechanical performance of polymeric materials (Adesina *et al.*, 2019). Also, in case of particulate reinforced composites the particle can be either randomly oriented or preferred oriented.

2.3.2.1 Metal matrix composites

Metal Matrix Composites are most commonly used in industrial applications due to their advantage in comparison to metal matrix composites. They have many excellent physical and mechanical properties such as high strength and stiffness, wear resistance, dimensional stability, capacity to withstand at high temperature excellent thermal and electrical conductivity (Arun *et al.*, 2020)

2.3.2.2 Ceramic matrix composites

One of the main objectives in producing ceramic matrix composites is to increase the toughness. Ceramics based composites are used at high temperature application (Low, 2006). Naturally it is hoped and indeed often found that there is a concomitant improvement in strength and stiffness of ceramic matrix composites. Ceramics have certain attractive properties such as high stiffness, hardness, compressive strength and relatively low density (Groover, 2010). However, they are brittle and have low fracture toughness

2.3.2.3 Polymer matrix composites

Most commonly used matrix materials are polymeric. The reasons for this are twofold. In general the mechanical properties of polymers are inadequate for many structural purposes. In particular their strength and stiffness are low compared to metals and ceramics. Glass-fibre reinforced composite materials showed limited applications in terms of construction and building industry for several years. Recently, well potential for the applications of fibre reinforced composite materials for the numerous applications due to expeditiously retrofit (Hazrol *et al.*, 2019).

The process of forming large molecules from small ones is called polymerization; that is, polymerization is the process of joining many monomers, the basic building blocks, together to form polymers. There are two important classes of polymerization:

a. Condensation polymerization

In this process a stepwise reaction of molecules occurs and in each step a molecule of a simple compound, generally water, forms as a by-product.

b. Addition polymerization

In this process monomers join to form a polymer without producing any by-product. Addition polymerization is generally carried out in the presence of catalysts. The linear addition of ethylene molecules (CH_2) results in polyethylene (a chain of ethylene molecules), with the final mass of polymer being the sum of monomer masses (Krishan, 2012).

2.4 Natural Fibres

All fibres which come from natural sources (plants and animals) and do not require fibre formation or reformation are defined as natural fibres (Niddles, 2001, Jacob *et al*., 2004). Natural fibres are used in the manufacture of composite because of their low cost, abundant, renewable, better formability and eco-friendly features. They have low mechanical strength; most composites have strong, stiff fibres in a matrix which is weaker and less stiff (Zhu *et al*.,

2003). These engineering composites are desired due to their low density, high corrosion resistance, ease of fabrication, and low cost (Ubi *et al*., 2015). Natural fibres derived from plants mainly consist of cellulose, hemicellulose, lignin, pectin and other waxy substances. Cellulose is the main chemical component of all plant-based natural fibres. It is the most noteworthy organic component produced by plants that is ample in the environment. Based on the source of origin of natural cellulosic fibres are recognized by the chemical structure of cellulose in the bundle which provides strength and stability to the plant cell walls and the fibre. The low spiral angle of structural cellulose, smaller fibre diameter, and together with longer fibre is preferable properties of natural fibre (Anteneh *et al.*, 2021). Cellulose is composed of a long chain of glucose polymer units that are connected to form microfibrils (Faridulhassan *et al.*, 2020).

In various applications, natural fibres extracted from plants are used as reinforcements in both thermoplastic and thermoset composites. Figure 2.2 shows the different structural constituents a plant fibre which consist of cellulose and other trace element, it can be seen that, cellulose is highly crystalline polymer which contain as much as 80% of crystalline regions.

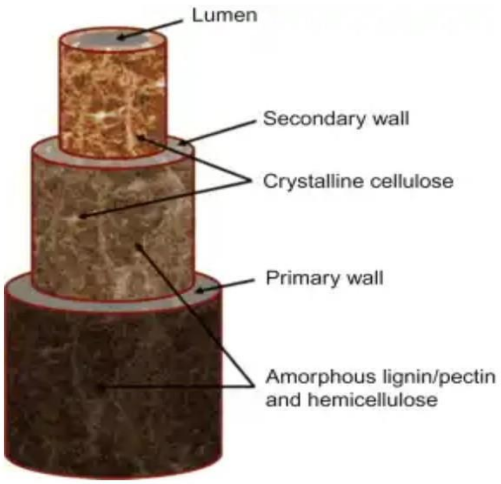

Figure 2.2: Structure of a plant fibre (Pilleriin *et al*., 2015)

Hemicellulose is made up of highly branched polysaccharides attached to the cellulose after the removal of pectin. Lignin is amorphous, stiffens the cell walls, and act as a protective barrier for the cellulose, (Pilleriin *et al*., 2015).

The reinforcing ability of natural fibres is usually enhanced by fibre treatment, which leads to improvement in the properties of fibre- reinforced resulting polymer composites (Idowu *et al.*,2016). Certain advantageous features, such as the biodegradability of natural fibres, coupled with the low cost, high specific strength and lighter weight than glass, have led to the extensive development of this environmentally friendly green material (Mohanty *et al*., 2000). Table 2.1 highlight some of the factors that differentiate between natural and synthetic fibres.

Table 2.1: Comparison between natural and synthetic fibre

Aspect	**Property**	**Natural Fibre**	**Synthetic Fibre**
Technical	Mechanical property	Moderate	High
	Moisture Sensitivity	High	Low
	Thermal sensitivity	High	Low
Environmental	Resource	Infinite	Limited
	Production	Low	High
	Recyclability	Good	Moderate

(Praveen *et al*., 2018)

2.4.1 Sources of natural fibres

Natural fibres are sourced from either plant or animals. Plant fibres are categorized as either primary as secondary depending on how they are used. Primary plants are grown basically for their fibre content, examples are; coir, oil palm, pineapple etc. while secondary plants are plants which fibres are produced as a by- product, examples are; Baobab pod fibres, hemp

and sisal. Table 2.2 shows the main plant fibres used commercially as composites which are produced throughout the world.

Table 2.2: Commercially measure fibre sources

Fibre source	World production (10^3 ton)
Bamboo	30,000
Jute	2300
Kenaf	970
Flax	830
Sisal	378
Hemp	214
Coir	100
Ramie	100
Abaca	70
Sugar cane bagasse	75,000
Grass	700

(Staiger *et al.*, 2008)

2.4.2 Classifications of natural fibres

Based on their origin, natural fibres can be classified as plant, animal and mineral fibres. Animal fibres such as hair, silk and mineral fibres have not been widely used as a reinforcement fibre, the detailed classification of natural fibres is shown in Figure 2.3.

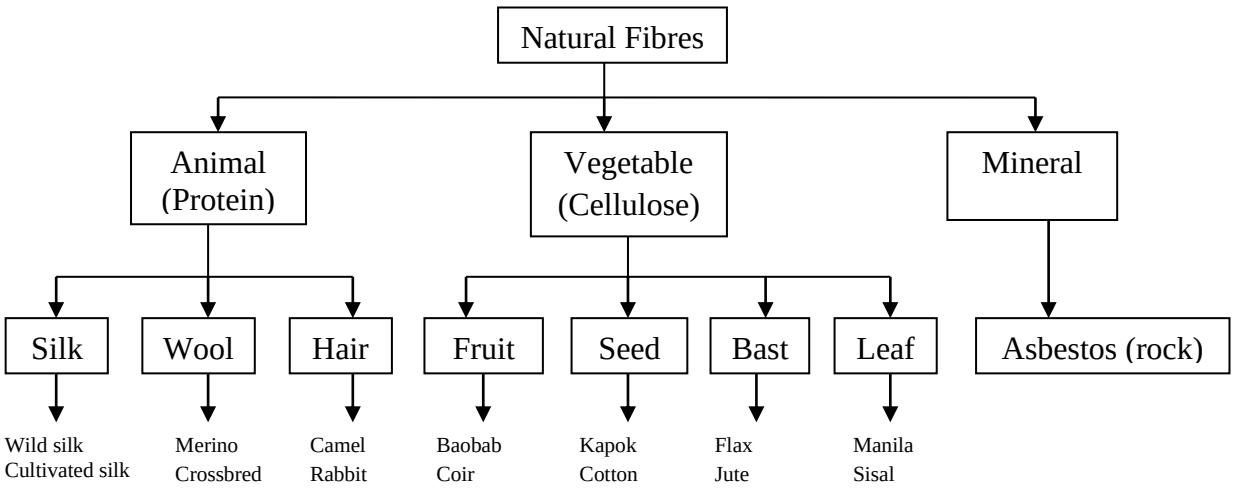

Figure 2.3: Classification of Natural Fibres (Praveenkumara *et al.*, 2018)

But several plants fibres have been used widely in biocomposites field for the applications in the area of automotive, marine and construction (Sanjay *et al*., 2016).

2.4.2.1 Animal fibres

Animal fibres are natural fibres that consist largely of particular proteins. Instances are silk, hair/fur (including wool) and feathers. Wool is the fibre derived from the fur of animals, principally sheep, but the hair of certain species of other mammals such as goats, alpacas, and rabbits may also be called wool is the fibre derived from the fur of animals, principally sheep, but the hair of certain species of other mammals such as goats, alpacas, and rabbits may also be called wool. The animal fibres used most commonly both in the manufacturing world as well as by the hand spinners are wool from domestic sheep and silk (Praveenkumara *et al.*, 2018).

2.4.2.2 Plant fibres

Plants are the natural sources of many raw materials used to produce textiles, ropes, twine, and similar products. Naturally available fruit fibres are pineapple, banana, coir, and palm fibre; Leaf fibres are manila and sisal fibres; Seed fibres are cotton and kapok fibres and also areca, bamboo, hemp, jute, kenaf and ramie fibres are the major plant fibres commonly used (Praveenkumara *et al.*, 2018).

2.4.2.3 Mineral fibres

Examples of mineral fibres are asbestos, graphite and glass. Asbestos occurs naturally as fibres. Asbestos is the only natural fibres obtained from varieties of rocks. It is fibrous form of silicate of magnesium and calcium containing iron and aluminium and other materials. It is acid proof, flame proof and rust proof, its particles are carcinogenic and hence its use is restricted. It can largely be used in fire-resistant substances (Praveenkumara *et al.*, 2018). They have higher stiffness and reasonable mechanical properties. It checks higher thermal

conductivity and hence this makes them particularly useful in thermal management system and satellite structures.

2.5 Manufacturing Methods for Natural Fibre Composites

Fibre reinforced plastics have been fabricated by several methods depending upon the shape of component to be manufactured. All those methods fall under a principle called polymerization (Srinivas *et al*., 2017). Polymerization is the process of joining large number of synthetic molecules together to form a rigid structure.

2.5.1 Compression moulding

Compression molding is a reliable method due to the high production rate and low processing time. Bio-composites fabricated through this process have adequate mechanical properties for different applications (Akampumuza *et al.*, 2017). Compression molding is used for bulk production, such as in automobile parts production (Alves *et al.*, 2010). Compression moulding is usually used for thermoplastic matrices with unfastened chopped fibre or mats of short or long fibre either randomly oriented or aligned, however can also be used with thermoset matrices. The fibres are commonly stacked alternately with thermoplastic matrix sheets earlier than stress and warmth are implemented. Compression molding is a technique of molding wherein the molding material, generally preheated, is first located in an open, heated mildew hollow space (Rong, 2001). Compression molding decreases fibre strength due to the dependency on initial fibre length and various process parameters such as melt viscosity and screw speed and design. The incompatibility of natural fibre with matrices also reduces fibre strength and the strength of bio-composite (Ho *et al.*, 2012).

In compression molding, fibres are placed between matrix layers. Furthermore, load and heat are applied in the process (Srinivas *et al.*, 2017). Compression molding is categorized into hot pressing and auto-clave methods. Sheet and bulk molding materials are starting materials

used to cover around 30–70 % mold cavity. The mold is closed correctly along with the application of pressure and heat. Natural fibres may break due to high pressure and temperature. Sometimes, short fibres are mixed prior to compression molding to reduce shrinkage and increase the strength of final products (Mallick *et al.*, 2007).

2.6 General Characteristics of Fibre Reinforced Composites

Common fibre reinforced composites are composed of fibres and a matrix. A high stiffness and strength to weight ratio is provided by polymeric materials reinforced with synthetic fibres such as glass and carbon (Abhishek, 2015). The polymer matrix used to make the composite can be a thermoplastic or thermosetting plastic depending on the application. There are a number of aspects that affects composite performance level or activities, of which to name a few are the following.

a. Orientation of fibre
b. Strength of fibres
c. Physical properties of fibres
d. Interfacial adhesion property of fibre

A fibre-reinforced composite depends as well on the contribution of some additional characteristics such as: matrix properties, fibre-matrix ratio, filler material, coupling agents and processing techniques (Pickering, 2016). The various types of natural fibre reinforcement is shown in Figure 2.4. As a consequence of imperfections in the manufacturing process, multi-layered fibre-reinforced composites are prone to early failure because of low adhesion between laminas that is, delamination (Chermoshentseva *et al.*, 2016).

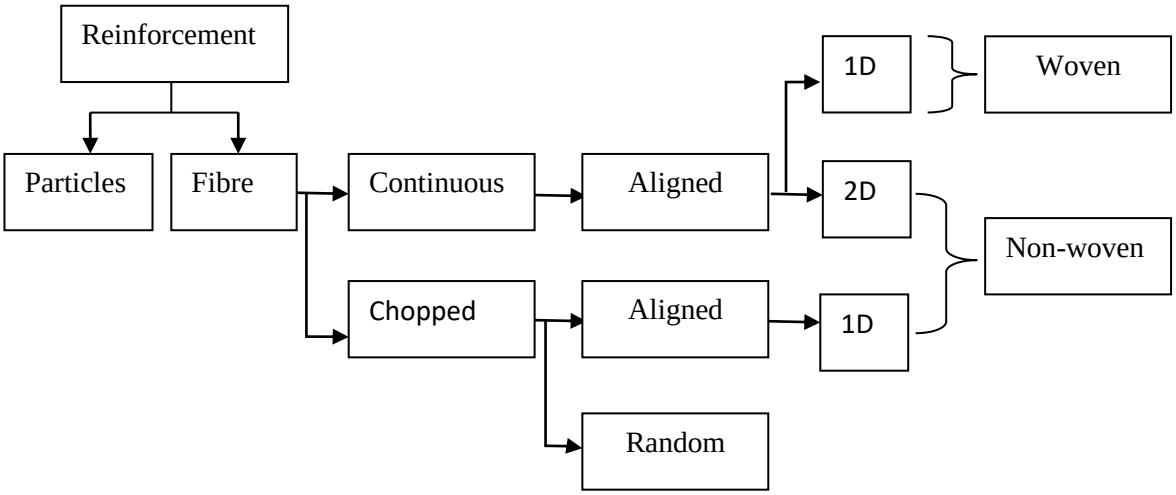

Figure 2.4: Type of natural fibre reinforcement (Mallick, 2007)

2.7 Chemical Compositions of Natural Fibres

Any natural fibre in nature contains different chemical compositions. It varies from plant to plant and the types of sources of fibre extracted such as stem, leaf, and root (Ramamoorthy *et al.,* 2014). The chemical composition of natural fibres such as wood, non-wood and bio residues is the most important factor for utilization of these sustainable materials. In order to produce many final products such as pulp, paper, composites and nanocellulose from these fibres, the chemical characteristics and their special qualities must be analyzed. These properties play an essential role in the technical aspects. In general, there are four major chemical ingredients in fibres derived from lignocellulosic materials as shown in Figure 2.5, and these are cellulose, hemicelluloses as well as lignin and extractives (Mehdi *et al*., 2015). Also the use of detergent fibre analysis developed by Peter Van Soest with the aid of Ankom 200 Fibre Analyzer^{TM} machine has been reported by several authors to be efficient in determining the chemical compositions of natural fibres. One of the limitations of detergent fibre analysis is that it cannot quantify the amount of pectin present in natural fibres.

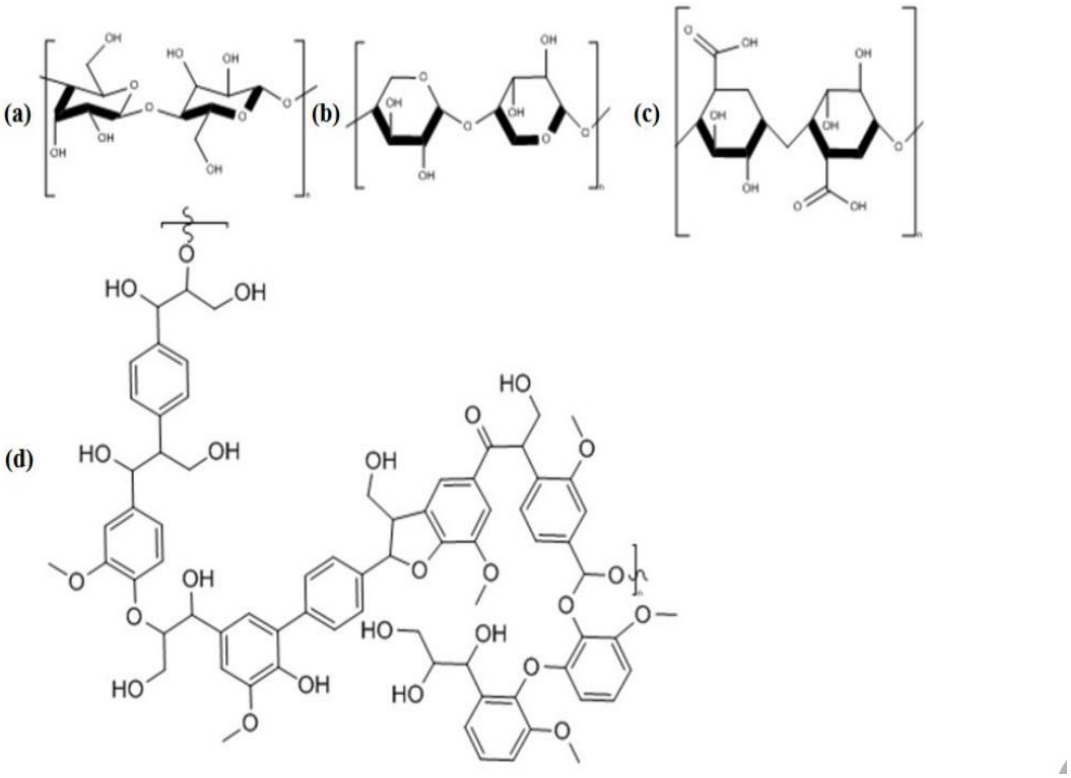

Figure 2.5: Chemical structures of (a) cellulose (b) hemicellulose (c) pectin (d) lignin (Odian, 2004)

Natural fibres are composed mainly of cellulose, hemicellulose, lignin, wax, pectin, and other materials. Among these, cellulose, hemicellulose and lignin are the basic components of Natural Fibres accounting for mechanical properties (Bledzki, *et al*., 1999). The significance of chemical composition investigation was to identify the amount of cellulose, hemicellulose, lignin, moisture, wax and ash contents in the existing fibres that help to selects the strength and bonding ability of the fibre materials (Anteneh *et al.*, 2021). Most of the modern fibres are almost identical in their morphology, cellulose-based fibres (cotton, linen, jute, sisal, viscose), which are very similar by their chemical composition, are difficult to differentiate from each other with IR-based methods (Peet *et al*., 2017). Table 2.3 summarized the chemical compositions of some natural fibres.

Table 2.3: Chemical composition of some natural fibres

Fibre	Cellulose (wt.%)	Hemicellulose (wt.%)	Lignin (wt.%)	Waxes (wt.%)
Bagasse	52.2	16.8	25.3	
Bamboo	26 – 43	30	21 – 31	–
Flax	71	18.6 – 20.6	2.2	1.5
Kenaf	72	20.3	9	–
Jute	61 – 71	14 – 20	12 – 13	0.5
Hemp	68	15	10	0.8
Ramie	68.6 – 76.2	13 – 16	0.6 – 0.7	0.3
Abaca	56 – 63	20 – 25	7 – 9	3
Sisal	65	12	9.9	2
Coir	32 – 43	0.15 – 0.25	40 – 45	–
Oil palm	65	–	29	–
Pineapple	81	–	12,7	–
Curaua	73.6	9.9	7.5	–
Wheat straw	38 – 45	15 – 31	12 – 20	–
Rice husk	35 – 45	19 – 25	20	14 – 17
Rice straw	41 – 57	33	8 – 19	8 – 38

(Faruk *et al*., 2000)

2.8 Hydrophilic Character of Natural Fibres

Setbacks associated with natural fibres have to be overcome before using them in polymer composites. The most serious concerned problem with natural fibres is its hydrophilic nature, which causes the fibre to swell and ultimately rotting takes place through attack by fungi. The hydrophilic nature of fibres prevents the use of bio-composites in various potential applications (Sgriccia *et al.*, 2008). Natural fibres are hydrophilic as they are derived from lignocellulose, which contain strongly polarized hydroxyl groups. These fibres, therefore, are inherently incompatible with hydrophobic thermoplastics, such as polyolefins. The major limitations of using these fibres as reinforcements in such matrices include poor interfacial adhesion between polar-hydrophilic fibre and nonpolar-hydrophobic matrix. Moreover, difficulty in mixing because of poor wetting of the fibre with the matrix is another problem that leads to composites with weak interface. A possible solution to improve the fibre polymer interaction is by using competibilizers and adhesion promoters which reduce the

moisture absorption. Surface treatments of the fibre with silane make the fibre more hydrophobic (Pott *et al.*, 1997). To reduce the moisture absorption, the fibre has to be changed chemically and physically. Hydrothermal treatment is one of the approaches to reduce moisture absorption of natural fibres, which can increase the crystallinity of cellulose and therefore, contributes to a reduced moisture uptake. Moreover, on hydrothermal treatment, a part of hemi-cellulose is extracted thereby decreasing the moisture absorbance (Pejis *et al.*, 1998).

2.9 Biodegradability of Natural Fibre Composites

Biodegradable matrices are environmental and eco-friendly. Disposal and the environmental problems of composites can be solved using renewable and biodegradable matrices and fibres (Narayan *et al.,* 2006). Biodegradation is referred to a type of degradation that involves biological activity. Biodegradation is expected to be the major mechanism of loss for most chemicals released into the environment. This process refers to the degradation and assimilation of polymers by living microorganisms to yield degradation products. The most significant organisms in biodegradation are fungi, bacteria and algae. (Leja, 2010).

High strength composites are resultants products of natural fibre reinforcement in polymers which also provide extra or improved biodegradability, low cost, light weight and enhanced properties related to mechanical structure (Sreekala *et al*., 2001). At temperatures as high as 240 ˚C, natural fibres start degrading whereas constituents of fibre, such as hemicellulose, cellulose, lignin, and others start degrading at different level of temperature; for example, at 200 ˚C lignin starts to decompose whereas at temperatures higher than this other constituents will degrade (Kabir *et al*., 2012).

Since thermal stability of the fibres is dependent on the structural constituent of fibres, it can be improved if the concentration levels or structural constituents are completely removed. Natural fibres have a short life span with minimum environmental damage upon degradation,

whereas synthetic ones effect environment due to pollution caused by degradation (Ramesh *et al*., 2014)

2.9.1 Factors affecting the biodegradability of plastics

The properties of plastics are associated with their biodegradability. Both the chemical and physical properties of plastics influence the mechanism of biodegradation. The surface conditions (surface area, hydrophilic, and hydrophobic properties), the first order structures (chemical structure, molecular weight and molecular weight distribution) and the high order structures (glass transition temperature, melting temperature, modulus of elasticity, crystallinity and crystal structure) of polymers play important roles in the biodegradation processes (Iwata *et al*, 1998).

The molecular weight is also important for the biodegradability because it determines many physical properties of the polymer. Increasing the molecular weight of the polymer decreased its degradability. Moreover, the morphology of polymers greatly affects their rates of biodegradation. The degree of crystallinity is a crucial factor affecting biodegradability, since enzymes mainly attack the amorphous domains of a polymer (Pranamuda *et al.*, 1997). The molecules in the amorphous region are loosely packed, and thus make it more susceptible to degradation. The biodegradation mechanisms of plastics as shown in this review can be applied to biomass that is composed of polymeric materials (i.e., cellulose, hemicellulose, lignin, chitin and silk fibroin) (Tsuji *et al.*, 2001).

Biodegradability of the polymer is essentially determined by the following important physical and chemical characteristics:

a. Availability of functional groups that increases hydrophilicity
b. Size, molecular weight and density of the polymer
c. Amount of crystalline and amorphous regions
d. Structural complexity such as linearity or presence of branching in the polymer

e. Presence of easily breakable bonds such as ester or amide bonds as against carbo – carbon bonds

f. Molecular composition (blend) and

g. Nature and physical form of the polymer such as whether it is in the form films, pellets, powder or fibres

2.10 Baobab Fibres

Adansonia digitata called the Baobab tree in both English and French is very characteristic of the Sahelian region and belongs to the Malvaceae family. The plant is a very massive tree with a very large trunk (up to 10 m diameter) which can grow up to 25 m in height and may live for hundreds of years. The plant is widespread throughout the hot and drier regions of tropical Africa (FAO, 1988). The fruit consists of large seeds embedded in a dry, acidic pulp and shell (Yezzie *et al*., 1994). The Baobab tree also known as the tree of life as shown in Plate I. It is huge tree with a very large trunk which can grow up to 25 meters in height and may live for hundreds of years.

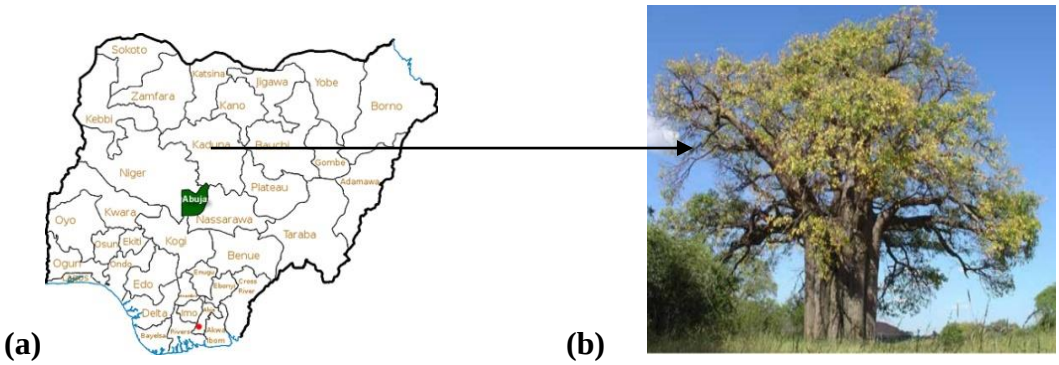

Plate I: Image showing (a) The location of Baobab tree and (b) Baobab tree

Baobab is a tree mostly found in Northern part of Nigeria. Both leaves and pulp are used in this region for human consumption. The pod (fruit) contains fibres as shown in Plate II. The plant also provides forage for wildlife and domestic animals (Nkafamiya *et al.*, 2007). Nutritional analysis of Baobab fruit pulp has shown that it is an excellent source of pectin,

calcium, vitamin C and iron. Its vitamin C content has been compared with oranges and found that it is about three times higher, (Osman, 2004).

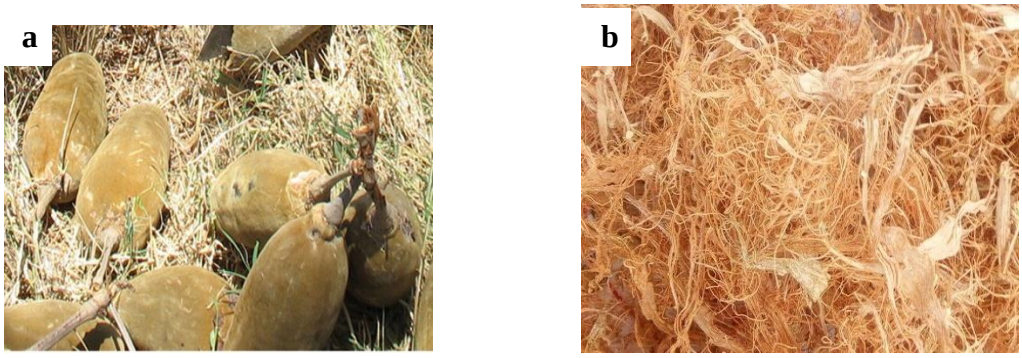

Plate II: Images showing (a) Baobab pods (b) Baobab pod fibre (FAO, 1988)

Baobab fibre is obtained from the pod and bark of the tree Adansonia digitata. Apart from Being a source of fibre, the fruit pulp, seeds, leaves, bark and root tubers have been studied by scientists for their useful properties. They all have interesting possibilities for use in pharmaceutical, nutritional, cosmetic and veterinary items (Joerg *et al*., 2018). Like other natural fibres, Baobab fibres are lignocellulosic fibres with high percentage extension at break and low density of 5.3 % and 1.40 g/cm^3 respectively compared to other natural fibres (Modibbo *et al*., 2009).

2.11 Chemical Treatments of Natural Fibres

Fibre modification helps to overcome various problems of natural fibre, such as poor fibre/matrix adhesion, moisture absorption, low fire resistance, inferior mechanical properties, low thermal resistance, and restrictive processing temperatures (Mohammed, 2021). Chemical treatments are considered in modifying the fibre surface properties. It is aimed at improving the adhesion between the fibre surface and the polymer matrix may not only modify the fibre surface but also increase fibre strength. This treatment provides chemical interlocking at the fibre/matrix interface to improve adhesion (Rahman *et al.*, 2007). Some of these chemical treatment methods are discussed below:

2.11.1 Mercerization

This is a traditional alkali treatment based on sodium hydroxide (NaOH, caustic soda), alkali treatment is a common method to clean and modify the surface of natural fibre to promote enhanced fibre-polymer adhesion. A number of studies have found that the alkali treatments can improve the properties of natural fibres and the interfacial adhesion to polymers. It improves the adhesive characteristics of the fibre surface by removing natural waxy materials, hemicellulose and artificial impurities, and produce good surface topography (Jacobs *et al.*, 2004).

Addition of aqueous sodium hydroxide (NaOH) to natural fibre promotes the ionization of the hydroxyl group to the alkoxide (Rohan *et al.*, 2018). The reaction mechanism for NaOH treatment of natural fibre is shown in Figure 2.6. This treatment removes a certain amount of lignin, wax and oils covering the external surface of the fibre cell wall, depolymerizes cellulose and exposes the short length crystallites (Mohanty *et al.*, 2001).

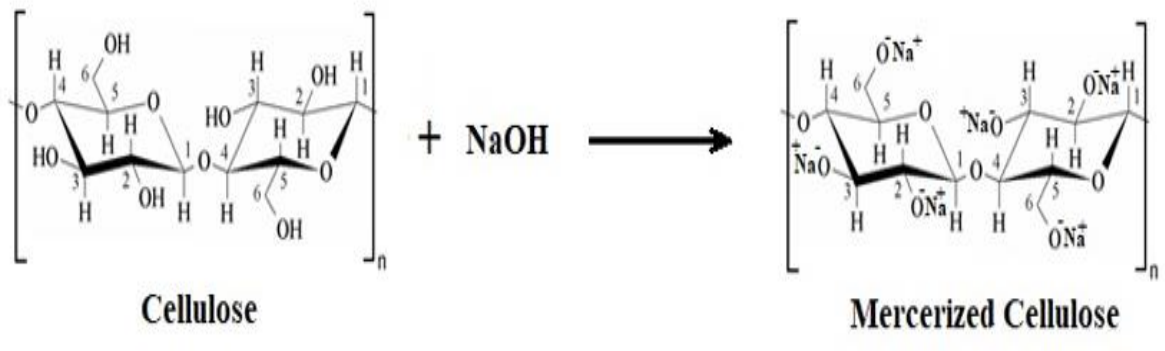

Figure 2.6: Mercerization of cellulose in natural fibre (Omid *et al.*, 2017)

2.11.2 Acetylation

This is a treatment of particular interest for natural fibres. In this treatment, acetic anhydrides substitute the cell wall hydroxyl groups of a natural fibre with acetyl groups, rendering the surface more hydrophobic and thus less susceptible to moisture uptake and biological attack and more compatible with polymer matrices. Acetylation is commonly applied to wood to

improve dimensional stability and environmental resistance. A typical process involves soaking the fibres in acetic acid, then treating them with acetic anhydride and then a final washing stage. If done properly, fibre properties such as strength and modulus are not reduced. The reaction of acetic anhydride with fibre is shown as:

$$\text{Fibre} - OH + CH_3 - C(=O) - O - C(=O) - CH_3 \rightarrow \text{Fibre} - OCOCH_3 + CH_3COOH$$

Acetylation can reduce the hygroscopic nature of natural fibres and increases the dimensional stability of composites. Acetylation was used in surface treatments of fibre for use in fibre-reinforced composites (Rong *et al.*, 2001)

2.11.3 Silane treatment

The use of silane in chemically modifying NFs has been reported in several studies to have been effective in enhancing the interface between the fibres and polymer matrix composites. Silane (SiH_4) is a multifunctional molecule which is used as a coupling agent to modify fibre surfaces and to let natural fibres adhere to polymer matrix, stabilizing the composite materials. The composition of silane forms a chemical link between the fibre surface and the matrix through a Sloane bridge (Wang *et al.,* 2007). Its application restrains the swelling of fibre by creating a crossed linked network due to coverlent bonding between matrix and fibre. Therefore, the hydrocarbon chains provided by the application of silane restrain the swelling of the fibre by creating a cross linked network due to covalent bonding between the matrix and the fibre. The reaction schemes are given as follows:

$$CH_2CHSi(OC_2H_5)_3 \xrightarrow{H_2O} CH_2CHSi(OH)_3 + 3C_2H_5OH$$

$$CH_2CHSi(OH)_3 + \text{Fibre} - OH \rightarrow CH_2CHSi(OH)_2O - \text{Fibre} + H_2O$$

Many researchers silane applied treatment in surface modification of glass fibre composites (Lee *et al*, 1997). Silane coupling agents were also found to be effective in modifying natural fibre–polymer matrix interface and increasing the interfacial strength.

2.11.4 Benzoylation treatment

Benzoylation is an important transformation in organic synthesis. Benzoyl chloride is most often used in fibre treatment. Benzoyl chloride includes benzoyl ($C_6H_5C{=}O$) which is attributed to the decreased hydrophilic nature of the treated fibre and improved interaction with the hydrophobic matrix. The reaction between the cellulosic hydroxyl group of the fibre and benzoyl chloride is shown in Equations (2.1) and (2.2) (Joseph *et al.*, 2000)

$$\text{Fibre} - OH + NaOH \rightarrow \text{Fibre} - O^- Na^+ + H_2O \quad (2.1)$$

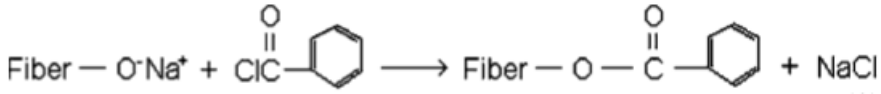

(2.2)

Benzoylation of fibre improves fibre matrix adhesion, thereby considerably increasing the strength of composite, decreasing its water absorption and improving its thermal stability.

2.11.5 Peroxide treatment

In organic chemistry, peroxide is a specific functional group or a molecule with the functional group ROOR containing the divalent ion O–O. Organic peroxides tend to decompose easily to free radicals of the form RO;RO then reacts with the hydrogen group of the matrix and cellulose fibres. For example, the peroxide initiated free radical reaction between polyethylene (PE) matrix and cellulose fibres is shown by the following equations (Paulo *et al.*, 2018):

$$RO - OR \rightarrow 2RO \quad (2.3)$$

$$RO + PE - H \rightarrow ROH + PE \quad (2.4)$$

$$RO + Cellulose - H \rightarrow ROH + Cellulose \quad (2.5)$$

$$PE + Cellulose \rightarrow PE - Cellulose \quad (2.6)$$

In peroxide treatment, fibres are coated with BP or DCP in acetone solution for about 30 min after alkali pre-treatment (Sreekala *et al.*, 2000).

2.12 Nanocellulose

Nanocellulose is a general term used for cellulose nanocrystals (CNC), cellulose nanofibers (CNF), and bacterial nanocellulose (BNC) (Farid *et al.*, 2020), They have essentially different extraction procedures as well as different morphologies. CNFs can be isolated using mechanical processes such as high pressure homogenization, grinding and refining (Wang *et al.*, 2007), whereas CNCs have been extensively isolated by using acid hydrolysis treatments (Habibi *et al*., 2009). Other works have also been reported for isolation of CNCs from biomass using other chemicals such as ammonium persulfate and hydrogen peroxide (Miyashiro *et al*., 2020). In general terms, wood and non-wood cellulose can be utilized as sources to prepare either CNFs or CNCs.

2.12.1 Cellulose nano fibres (CNF)

The cell wall in lignocellulosic fibre possesses basic structural units that are known as elementary fibrils. These elementary fibrils are about 2–20 nm in diameter and a few micrometers in length (Wang *et al.*, 2007). These CNFs include groups of cellulose chains that are bound together by hydrogen bonding. Isolation of CNFs can be performed by a wide variety of mechanical techniques such as refining, grinding, high pressure homogenization and cryocrushing. In combination with a suitable matrix polymer, CNF networks show considerable potential as an effective reinforcement for high-quality specialty applications of

bio-based composites (Mehdi *et al.,* 2015). The combination of their flexibility, strength and aspect ratio provides a number of alternatives potentials to using CNFs in many applications.

2.12.2 Cellulose nanocrystals (CNCs)

Different terms have been used in the literature to designate these rod-like nanoparticles. They are mainly referred to as ‘‘crystals’’ or cellulose nanocrystals. CNCs are the crystalline regions of the CNFs and are described as the monocrystalline region of cellulose (Azizi Samir *et al*., 2005). The size of CNCs depends on the source from which they are generated and can vary from 100 to 1,000 nm in length and 4 to 25 nm in diameter. Regarding the extraction of crystalline cellulosic regions, in the form of CNCs, a simple process mostly based on acid hydrolysis is generally utilized. Acid hydrolysis is therefore a well-known process to produce CNC. It is believed that this method leads to isolation of CNCs with a high degree of crystallinity by removing the amorphous part of the raw material (Habibi *et al.,* 2010). Although acid hydrolysis is usually performed using HCl or H_2SO_4, microbial hydrolysis has also been utilized to produce nanocrystals (Satyamurthy *et al*., 2011)

2.13 Nanocomposites

Nanotechnology is revolutionizing the world of materials. It has very high impact in developing a new generation of composites with enhanced functionality and a wide range of applications. are composites in which at least one of the phases shows dimensions in the nanometre range (1 nm = 10^{-9} m). Recently, nanoparticles have become more popular for enhancing the mechanical and functional performances (flame retardancy, antibacterial, and anticorrosion (Farid *et al*., 2020). Nanofillers are replacing traditional micro scale filler. The data on processing, characterization and applications helps researchers in understanding and utilizing the special chemical and material principles underlying these cutting-edge polymer nanocomposites (Namita, 2015).

Replacement of traditional micro-composites with nanocomposite materials grew quickly in the last 20 years to overwhelm the restrictions of the micrometer scale, synthesizing novel structures and materials having extraordinary flexibility, enhanced physical performances, and noteworthy industry impact (Michael and Philippe 2000 (Thomas *et al.*, 2007).

A nanocomposite is a class of materials in which one or more phases with nanoscale dimensions are embedded in a metal, ceramic, or polymer matrix The properties of nanocomposites rely on a range of variables, particularly the matrix material, which can exhibit nanoscale dimensions, loading, degree of dispersion, size, shape, and orientation of the nanoscale second phase and interactions between the matrix and the second phase. Most nanocomposites that have been developed and that have demonstrated technological importance have been composed of two phases, and can be microstructurally classified into three principal types:

As with conventional composites, the properties of nanocomposites can display synergistic improvements over those of the component phases individually. However by reducing the physical dimensions (s) of the phase (s) down to the nanometer length scale, unusual and often enhanced properties can be realized. An important microstructural feature of nanocomposites is their large ratio of interphase surface area to volume (Shivani, 2015)

2.13.1 Structure and properties of nanocomposites

The structure of nanocomposites usually consists of the matrix material containing the nanosized reinforcement components in the form of particles, whiskers, fibres, nanotubes, etc. (Franki *et al*., 2003). Different investigators have employed various equipments and techniques for the characterization of nanocomposites. In addition, theoretical calculations/simulations have been worked out to predict strength properties, including

stress/strain curves. Similarly, theoretical thermal and electrical conductivities are comparable with that of diamond, with an almost negligible thermal expansion coefficient (Kojima *et al*., 1993). They also exhibit high thermal stability both in air and in vacuum, compared to the lower values obtained for metal wires in microchips, and high parallel and perpendicular magnetic susceptibilities (Dresselhaus *et al.*, 2005).

2.13.2 Classification of nanocomposites

Nanocomposites can be classified into two major groups:

a. Polymer based

b. Non polymer based

2.13.2.1 Polymer based nanocomposites

Nanomaterials have very good mechanical, optical, and thermal characteristics that can be easily implemented as Nanofillers for functionalizing various nano bio composites (Nguyen *et al*., 2020). Polymer nanocomposites are composites with a polymer matrix and filler with at least one dimension less than 100 nm. Polymer–nanoparticle composite materials have also attracted the interest of a number of researchers, due to their synergistic and hybrid properties. Polymer based nano composites can be classified into different categories as shown in Figure 2.7. Ease of processability of organic polymers combined with the better mechanical and optical properties of nanoparticles has led to the fabrication of many devices.

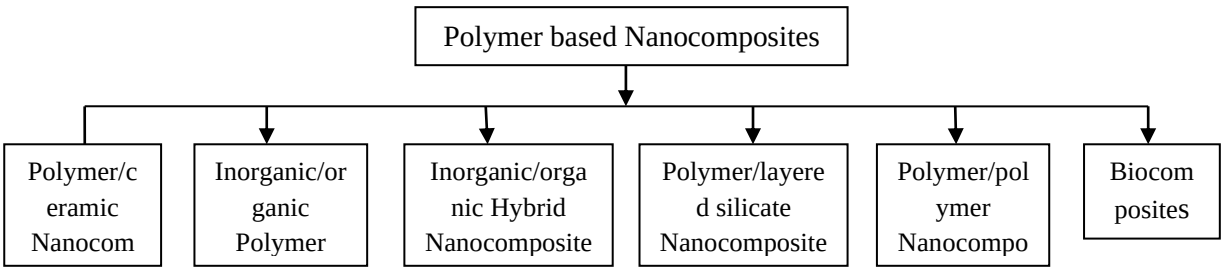

Figure 2.7: Classification of polymer based Nanocomposites (Shivani, 2015)

2.13.2.1 Non polymer based nanocomposites

Non- polymer based nanocomposite materials can be classified as shown in Figure 2.8.

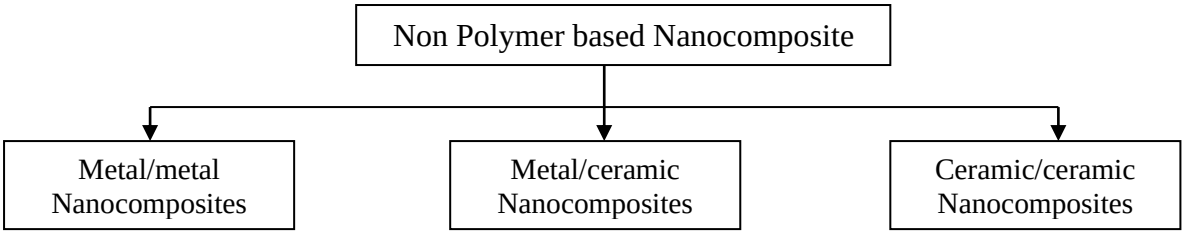

Figure 2.8: Classification of non-polymer based nanocomposites (Shivani, 2015)

a. Metal/Metal nanocomposite

Bimetallic nanoparticles either in the form of alloy or core-shell structures or being investigated in some depth because of their improved catalytic properties and changes in the electronic/optical properties related to individual, separate metals. It is postulated their interesting physico-chemical properties, result from the combination of two kinds of metals and their fine structures (Schmidt, 2002).

b. Metal/Ceramic nanocomposites

In these types of composites, the electric, magnetic, chemical, optical and mechanical properties of both phases are combined. Size reduction of the components to the nanoscale causes improvement of the above mentioned properties and leads to new application. The polymer precursor's techniques offer an attractive rough to such composites proving a chemically inert and hard ceramic matrix (Subramanian, 2005)

c. Ceramic/Ceramic nanocomposites

Ceramic Nano composites could solve the problem of fracture failures in artificial joint implants; these would extend patient's mobility and eliminate the high cost of surgery. The

use of Zirconia-toughened alumina nanocomposite to form Ceramic/ceramic implants with potential life spends of more than 30 years (Schmidt, 2002).

2.13.3 Polymer matrix- reinforcement nanocomposites

The reinforcing materials employed in the production of polymer nanocomposites can be classified according to their dimensions. Example, when the three dimensions are in the nanometre scale, they are called isodimensional nanoparticles. Examples include spherical silica, metal particles and semiconductor nanoclusters. The second kind of reinforcement is formed by nanotubes or whiskers, which contain two dimensions in the nanometre scale and one larger, forming an elongated structure. Carbon nanotubes and cellulose whiskers, extensively studied as reinforcing nanofillers, can be included in this second category (Bafna *et al.*, 2003).

The third type of reinforcement is characterized by only one dimension in the nanometre range 220-222. In this group, the filler contains sheets one to a few nanometres thick and hundreds to thousands nanometres long. This family is called polymer-layered nanocomposites (Fischer *et al.*, 2003). These materials are obtained by intercalation of the polymer (or a monomer subsequently polymerized) inside the galleries of the layered host (Chen *et al.*, 1997). Many synthetic and natural crystalline hosts that are able, under specific conditions, to intercalate a polymer have been described. Nanocomposites based on clay and layered silicates have been widely investigated due to the availability of clay starting materials and their well-known intercalation chemistry (Ogawa *et al.*, 1997).

2.13.4 Applications of nanocomposites

From the foregoing, it becomes evident that nanocomposites may provide many benefits such as enhanced properties, reduction of solid wastes [lower gauge thickness films and lower

reinforcement usage] and improved manufacturing capability, particularly for packaging applications (Schmidt *et al*., 2002).

Improvements in mechanical property have results in major interest in nanocomposite in various automotive and general/industrial applications. These include potential for utilization as mirror housing on various vehicles types, door handles, engine covers and intake manifolds and timing belt covers. More general applications currently being considered include usage as impellers and blades for vacuum cleaners, power tool housings, mower hood and covers for portable electronic equipment such mobile phones, pagers (Bledzki *et al*., 1999).

Nano-particles and nano-layers have very high surface-to-volume and aspect ratios and this makes them ideal for use in polymeric materials. Such structures combine the best properties of each component to possess enhanced mechanical and superconducting properties for advanced applications. The properties of nano-composite materials depend not only on the properties of their individual parents but also on their morphology and interfacial characteristics. Some nanocomposite materials could be 1000 times tougher than the bulk component. The general class of nanocomposite organic/inorganic materials is a fast growing area of research (Obor *et al*., 2018).

As it can be observed, the promising applications of nanocomposite systems are numerous, comprising both the generation of new materials and the performance enhancement of known devices such as fuel cells, sensors and coatings. Although the use of nanocomposites in industry is not yet large, their massive switching from research to industry has already started and is expected to be extensive in the next few years (Voevodin and Zabinski, 2005).

In general, nanocomposites exhibit gains in barrier, flame resistance, structural, and thermal properties yet without significant loss in impact or clarity. Because of the nanometer-sized

dimensions of the individual platelets in one direction, exfoliated nanoclays are transparent in most polymer systems. However, with surface dimensions extending to 1 micron, the tightly bound structure in a polymer matrix is impermeable to gases and liquids, and offers superior barrier properties over the neat polymer. Nanocomposites also demonstrate enhanced fire resistant properties and are finding increasing use in engineering plastics (Yoldas *et al*., 2013).

2.13.5 The future of nanocomposites

The number of commercial applications of nanocomposites has been growing at a rapid rate. It has been reported that in less than two years, the worldwide production is estimated to increase and is set to cover the following key areas in the future: Drug delivery systems, anti-corrosion barrier coatings, UV protection gels, lubricants and scratch free paints new fire retardant materials and new scratch/abrasion resistant materials (Tan *et al*., 2015).

Superior strength fibres and films Improvements in mechanical property have resulted in major interest in nanocomposite materials in numerous automotive and general/industrial applications. These include potential for utilization as mirror housings on various vehicle types, door handles, engine covers and intake manifolds and timing belt covers. More general applications currently being considered include usage as impellers and blades for vacuum cleaners, power tool housings, mower hoods and covers for portable electronic equipment such as mobile phones and pagers (Yoldas *et al*., 2013)

2.14 Polymer Matrix

Polymers are composed of many repeating subunits, such as monomers, that are chemically bonded. They are mainly classified into two categories: one is natural polymers (like cellulose, pectin, protein, lignin, and hemicellulose) and the other is synthetic polymers (Chandar *et al*., 2016).

There are also other types of modified natural polymers, such as viscose. The structure of thermoplastics can be crystalline, amorphous, or even semi crystalline, and is affected by the different processing technologies of the polymers (Farid *et al*., 2020).

Thermoplastic polymers are made by different methods, such as injection molding, extrusion, and compression molding (Al-Oqla *et al*., 2015). Different natural fibres are used for reinforcements, along with the matrix, to enhance the strength and performance of the composites (Wu *et al*., 2020).

2.14.1 Polyethylene

Polyethylene is a light weight, durable thermoplastic with variable crystalline structure. It is one of the most widely produced plastics in the world. It's used in applications ranging from films, tubes, plastic parts and laminates. Polyethylene is made from the polymerization of ethylene (or ethane) monomer. Polyethylene chemical formula is $(C_2H_4)n$, the molecular structure of polyethylene is represented in Figure 2.9. Polyethylene belongs to polyolefin family of polymers and is classified by its density and branching (Rong *et al*., 2001).

Figure 2.9: Molecular structure of polyethylene

2.14.1.1 Low density polyethylene (LDPE)

Low-Density Polyethylene (LDPE) is sometimes recycled. It is a very healthy plastic that tends to be both durable and flexible. Items such as cling-film, sandwich bags, squeezable bottles, and plastic grocery bags are made from LDPE. Compared to high density polyethylene, it has a higher degree of short and long side-chain branching. It is produced at high pressure via free radical polymerization process Its tough and flexible, soft, has waxy

surface, good moisture barrier properties, low melting point and stable electrical properties (Lavanya *et al*., 2015).

2.14.1.2 High density polyethylene

High-Density Polyethylene (HDPE) products are very safe and are not known to transmit any chemicals into foods or drinks. HDPE products are commonly recycled. Items made from this plastic include containers for milk, motor oil, shampoo, conditioners, soap bottles, detergents, and bleaches.

2.14.1.3 Polyethylene terephthalate

Polyethylene Terephthalate (PET) sometimes absorbs odours and flavours from foods and drinks that are stored in them. Items made from this plastic are commonly recycled. PET plastic is used to make many common household items like beverage bottles, medicine jars, rope, clothing and carpet fibre. PET has good gas and moisture barrier properties, High heat resistance, Solvent resistant, clear, hard and though (Thomas *et al.*, 2007).

2.14.1.4 Polyvinyl chloride

Polyvinyl Chloride (PVC) is sometimes recycled. PVC is used for all kinds of pipes and tiles, but is most commonly found in plumbing pipes. This kind of plastic should not come in contact with food items as it can be harmful if ingested. It has excellent transparency, hard, good chemical resistance, long term stability, stable electrical properties and good weathering ability.

2.14.1.5 Polypropylene

Polypropylene (PP) is occasionally recycled. PP is strong and can usually withstand higher temperatures. It is used to make lunch boxes, margarine containers, yogurt pots, syrup bottles, prescription bottles. Plastic bottle caps are often made from PP. Polypropylene has excellent

chemical resistance, high melting point, translucent, hard, strong but flexible (Sanjay *et al*., 2016).

2.15 Applications of fibre reinforced composites

Fibre reinforced composites has lot of significance in our everyday life ranging from chemical industries, Automotive industries to construction industries (Wu *et al*., 2020). Fibre reinforced polymers (FRPs) find wide application in many industries as summarized in the Table 2.4.

Table 2.4: Summary of Applications of Composites

Industry	Examples	Comments
Aircraft	Door, elevators	20-35 % Weight savings
Aerospace	Space Shuttle, Space stations, control surfaces in airplanes, for the rotor assembly in helicopters.	Great weight saving
Automotive	Body frames, engine components, racing cars.	Components High stiffness and damage tolerance
Chemical	Pipes, Tanks, Pressure vessels	Corrosion resistance
Construction	Structural and decorative panels, Fuel tanks etc.	Weight savings, portable.
Sport	Shafts for golf clubs, handles of rackets	Weight savings, portable.

(Wu *et al*., 2020)

2.15.1 Use of Fibre reinforced Composites for automotive applications.

More interest has now been shown in the investigation of the suitability of natural fibre composites in automotive applications where moderate strength, lower cost and environmental friendly features are required. Vegetable fibres are used in the interior of passenger cars and truck cabins. For example, in automotive industry the kenaf, hemp, flax, sisal, jute blended with thermoplastic polymers, such as polypropylene and polyester can be used. These materials collectively make an excellent application for automotive seat backs,

headliners, door panels, package trays, pillars, and the list goes on to a broad range of products. Moreover, the most important variables for changing into new materials are mass, material, internal energy and head Injury criterion (Zahra *et al*., 2020).

CHAPTER THREE

3.0 MATERIALS AND METHODS

This chapter present the materials and experimental methods used and procedures followed to achieve the set objectives of this research.

3.1 Materials

Ripe and mature Baobab pods were collected from Baobab trees. Low density polyethylene (LDPE) was obtained from Nigeria Institute of Leather and Science Technology (NILEST) Samaru-Zaria, Kaduna state, Nigeria. Sodium hydroxide (NaOH) pellets (98 % purity, analytical grade), Sodium Chlorite ($NaClO_2$), Acetic acid and distilled water (100 % purity) were supplied by a vendor. All chemicals were used as received. List and sources of Equipments used are summarized in Table 3.1

3.2 Equipments

Table 3.1: Equipment used with their sources

S/N	Equipment	Description	Source
1	Weighing machine	Kern and Solm Company Berlingen Germany (Model No D72336).	National Research Institute for Chemical Technology (NARICT) Zaria.
2	Centrifuge	China Lab Model HY800N, Basket diameter; 800m, Rotation speed; 700-900 rpm, output capacity; 5-10 t/h, motor power; 22kw, moisture content of solid cake;3-5%, solid material recovery; above 95%.	Department of Chemical Engineering, Kaduna Polytechnic, Kaduna,

3	Two roll mill	Reliable Rubber and Machinery Company North Bergen New Jersey U.S.A (Model No 5183).	College of Leather Research and Chemical Technology, Zaria
4	Compression moulding Machine	Carver Incorporation New Jersey, U.S.A Model No 12000.	College of Leather Research and Chemical Technology, Zaria.
5	Tensile Strength testing Machine	Instron Machine Model 3369, GBT. Number 3369K1781,Capacity 50 kN, weight 141 kg, Maximum speed 500 mm/min, Power Requirement 100/120/220/240V, Maximum Vertical Test space 1193 mm.	Nuhu Bamalli Polytechnic Zaria.
6	Charpy Impact Testing Machine	Capacity 15 J and 25 J, Serial Number 412-07-15269C, Norwood Instruments Limited, Great Britain.	Department of Metallurgical and Materials Engineering ABU Zaria.
7	Flexural Testing Machine	Universal Materials Testing Machine, Norwood Instruments Ltd. Serial Number Cat. Nr 261, 100 kN capacities.	Strength of Material Laboratory of the Department of Mechanical Engineering Ahmadu Bello University Zaria.
8	Hardness Testing Machine	Vickers Hardness Tester. DIN 53505 ISO 868 ASTM D2240, Serial Number 07/2012-1329, Model MV1-PC	Shell Complex, Ahmadu Bello University Zaria
9	Fourier Transform Infrared Spectroscopy (FT-IR)	Agilent Technologies	National Research Institute for Chemical Technology (NARICT) Zaria.

10	Scanning Electron Microscopy (SEM) Machine	ZEISS Technologies Germany, machine model Hitachi S3000N VP	South Africa
11	Thermogravimetric Analysis (TGA) Machine	Perkin Elmer Thermal Analysis. Q20 V4.5A (TA instruments, USA)	Step-B, Federal University of Technology. Minna
12	X-ray Detraction (XRD) Machine	PANalytical Empyrean X-ray diffractometer UK. Radiation = 1.540598 , Pattern : 00-003-0289	South Africa

3.3 Material Preparation

Baobab pods were sliced open mechanically using a knife. The fibres were screened out from the pods by hand, and then washed in a running tap water to remove the remaining pulp on the fibres. Finally, the fibres were allowed to dry for 24 h. The dried Baobab fibres were subjected to size reduction by grinding using local milling machine.

The block diagram for the process summarizes step by step procedure in the production of the reinforced composite. The Flowchart for Baobab pod fibre CNC/LDPE composite production is represented by Figure 3.1.

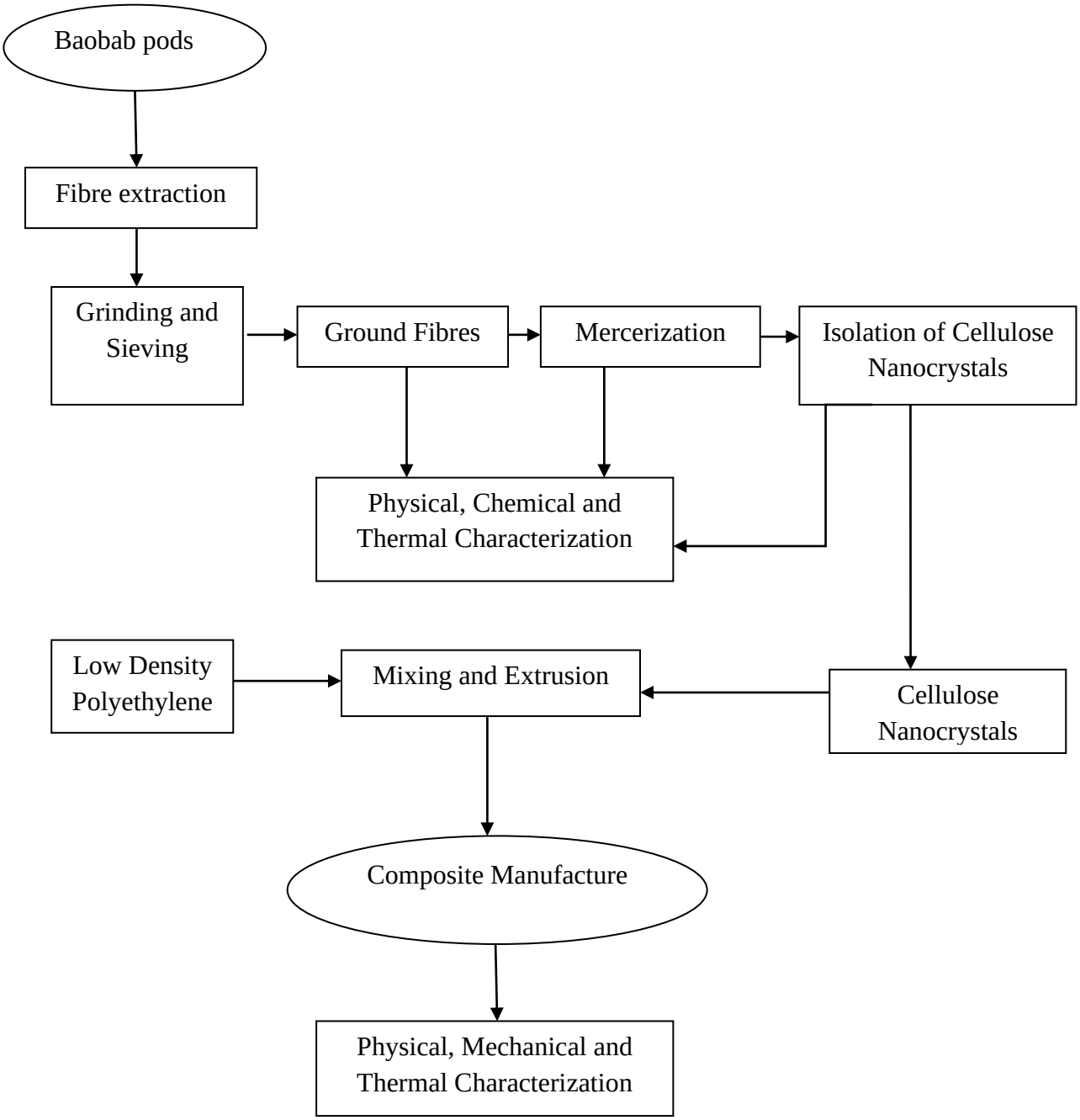

Figure 3.1: Flowchart for Baobab pod fibre CNC/LDPE composite production

3.4 Characterization of Baobab Pod Fibres (BPFs)

In order to fully comprehend the behaviour of Baobab pod fibres and to have a good understanding of its properties, different physical, thermal, chemical and mechanical tests were carried out. These include diameter measurement, density measurement, proximate analysis, ultimate analysis, chemical analysis, tensile test, water absorption measurements,

Fourier Transform Infra-red (FTIR) analysis, Scanning Electron Microscopy/Energy dispersive X-ray spectroscopy (SEM/EDS), X-ray Diffraction (XRD) analysis and Thermogravimetric Analysis (TGA).

3.4.1 Length and diameter measurement

Single fibre measurement was achieved using a ruler. Twelve fibres were chosen at random and their individual lengths were measured and recorded, mean average was then taken. The length obtained was 50 ± 0.2 mm.

The diameter of the Baobab pod fibre was determined using a micrometer screw gauge. Twelve fibres were chosen at random and diameter measurements were obtained for the different fibres after which the mean average was taken. The average diameter obtained was 0.28 ± 0.02 mm.

3.4.2 Density measurement of BPFs

The density (ρ) in g/cm^3 of the fibre was obtained using Equation 3.1:

$$\rho = \frac{m}{v} \tag{3.1}$$

ρ = density

m = the mass of the ground BPFs measured using the weighing scale

v = the volume of the samples measured

The sample was weighed using a weighing balance, then volume was measured by displacement of the amount of water when sample was inserted in measuring cylinder containing known amount of distilled water at 23 °C. Density was then calculated. The mass

of the ground BPFs was measured using the weighing scale; the volume of the samples was measured using a pycnometer.

3.4.3 Proximate analysis of BPFs

Proximate analysis is a method of partitioning of the compounds in the fibre. This system consist of the analytical determination of water (moisture) content, ash content, volatile content and fixed carbon content. The methods of the analysis are thus:

3.4.3.1 Moisture content

Each sample of mass 10 g were measured and placed in the porcelain separately. The porcelain and its content were then dried in an oven at 110 ˚C to a constant weight for 3 h. The moisture content was calculated using Equation 3.2

$$\% \text{ Moisture content} = \frac{(g-x)}{g} \times 100 \qquad (3.2)$$

Where,

g = weight of sample

x = weight of dry matter

(g – x) = loss in weight

3.4.3.2 Ash content

The total ash content equals the weight of the ash divided by the weight of the original sample multiplied by 100 %. The formula is given in equation 3.3

$$\% \text{ Ash} = \left(\frac{X}{g}\right) \times 100 \qquad (3.3)$$

Where,

g = weight of sample

x = weight of ash

3.4.3.3 Volatile matter

The volatile matter of the fibre is calculated using Equation 3.4:

$$\% \text{ Volatile matter} = \left(\frac{x-y}{g}\right) \times 100 \quad (3.4)$$

Where,

x = weight of sample

y = weight of dry matter

g = weight of residue

3.4.3.4 Fixed carbon

The percentage of fixed carbon was determined using Equation 3.5:

$$\% \text{ fixed carbon} = 100 - (\text{VM} + \text{Ash} + \text{MC}) \quad (3.5)$$

Where,

VM = Volatile matter

Ash = Ash content

MC = Moisture content

3.4.4 Elemental analysis of BPFs

The elemental analysis simply refers to the chemical contents of the fibre; it gives the carbon content, hydrogen content, nitrogen content and oxygen content. The formula used for determining the constituent of the ultimate analysis is according to (Jenkins *et al*., 2008)

3.4.4.1 Carbon content

The non aqueous titration method was used for this analysis. The carbon content was determined using Equation 3.6

$$\% \text{ Carbon} = \frac{(B-T) \times M \times 0.003 \times 100 \times 1.33}{g} \quad (3.6)$$

Where,

B = Blank titre

T= S ample titre

M = Molarity of the acid used

g = weight of sample

3.4.4.2 Hydrogen content

The non aqueous titration method was used for the determination of hydrogen content of the fibre sample. The hydrogen content was determined using Equation 3.7

$$\% \text{ Hydrogen} = \frac{wt\ of\ H_2O \times 0.1119 \times 100}{wt\ of\ pellet} \quad (3.7)$$

3.4.4.3 Nitrogen content

The non aqueous titration method was also used for this analysis. The Nitrogen content was determined using Equation 3.8

$$\% \text{ Nitrogen} = \frac{T \times M \times 0.014 \times DF}{g} \times 100 \quad (3.8)$$

Where,

M = Molarity of the acid used

g = Weight of sample

T = Titre value

DF = Dillusion factor diluted

3.4.4.4 Oxygen content

The total amount of all substances including ash content subtracted from 100% gives the percentage of Oxygen present in the sample. The Oxygen content was determined using Equation 3.9

$$\% \text{ Oxygen} = 100 - (C + H + N + S + \%Ash) \quad (3.9)$$

3.4.5 Determination of chemical composition of BPFs

The determination of chemical composition (cellulose, hemicellulose, and lignin contents) of Baobab pod fibres (BPFs) before and after treatment was achieved by acid digestion using a Fibre Analyzer. The standard acid detergent fibre (ADF), neutral detergent fibre (NDF) and acid detergent lignin (ADL) analysis were carried out using Ankom 200 Method 5, Method 6

and Method 8, respectively. 0.5 g of ground fibres was used for each analysis. The percentages of cellulose, hemicellulose and lignin content were determined from the following Equations 3.10 – 3.12

Lignin (% dry matter) = ADL (3.10)

Cellulose (% dry matter) = ADF – ADL (3.11)

Hemicellulose (% dry matter) = NDF – ADF (3.12)

3.4.6 Tensile strength test

Tensile properties of raw Baobab pod fibres were determined using a universal testing machine. Treated and untreated single Baobab fibres were tensile tested according to the ASTM D3379 standard test for Tensile strength (TS) and young Modulus of Elasticity (MOE) for high-modulus single filament materials. The machine was set at a crosshead speed of 1 mm/min and fibre length of 50 mm, diameter of 19.16 mm, area of 958 mm^2, displacement of 1.69 mm and a force of 776 MPa was used.

3.4.7 Water absorption of BPFs

The purpose of this test was to determine the water absorption capacity of dry Baobab pod fibres when immersed in water. ASTM D5229 was used, baobab pod fibres were dried in the in the sun for three days and the weight was determined using a weighing scale, the fibres were then immersed in distilled water at room temperature for 4 h and weighed immediately recorded. The water content of the fibres (in wt. %) was computed using Equation 3.13

$$\% \text{ absorption} = \frac{W_2 - W_1}{W_1} \times 100 \quad (3.13)$$

W_1 = weight of dried Baobab pod fibres

W_2 = weight of Baobab pod fibres immersed in distilled water

3.4.8 SEM/EDX analysis

Scanning electron microscopy (SEM) machine model Hitachi S3000N VP was used. Prior to SEM measurements, the samples were coated with a gold layer using an Edwards sputter coater model Pirani 50 I.

3.4.9 FTIR analysis

The surface chemistry of natural fibres can be altered by chemical treatments; these changes are investigated by using Fourier Transform Infrared (FTIR). It identifies the different functional groups present in the fibres before and after chemical treatments. Shift in the spectre and the complete disappearance of some functional groups helps in detecting the changes that happens during chemical treatments. The effect of NaOH treatment on the chemical structure of Baobab pod fibres was analysed using Shidmazu/IRTracer-100. The FTIR spectra with percentage transmittance (%T) versus wavelength (cm^{-1}) were recorded within the scanning range of 650 - 4000 cm^{-1}.

3.4.10 XRD Analysis

X-ray diffraction measurement of BPFs was carried out using a PANalytical Empyrean X-ray diffractometer with a C_o target, rotating stage and goniometer in 2θ configuration. The wavelength of C_o radiation is 0.179 nm. The generator was utilized at 40 kV and 45 mA. The intensities were measured from 5^o to 110^o at 2θ with step size of 0.0167° and a scan speed of 0.015 deg/sec. The radiation used was full spectrum Co ($K\alpha_1$, $K\alpha_2$) with the K_β filtered out with a diffracted side Fe filter. The empirical Equation (3.14) was used to estimate the degree of crystallinity (crystallinity index, CI) of ground Baobab pod fibres from the XRD results.

$$I_{Cr} = \frac{I_{002} - I_{am}}{I_{002}} \times 100 \qquad (3.14)$$

Where

I_{002} is the maximum intensity of the 002 lattice reflection (the highest peak for native cellulose) of the cellulose crystallographic form at $2\theta = 22.5°$

I_{am} is the intensity of diffraction of the amorphous material at $2\theta = 18.5°$ (Mwaikambo and Ansell, 1999).

The average crystallite particle size was determined from the XRD patterns of the CNC using Scherer equation represented by Equation 3.15

$$D = \frac{k\,\lambda}{\beta cos\theta} \tag{3.15}$$

Where

D = the particle size diameter

β = the full width at half maximum

λ = the wave length of X-ray

θ = the diffraction angle and

K = the Scherer constant.

3.5 Design of Experiment

3.5.1 Optimization of NaOH treatment conditions of BPFs using RSM

Design-Expert software was used to analyze the experimental data and to establish the design matrix. Numerical and graphical optimization techniques were used and the responses are single fibre tensile strength (TS) and modulus of elasticity (MOE). NaOH concentration (A), soaking time (B), and soaking temperature (C) were selected (based on pilot experiments) to describe this system with reasonable ranges as follows:

$$5\ \% \leq \text{NaOH concentration (A)} \leq 10\ \%$$

$$20\ ℃ \leq \text{temperature (C)} \leq 90\ ℃$$

In this study, the test was based on a three-factor three-level Box–Behnken design, as presented in Table 3.2. An RSM was applied to the experimental data using Design-Expert software V10; polynomial equation was fitted to the experimental data to obtain the regression equation for the TS and MOE. The statistical significance of the terms in the equations was examined using the sequential F-test, lack-of-fit test, and other adequacy measures using the same software to obtain the best fit.

Table 3.2: NaOH treatment conditions for Baobab pod fibres

		Factor 1	Factor 2	Factor 3	Response 1	Response 2
Std	Run	A:NaOH Conc. %	B:Soaking Time min	C:Soaking Temp ℃	Tensile Strength MPa	Young Modulus MPa
17	1	6	240	67.5		
3	2	2	360	67.5		
16	3	6	240	67.5		
12	4	6	360	100		
7	5	2	240	100		
4	6	10	360	67.5		
11	7	6	120	100		
14	8	6	240	67.5		
15	9	6	240	67.5		
2	10	10	120	67.5		
1	11	2	120	67.5		
6	12	10	240	35		
13	13	6	240	67.5		
9	14	6	120	35		
8	15	10	240	100		
10	16	6	360	35		
5	17	2	240	35		

3.6 Pilot Experiment for Chemical Treatments of BPFs

Mercerization method of fibre treatment was adopted for the purpose of this study; analytical grade NaOH was used. Different concentrations of aqueous NaOH were prepared (2 %, 6%, and 10 % by weight) by dissolving NaOH pellets in distilled water. Ground BPFs were then immersed into the solution and heated at 67.5 ˚C for 240 min with a solution to fibre ratio of 40 cm^3 to 1 g. Plate III shows the colour of the sodium hydroxide solution before and after chemical treatments of ground BPFs. After the immersion, the fibres were washed thoroughly with tap water and subsequently with distilled water to get a neutral pH and to ensure no NaOH was left in the fibres. Subsequently, the fibres were dried at 60 ℃ for 24 h. Plate IV shows an image of the treated fibres. The reaction of sodium hydroxide with cellulose is as follows:

$$Cell - OH + NaOH \rightarrow Cell - O^{-}Na^{+} + H_2O + [surface\ impurities]$$

The quantity of NaOH used in terms of percentage was calculated thus;

1Molar of NaOH must be dissolved in 1000 cm^3 of water (1liter) and as

1M NaOH = (Na =23 g, O = 16 g, H = 1g)

$\Rightarrow$ (23 g + 16 g +1 g = 40 g)

That is, 40 g of NaOH to be dissolved in 1liter.

In term of percentage: (40 g/1000 g) × 100 = 4 % NaOH.

That is, 3 % of NaOH =30 g, 5 % NaOH = 50 g and 10 % NaOH =100 g.

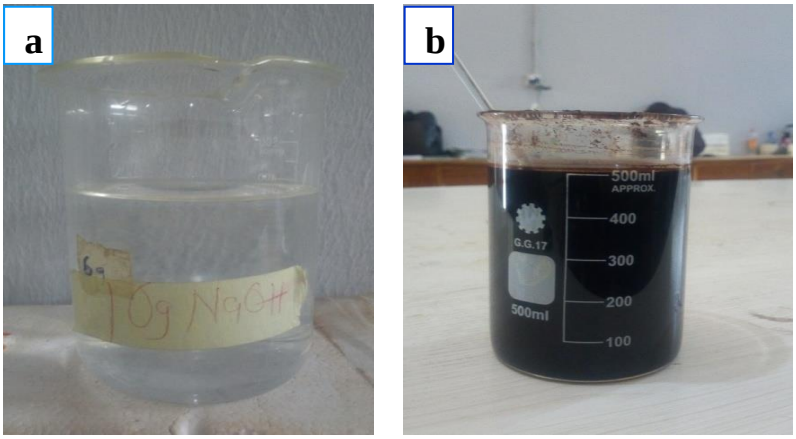

Plate III: Images of Sodium hydroxide solution (a) before and (b) after treatment

Plate IV: Treated Baobab Pod Fibres

3.7 Isolation of Cellulose Nanocrystals from BPFs

Three stages were involved in the isolation of cellulose nanocrystals from Baobab pod fibres, these includes sodium hydroxide treatment, bleaching with sodium chlorite and acid hydrolysis using a mixture of nitric and acetic acid.

3.7.1 Bleaching with Sodium chlorite ($NaClO_2$)

Sodium chlorite ($NaClO_2$) method was used for the bleaching of Baobab pod fibre, it is an excellent bleaching agent which helps in the removal of lignin and produces holocellulose (cellulose + hemicellulose). 1.8 w/v% $NaClO_2$ was prepared in a 500 cm^3 beaker and Baobab pod fibres were immersed into the solution and heated for 4 h at 70 ℃. The fibres were then washed with water and finally with distilled water, the fibres were then dried in an oven for 2 h at 50 ℃. Initially, the Baobab pod fibres were dark brownish in colour due to the presence of hemicellulose, lignin, extractives such as wax and pectin but after bleaching, the colour changes due to the removal of lignin and extractives as can be seen in the image represented in Plate V.

Plate V: Image of BPFs, after bleaching with sodium chlorite ($NaClO_2$)

3.7.2 Acid Hydrolysis

A formulation of 60 % Nitric acid (HNO_3) and 40 % acetic acid mixture was used for the isolation of cellulose. 7 g of bleached BPFs were placed in a conical flask. 160 cm^3 of 40 % acetic acid and 240 cm^3, 60 % of nitric acid (w/w) were added and the flask was then closed

using a cork. It was then placed on a heating mantel at a temperature of 83 °C (boiling point of Nitric acid) for 40 min. The flask was then removed from the heating mantel and cooled before 70 cm^3 distilled water was added. It was filtered and repeatedly washed with distilled water and ethanol to remove nitric acid. The residue was dried in an oven at 60 °C. The experimental set-up for the process is shown in the image represented in Plate VI.

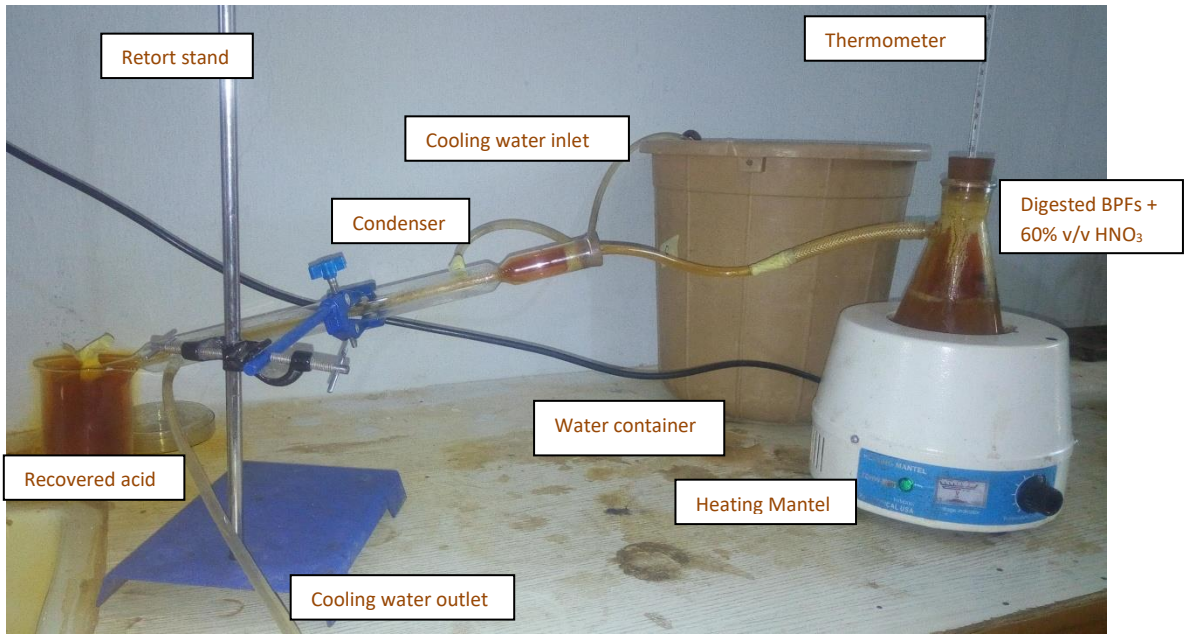

Plate VI: Experimental set-up for the isolation of CNC from BPFs

3.7.3 Centrifugation

A centrifuge was used to wash the hydrolysed cellulose five times; the centrifugation took place at 1000 rpm, 10 min and 10 ℃. the products were then neutralized to a pH of 7 using NaOH.

3.8 Production of BPFs Reinforced Low Density Polyethylene Composites

From the Acid Hydrolysis process, 100 g of Cellulose Nanocrystals (CNC) was produced from treated Baobab Pod Fibres (BPFs). Table 3.3 presents the formulation used for the production of the composites:

Table 3.3: Formulation for the Production of Baobab CNC/LDPE Composites

Formulation (%)	Code Name	Low density polyethylene (%)	(g)	BPFs Cellulose Nanocrystals (%)	(g)
100	Control	100	100	0	0
90:10	A	90	90	10	10
80:20	B	80	80	20	20
70:30	C	70	70	30	30
60:40	D	60	60	40	40

3.8.1 Two roll machine and process of mixture

The two-roll mill machine was heated to a temperature of 150 ^{o}C for 30 min, which is the melting temperature of low density polyethylene. The Baobab pod fibres cellulose nanocrystals were mixed with low density polyethylene by a way of compounding using two-roll. 90 wt% of LDPE were poured into the preheated two-roll mill to melt the LDPE for 5 min, followed by gradual pouring of 10 wt% Baobab pod fibres CNC into the melted LDPE and a complete mixing of the fibre with the matrix was achieved. Finally, the compounded Baobab/LDPE was scraped from the mill and sheet was formed.

The resulting compounded sheet was pressed using a compression moulding machine. At the start, the compounded Baobab pod fibres CNC/LDPE sheet scraped from the two role mill was introduced into a rectangular mould of 100 mm × 120 mm × 3 mm (Plate VII)

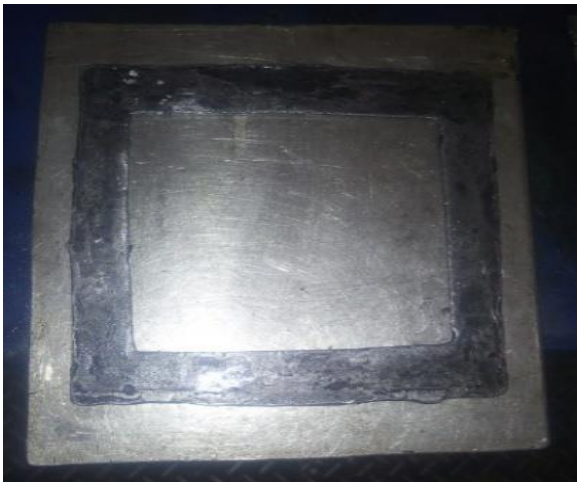

Plate VII: Image of Rectangular Mould

The compression moulding machine was heated for 30 min at the set temperature of 150 ^{o}C. After which the compounded sample was placed inside a rectangular mould. The arrange mould coated with aluminium foil paper and taken into the preheated compression mould machine. The hydraulic press was held under a pressure of 10 KN for a period of 6 min. Thereafter, the sample was removed from the press and allowed to cool before removing the composite sample from the mould.

The procedure was repeated for 20 wt%, 30 wt%, 40 wt% and 0 wt% of Baobab pod fibre CNC with the corresponding 80 wt%, 70 wt% , 60 wt% and 100 wt% matrices of low density polyethylene (LDPE).

3.9 Characterization of BPFs Nanocellulose Reinforced LDPE Composites

3.9.1 Density measurement

Standard method of test for density ASTM D 1475 was used; samples measuring 12.5 mm × 12.5 mm × 3.2 mm were used for density measurement. Equipment used were, Mettler Analytical weigh Balance and 50 cm^3 measuring cylinder with 10 mL distilled water inside for displacement. The specimen was weighed using a weighing balance, then volume was

measured by displacement of the amount of water when sample was inserted in measuring cylinder containing known amount of distilled water at 23 °C. Density is then calculated using Equation 3.15:

Density, kg/m^3 = (mass of sample / volume of sample) (3.15)

3.9.2 Tensile test of composites

The tensile test was conducted according to ASTM D638 using the Instron universal testing machine. The dimensions, gauge length and cross-head speeds are chosen according to the ASTM D638 standard. Sample was placed in grips of the universal testing machine at a specified grip separation and pulled until failure. An extensormeter is used to determine the elongation and tensile modulus. A drawing representing the specimen for tensile test is shown in Figure 3.2.

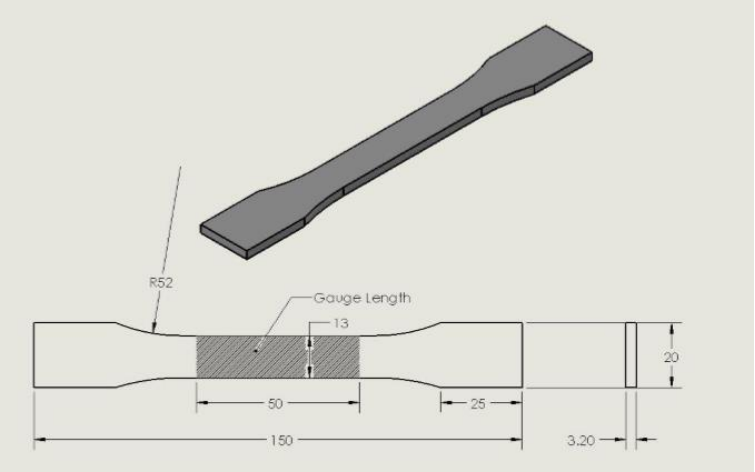

Figure 3.2: Dumb-bell shaped specimen for tensile test

3.9.3 Flexural test of Composites

Flexural strength was measured under a three-point bending approach using a universal testing machine according to ASTM D790 as shown in Plate VIII. Samples measuring 127 mm × 12.7 mm × 3.2 mm were tested at a crosshead speed of 4 mm/min.

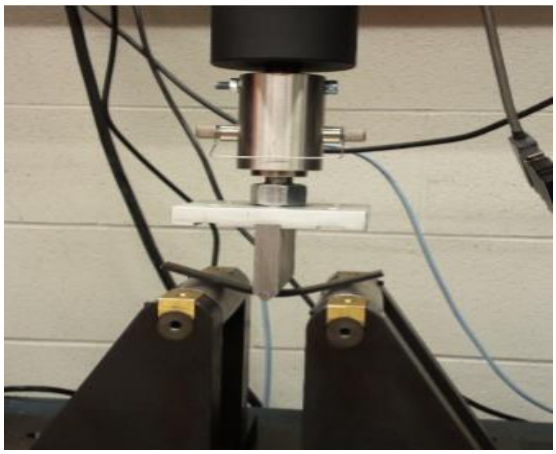

Plate VIII: A picture showing a typical flexural test on a sample

3.9.4 Charpy Impact test of composites

The impact test was conducted according to ASTM D256 using the charpy V-notch impact testing machine. The dimensions, gauge length and V-notch were chosen according to the standard. The specimen was placed between a special holder with the notch oriented vertically and towards the origin of impact. The specimen as represented by Figure 3.3 was struck by a "tup" attached to a swinging pendulum. The specimen breaks at its notched cross-section upon impact, and the upward swing of the pendulum was used to determine the amount of energy absorbed in the process.

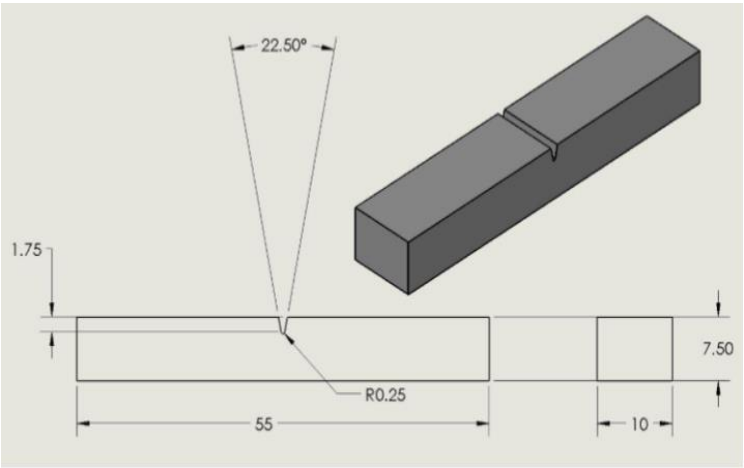

Figure 3.3: Charpy impact test sample

3.9.5 Vickers hardness test of composites

The Vickers hardness (HV) test method involves indenting the composites materials with a diamond indenter in the form of a right pyramid with a square base and an angle of 136° between opposite faces subjected to a load of 70 kgf for 10 s. The two diagonals of the indentation left in the surface of the composite material after removal of the load were measured using a microscope and their average was calculated. The Vickers hardness is the quotient obtained by dividing the kgf load by the square mm area of indentation.

$$HV = 1.854 \frac{F}{d^2} \tag{3.16}$$

F = Load in kgf

D = arithmetic mean of the two diagonals, d_1 and d_2 in mm

3.9.6 Water absorption of composites

The water absorption behaviour of the formed composites was determined by immersing samples measuring 20 mm (length) x 25 mm (thickness) x 3 mm (width) in distilled water at room temperature. Apparatus used were: An analytical balance capable of reading 0.0001 g and an Oven, capable of maintaining uniform temperatures of 50 to 63 ℃ and of 105 to 110 ℃. Samples were weighed before immersing in distilled water at room temperature following ASTM D 570-98 standard. At a regular time, interval (every 24 h), the samples were removed, and the surface moisture was wiped, and then weighed. This process was repeated until the samples reached their saturation limit. The percentage water absorbed was determined using Equation 3.17

$$M_t = \frac{W_{t-W_0}}{W_0} \tag{3.17}$$

Where,

W_0 = the dry weight of the BPFs

W_t = the weight of the BPFs after specific time t.

3.9.7 Thermal analysis of composite

To determine the thermal stability and decomposition pattern of Baobab fibre isolated cellulose, thermogravimetric analysis (TGA), was performed in an SDT Q600 instrument. For each measurement, approximately 5 mg of the sample was used. Patterns were recorded under a nitrogen atmosphere at a flow rate of 100 mL / min by heating the material from room temperature to 500 °C at a heating rate of 20 °C/min.

CHAPTER FOUR

4.0 RES ULTS AND DISCUSSION

4.1 Physical Behaviour of Raw BPFs

In order to fully comprehend the characteristics of Baobab pod fibres, some important physical characteristics were analyzed. Table 4.1 summarized the properties that were determined. Average length of the fibre obtained was 50.42 mm which indicates it is a short fibre when compared to that of other plants like, flax fibres which length is of up to 90 cm, ramie fibres with length range of up to 100 cm and sisal fibres with average length of up to 1 meter. Baobab fibres has a very low density of 0.65 g/cm^3 when compared to that of ramie, flax and hemp fibres, all with densities of 1.5 g/cm^3 (Pickring *et al.*, 2016). Plate VI (a) shows the images of Baobab pod fibres after extraction from the pod. The ground fibres were then sieved as shown in Plate IX (b), in order to ensure equal distribution of the fibres.

Plate IX: The Images of (a) Raw Baobab Pod fibres (b) Ground Baobab pod fibres

Table 4.1: Comparison of physical properties of BPFs with other natural fibres

Fibre	Length (mm)	Diameter (mm)	Density (g/cm^3)	Tensile strength (MPa)	Elongation (%)	Reference
BPFs	50.42	0.28	0.65	40.15	1.7	This study
Coir	134	0.86	0.9	13.05	2.1	Ayyavoo *et al.*, 2013
Polyester	600	1.77	1.3	67.8	2.3	Azzedine *et al.*, 2013
Flax	900	1.85	1.5	143	3.4	Pickring *et al.*, 2016
Raffia	140	1.63	1.5	67.7	2.5	Fadele, 2017
Sisal	1000	-	1.5	379	4.7	Kabir *et al*., 2012

The mean average for the tensile strength was obtained to be 40.17MPa, variance was obtained to be 0.33 and standard deviation was obtained as 0.57. The fibre exhibited better tensile property when compared to other short fibres of similar length like that obtained for coir at 13.05 MPa.

4.1.1 Proximate analysis of raw BPFs

The result for the proximate analysis of raw Baobab pod fibres is shown in Table 4.2. The moisture content of the fibre has a great effect on performance of composites, the higher the moisture content, the more detrimental it is to the performance of composites, it reduces stiffness and flexural strength. Moisture content of 9.4 % for BPFs is considered good as compared to other natural fibres. The proximate analysis of the BPFs reveals that, the fixed carbon 71.9 % which is the major component and the remaining composition is volatile content and ash amounting to about 18.4 %. Amount of ash content have direct correlation with the flexural properties, fixed carbon and volatile matter which indicates the amount of inorganic substituent in the carbon. High ash content is not suitable because adsorption capacity of fibre will be reduced. The low moisture content and low ash content of the BPFs makes it an excellent candidate for polymer reinforcement. Proximate and mineral

composition of the pod fibres as presented indicates that Baobab pods fibres could be a good candidate for polymer composite production.

Table 4.2: Proximate analysis of Raw, Treated and CNC

Description	Moisture (%)	Ash (%)	Volatile Content (%)	Fixed Carbon (%)
Raw BPFs	9.4	8.3	9.1	71.9
Treated BPFs	6.7	2.1	8.4	82.8
CNC	4.8	1.2	5.4	89.8

4.1.2 Ultimate analysis of raw BPFs, treated and CNC

The value of elemental carbon was consistent with that of the fixed carbon in the proximate analysis. Table 4.3 summarizes the results for the ultimate analysis, it can be seen that the sample consist predominantly of carbon greater than 60 % which indicates a good percentage of cellulose present in the fibre.

Table 4.3: Ultimate analysis of Raw, Treated and CNC

Description	Carbon (%)	Hydrogen (%)	Nitrogen (%)	Oxygen (%)
Raw BPFs	63.6	0.51	16.3	19.6
Treated BPFs	79.2	0.21	8.6	11.9
CNC	88.6	-	4.7	6.7

Baobab fibres constitute elements that make it an excellent candidate for composite production. Table 4.4 presents a comparison of the elemental composition of Baobab fibres with some natural fibres.

Table 4.4: Comparison of elemental composition of BPFs with other Natural fibres

Fibres	C	H	N	O	Moisture	Ash	Volatile	Reference
BPFs	64	0.5	16	20	9.4	8.3	9.1	This study
Raffia	78.2	2.1	8.4	11.6	7.3	2.4	6.4	Fadele, 2017
Rice husk	82	1.2	13	4.4	9.1	32	23	Rohan *et al*., 2018
Marshmallow	70.2	-	3.4	8.2	-	-	-	Mehmet *et al*., 2014
Aloe Vera	23	9	45	5.6	32	-	57	Saurabh, 2016
Corn husk	67	2,1	8.8	4.2	5,7	25	34	Kambli *et al.,* 2017

The cellulose nanocrystals isolated from Baobab pod fibres also exhibit excellent properties in comparison to that obtained from other fibre as shown in Table 4.5. Increased carbon and nitrogen content gives a good tendency of proper adhesion between fibre and matrix.

Table 4.5: Comparison of elemental composition of Baobab CNC with CNC from other Natural fibres

CNC	C	H	N	O	Moisture	Ash	Volatile	Reference
BPFs	88.6	-	11	6.7	4.8	1.2	4.5	This study
Raffia	78.2	2.1	8.4	11.6	7.3	2.4	6.4	Fadele, 2017
jackfruit	67.8	1.5	6.8	10.7	8.8	0.9	12.3	Costa *et al*., 2019
Flax	64.9	-	3.7	8.5	8.2	4.5	9.7	Russo *et al*., 2020
Pineapple	46.8	-	5.8	4.2	8.8	4.5	6.4	Zwawi, 2021
Bagasse	41.	-	32	12.4	12.3	15.7	3.1	Aliotta *et al*., 2020

4.2 Chemical Composition of Baobab Pod Fibres

The chemical composition of natural fibres constitutes mainly of cellulose, hemicellulose, lignin and other impurities. The high percentage in cellulose increases the tendency of proper adhesion between natural fibres and the reinforcing material. Raw Baobab pod fibres have 53.2 % of cellulose which is higher than that of other short fibres like Bamboo fibres, Coir

fibres, flax and corn husk as indicated in Table 4.6 This increases its potentiality for reinforcement with synthetic materials.

Table 4.6: Comparison of chemical properties of BPFs with other Natural fibres

Fibres	Cellulose (%)	Hemicellulose (%)	Lignin (%)	Pectin (%)	Waxes (%)	Reference
Baobab	53.2	15.7	26.1	3.7	1.3	This study
jackfruit	20.08	24.4	1.85	52.18	-	Anteneh *et al*., 2020
Coir	53.6	22.5	2.6	15.3	-	Adesina *et al*,2019
Corn husk	43.4	23.8	21.1	-	1.1	Kambli., 2017
Raffia	50.1	11.7	22.3	15.8	6.1	Fadele, 2017
Flax	33.4	22.3	21.5	16.9	-	Zhu 2013

4.2.1 Chemical composition of BPFs, treated and CNC

Table 4.7 gives the chemical composition of raw Baobab pod fibres. Alkaline treatment increases the cellulose content of natural fibres and reduces lignin and other impurities contained in the fibres.

Table 4.7: Chemical Composition of Raw, Treated and CNC of Baobab Fibres.

Description	Cellulose	Hemicellulose	Lignin	Pectin	Waxes
Raw BPFs	53.20	15.70	26.10	3.70	1.30
Treated BPFs	71.10	11.20	14.50	2.30	0.90
CNC	75.73	20.54	2.71	0.92	0.30

Raw Baobab pod fibres nanocellulose has 75.73 % of cellulose which is higher than that of Kenaf fibres with 31-39 %, Coir fibres with 41 % and Bamboo with 43 % (Bledzki *et al.*, 1999). This increases its potentiality for reinforcement with synthetic materials. Table 4.8 present the comparison of the chemical composition of Baobab cellulose nanocrystals with other natural fibres.

Table 4.8: Comparison of chemical properties of Baobab CNC with other fibre CNCs

CNC	Cellulose (%)	Hemicellulose (%)	Lignin (%)	Pectin (%)	Reference
Baobab	75.73	20.54	2.71	0.92	This study
Bamboo	43	30	31	-	Damfeu *et al.*, 2016
Coir	41	0.25	40	12	Anteneh *et al*., 2021
Wheat	45	31	20	-	Anteneh *et al.*, 2021
Kapok	35	32	22	8	Farid *et al*., 2021
Sisal	65	12	9.9	4	Faruk *et al*., 2017

4.3 Optimization of NaOH Treatment Conditions of BPFs using RSM

4.3.1 Mechanical behaviour of NaOH treated BPFs

Chemical treatments are required to enhance the fibre matrix interfacial strength and to minimize moisture absorption by these fibres which improves their mechanical properties. . Table 4.9 shows the responses of the treated Baobab Pod Fibres

Table 4.9: Responses of Treated BPFs using BBD

		Factor 1	Factor 2	Factor 3	Response 1	Response 2
Std	Run	A:NaOH Conc. %	B:Soaking Time min	C:Soaking Temp ℃	Tensile Strength MPa	Young Modulus MPa
17	1	6	240	67.5	43.6	23.04
3	2	2	360	67.5	31.1	19.32
16	3	6	240	67.5	42.9	22.11
12	4	6	360	100	44.1	30.69
7	5	2	240	100	24.2	20.4
4	6	10	360	67.5	39.6	24.34
11	7	6	120	100	41.5	25.28
14	8	6	240	67.5	42.7	22.51
15	9	6	240	67.5	43.3	21.87
2	10	10	120	67.5	37.3	20.01
1	11	2	120	67.5	26.6	15.43
6	12	10	240	35	21.2	19.46
13	13	6	240	67.5	42.9	22.02
9	14	6	120	35	26.7	21.46
8	15	10	240	100	44.2	22.44
10	16	6	360	35	31.9	21.87
5	17	2	240	35	20.2	12.39

Table 4.10 presents the analysis of variance for Tensile strength response surface quadratic model.

Table 4.10: Tensile Strength ANOVA for Response Surface Quadratic model

Analysis of variance table [Partial sum of squares - Type III]

Source	Sum of Squares	df	Mean Square	F Value	p-value Prob> F	
Model	1247.68	9	138.63	917.22	< 0.0001	significant
A-NaOH Conc	202.01	1	202.01	1336.52	< 0.0001	
B-Soaking Time	26.65	1	26.65	176.29	< 0.0001	
C-Soaking Temp	364.50	1	364.50	2411.63	< 0.0001	
AB	1.21	1	1.21	8.01	0.0254	
AC	90.25	1	90.25	597.12	< 0.0001	
BC	1.69	1	1.69	11.18	0.0124	
A^2	342.19	1	342.19	2264.02	< 0.0001	
B^2	0.73	1	0.73	4.80	0.0646	
C^2	184.25	1	184.25	1219.01	< 0.0001	
Residual	1.06	7	0.15			
Lack of Fit	0.53	3	0.18	1.34	0.3800	not significant
Pure Error	0.53	4	0.13			
Cor Total	1248.74	16				

The Model F-value of 917.22 implies the model is significant. There is only a 0.01% chance that an F-value this large could occur due to noise. Values of "Prob> F" less than 0.0500 indicate model terms are significant. In this case A, B, C, AB, AC, BC, A^2, C^2 are significant model terms. Values greater than 0.1000 indicate the model terms are not significant. If there are many insignificant model terms (not counting those required to support hierarchy), model reduction may improve your model. The "Lack of Fit F-value" of 1.34 implies the Lack of Fit is not significant relative to the pure error. There is a 38.00%

chance that a "Lack of Fit F-value" this large could occur due to noise. Non-significant lack of fit is good -- we want the model to fit.

Table 4.11: Standard Deviation in Terms of Coded Factors for TS

Std. Dev.	0.39	R-Squared	0.9992
Mean	35.53	Adj R-Squared	0.9981
C.V. %	1.09	Pred R-Squared	0.9925
PRESS	9.30	Adeq Precision	78.981
-2 Log Likelihood	1.04	BIC	29.37
		AICc	57.70

The "Pred R-Squared" of 0.9925 is in reasonable agreement with the "Adj R-Squared" of 0.9981; i.e. the difference is less than 0.2. "Adeq Precision" measures the signal to noise ratio. A ratio greater than 4 is desirable. The ratio of 78.981 indicates an adequate signal. This model can be used to navigate the design space.

Final Equation in Terms of Coded Factors:

$$TS = +43.08 + 5.03A + 1.83B + 6.75C + 0.55AB + 4.75AC - 0.65BC - 9.02A^2 - 0.42B^2 - 6.61C^2 \quad (4.1)$$

Table 4.12 : Young Modulus ANOVA for Response Surface Quadratic model

Analysis of variance table [Partial sum of squares - Type III]

Source	Sum of Squares	df	Mean Square	F Value	p-value Prob> F	
Model	242.16	9	26.91	95.08	< 0.0001	significant
A-NaOH Conc	43.76	1	43.76	154.63	< 0.0001	
B-Soaking Time	24.64	1	24.64	87.07	< 0.0001	
C-Soaking Temp	69.80	1	69.80	246.64	< 0.0001	
AB	0.048	1	0.048	0.17	0.6916	
AC	6.33	1	6.33	22.35	0.0021	
BC	6.25	1	6.25	22.09	0.0022	

A^2	79.44	1	79.44	280.73	< 0.0001	
B^2	13.78	1	13.78	48.68	0.0002	
C^2	2.10	1	2.10	7.42	0.0296	
Residual	1.98	7	0.28			
Lack of Fit	1.09	3	0.36	1.63	0.3163	not significant
Pure Error	0.89	4	0.22			
Cor Total	244.14	16				

The Model F-value of 95.08 implies the model is significant. There is only a 0.01% chance that an F-value this large could occur due to noise. Values of "Prob> F" less than 0.0500 indicate model terms are significant. In this case A, B, C, AC, BC, A^2, B^2, C^2 are significant model terms. Values greater than 0.1000 indicate the model terms are not significant. If there are many insignificant model terms (not counting those required to support hierarchy), model reduction may improve your model. The "Lack of Fit F-value" of 1.63 implies the Lack of Fit is not significant relative to the pure error. There is a 31.63% chance that a "Lack of Fit F-value" this large could occur due to noise. Non-significant lack of fit is good -- we want the model to fit.

Table 4.13: Standard Deviation in Terms of Coded Factors YM

Std. Dev.	0.53	R-Squared	0.9919
Mean	21.45	Adj R-Squared	0.9815
C.V. %	2.48	Pred R-Squared	0.9228
PRESS	18.84	Adeq Precision	45.738
-2 Log Likelihood	11.70	BIC	40.03
		AICc	68.37

The "Pred R-Squared" of 0.9228 is in reasonable agreement with the "Adj R-Squared" of 0.9815; i.e. the difference is less than 0.2. "Adeq Precision" measures the signal to noise

ratio. A ratio greater than 4 is desirable. The ratio of 45.738 indicates an adequate signal. This model can be used to navigate the design space.

$$YM = +22.31 + 2.34A + 1.75B + 2.95C + 0.11AB - 1.26AC + 1.25BC - 4.34A^2 + 1.81B^2 + 0.71C^2 \quad (4.2)$$

Table 4.14 gives the optimization solution for the alkali treatment of Baobab pod fibres; this solution predicts the best conditions for the treatment which is further validated through experimentation. The desirability of unity (1) throughout confirms the accuracy of the optimization solution.

Table 4.14: RSM Solution for optimization of chemical treatment of BPFs

Number	NaOH Conc.	Soaking Time	Soaking Temp	Tensile Strength	Young Modulus	Desirability	
1	6.112	359.291	99.788	44.27	30.738	1	
2	6.654	359.915	99.014	45.429	30.694	1	
3	6.618	357.738	99.752	45.228	30.699	1	
4	6.239	359.394	99.714	44.552	30.757	1	
5	6.827	359.226	99.775	45.538	30.764	1	
6	6.859	359.957	99.946	45.551	30.828	1	
7	6.963	359.963	99.763	45.716	30.778	1	Selected
8	6.147	359.908	99.951	44.311	30.808	1	
9	6.891	357.619	99.987	45.581	30.7	1	
10	6.369	358.572	99.747	44.798	30.735	1	

4.3.2 3D Interactions between variables for Young Modulus

The 3D plots shows the effect of interaction among the variables; Soaking temperature, Soaking time and NaOH concentration and Figure 4.1 show the interaction of the variables for Young Modulus,. The interaction between soaking time and NOH concentration shows increase in young modulus from 15 to 27 Pa. the interaction between soaking temperature shows increase from 20 to 27 Pa and then decrease to 21 Pa, that between soaking time and soaking temperature shows increase from 24 to 31 Pa and then decrease to 22 Pa.

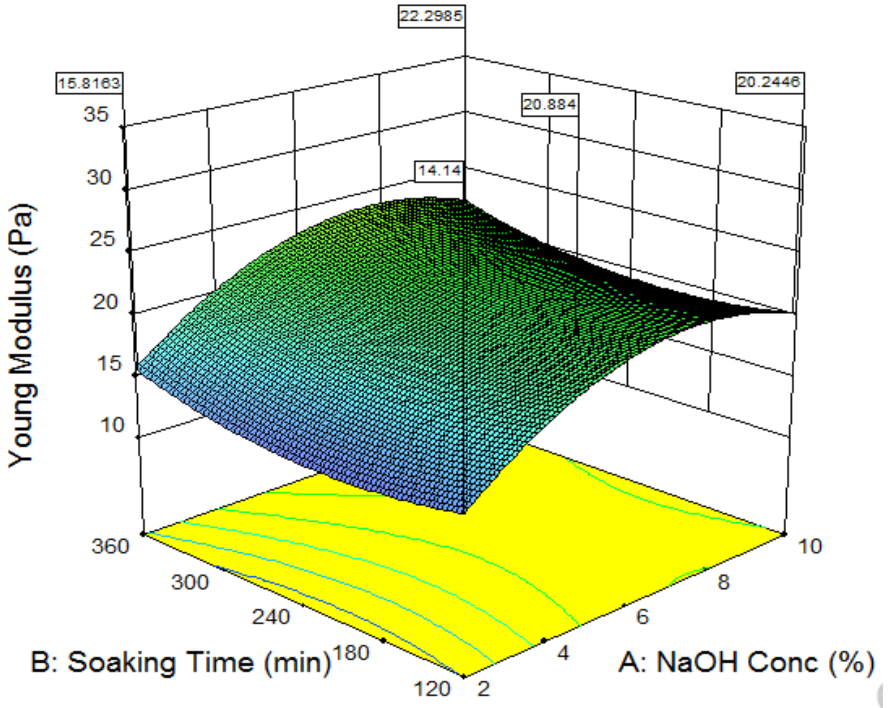

Figure 4.1: 3D Interaction between soaking time and NaOH Concentration for YM

Figure 4.2 shows the 3D Interaction between Soaking temp and NaOH Concentration for Young modulus and figure 4.3 shows 3D Interaction between soaking temp and soaking time for young modulus

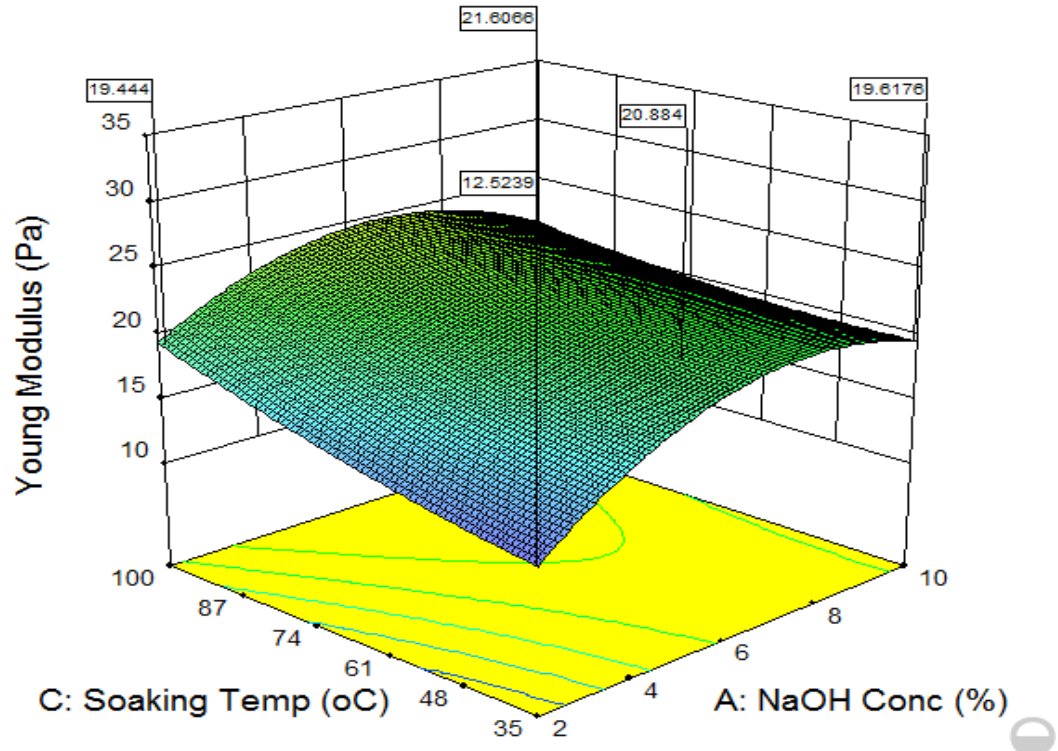

Figure 4.2: 3D Interaction between Soaking temperature and NaOH Concentration for YM

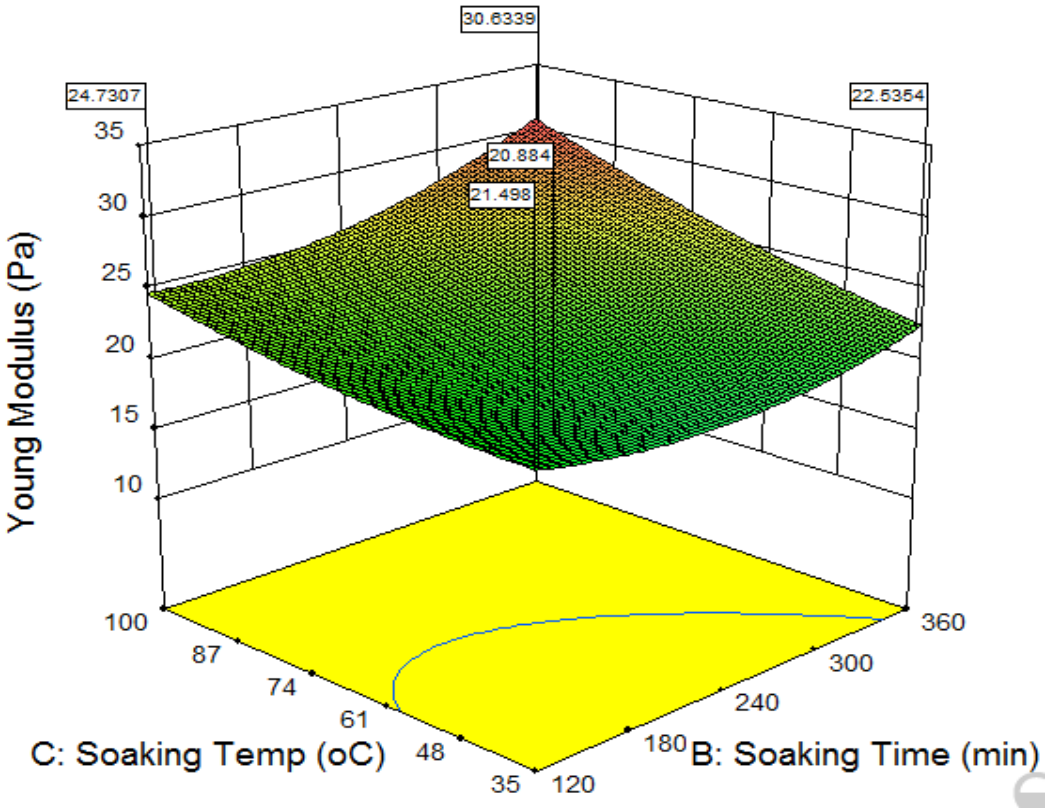

Figure 4.3: 3D Interaction between soaking temperature and soaking time for YM

4.3.3 3D Interactions between variables for Tensile Strength

The 3D plots shows the effect of interaction among the variables; soaking temperature, soaking time and NaOH concentration and Figure 4.4 show the interaction of the variables for Tensile Strength. Interaction between soaking time and NaOH concentration shows tensile strength increases from 27 to37 MPa while that of between soaking temperature and concentration increases from 24 to 45 MPa. Meanwhile, the interaction between soaking temperature and soaking time indicates decrease in tensile strength from 42 to 9 MPa.

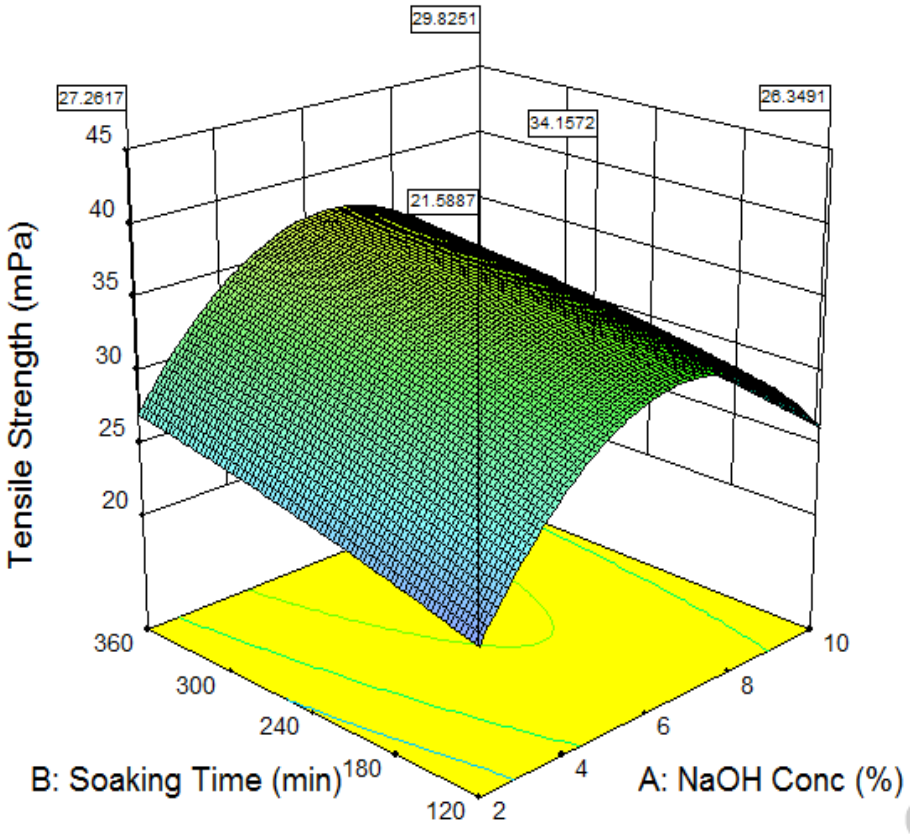

Figure 4.4: 3D Interaction between soaking time and NaOH Concentration for TS

Figure 4.5 shows the 3D Interaction between Soaking temp and NaOH Concentration for young modulus and Figure 4.6 shows 3D Interaction between soaking temp and soaking time for tensile strength.

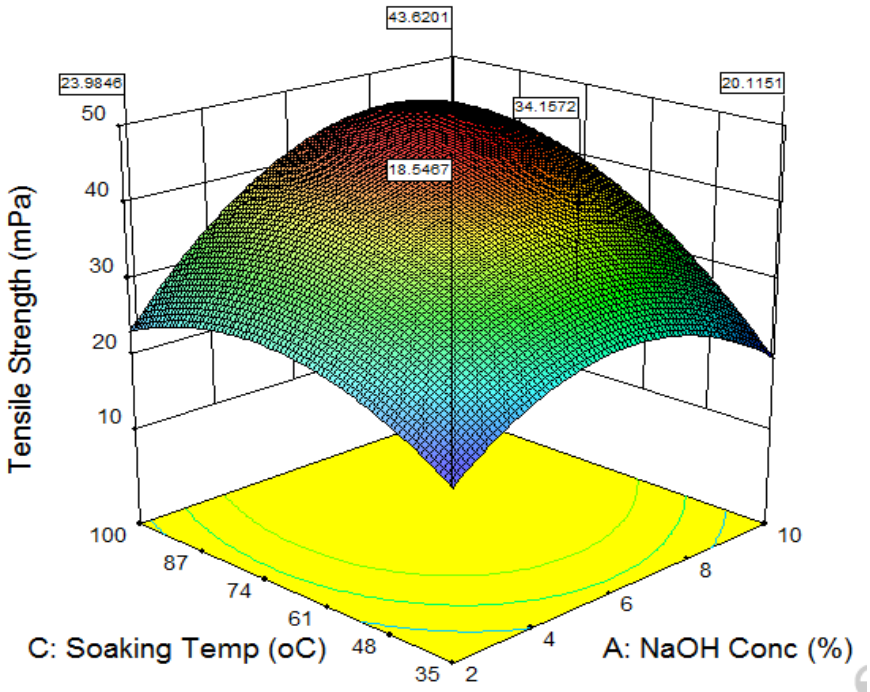

Figure 4.5: 3D Interaction between soaking temp .and NaOH Concentration for TS

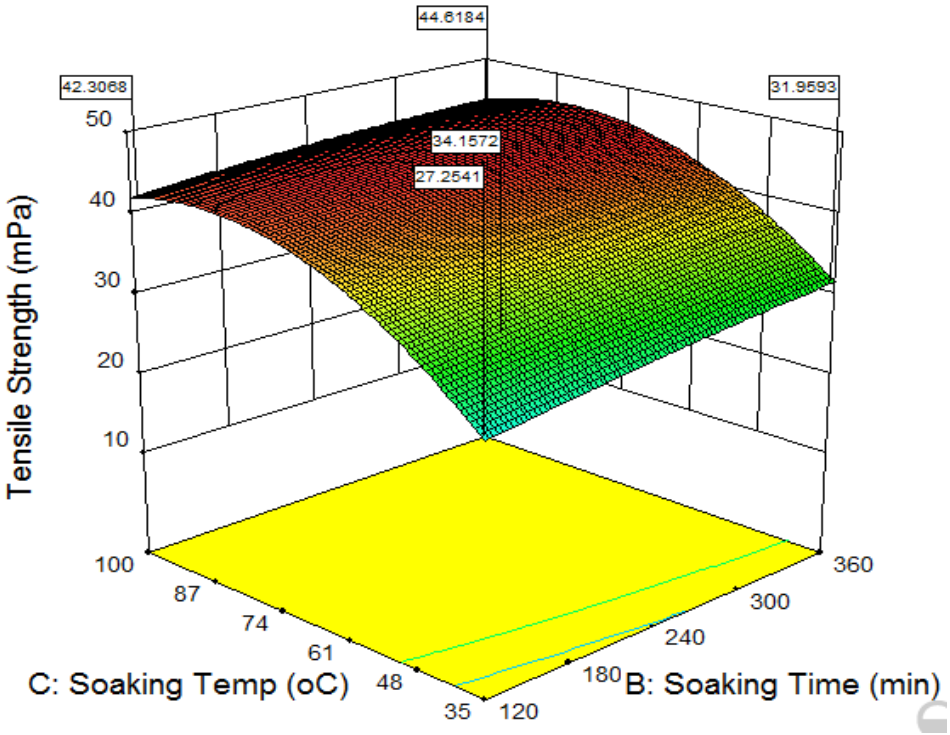

Figure 4.6: 3D Interaction between soaking temp and soaking time for TS

4.3.4 Validation of predicted model

In order to validate the optimization solution, the first and seventh predictions were taken and real experiments were carried out to determine the authenticity of the model. The percentage error for both TS and YM was obtained by subtracting the predicted results from the actual. Table 4.15 shows the validation test results for both TS and YM.

Table 4.15: Validation of Predicted Results

Concentration (%)	Time (min)	Temp ^{o}C		TS (MPa)	YM (MPa)
			Actual	42.21	27.47
6.112	359.291	99.788	Predicted	44.27	30.738
			Error%	3.06	3.268
			Actual	43.78	28.66
6.963	359.963	99.763	Predicted	45.716	30.778
			Error%	1.936	2.118

4 .4 FTIR Analysis for Raw BPFs, Treated and CNC

The absorbance peaks of interest are clearly marked in the FTIR spectra in Figure 4.7. The peak at 891 cm-^{1} correspond to v(C−H) stretching, which indicates the presence of hemi-cellulose for raw untreated fibres (Himmelsbach *et al.,* 1998). The absorption peak at 1733 cm^{-1} is attributed to v(C=O) stretching of methyl ester and carboxylic acid in pectin.. The absorbance peak of natural fibres in the region of 1610 cm^{-1} indicates the presence of fatty acids (Chan *et al.,* 2013) and is attributed to v(C=C) stretching confirming the traces of oils. The untreated fibre spectra also exhibit weak absorption peak at 1378 cm^{-1}, which indicates the presence of lignin and is attributed to v(C=C) stretching (Mwaikambo *et al.,* 2002). The absence of peaks at 1413, 1533, 1726, 1244 cm^{-1} shows the absence of hemicellulose and

lignin in the alkaline treated fibres. Thus, the FTIR spectrum for CNC confirms the purity of cellulose and the absence of hemicellulose and lignin.

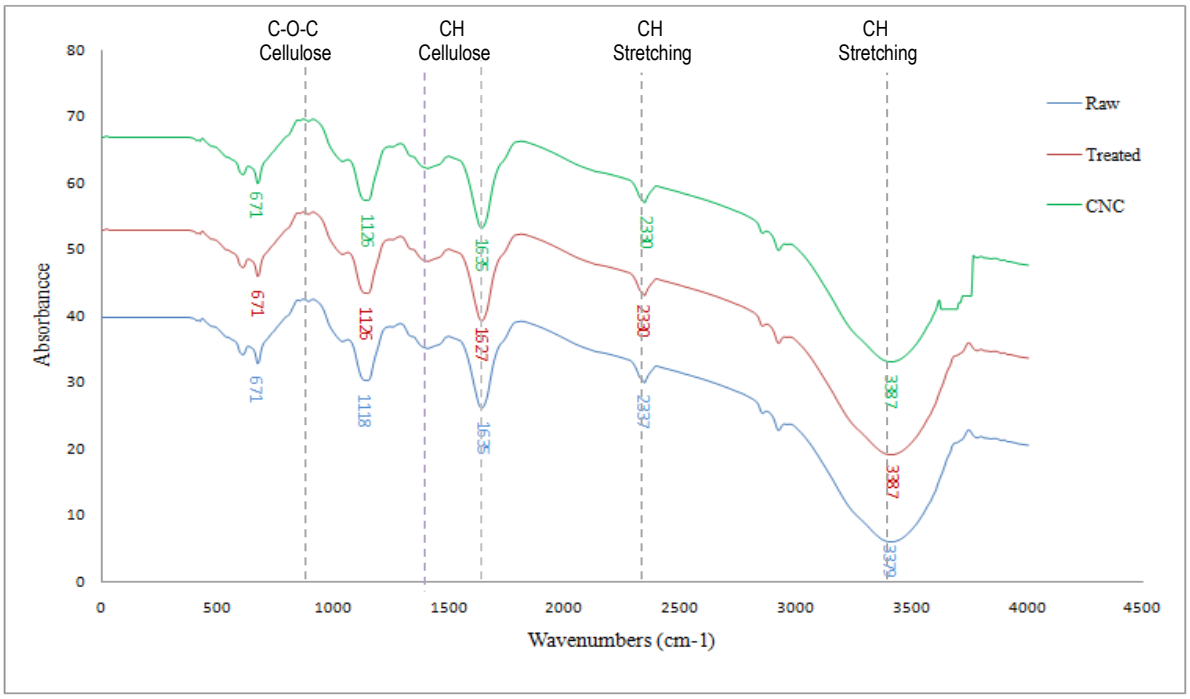

Figure 4.7: FTIR Spectrum for Raw, Treated and CNC BPFs

The FTIR spectrum of the CNC displayed absorption patterns corresponding to the specific functional groups of cellulose, and was also in good agreement with the reported cellulose by Shehu *et al* (2017). The peak at 1635 cm^{-1} was formed due to the bending mode of adsorbed water. The peak at 1118 cm^{-1} may be due to CH_2 bending vibration. The sharp transmittance peak around 1384 cm^{-1} represents a bending of OH groups. The peak at 1174 and 1120 cm^{-1} corresponds to C-O asymmetric bridge stretching.

4.5 Scanning Electron Microscopy (SEM) Analysis

In this study, a simple way to examine the raw (untreated), treated and isolated nano-crystalline cellulose of BPFs by conventional scanning electron microscopy (SEM) was investigated. The SEM indicates three distinct regions: an inner region (lumen), a middle

region (cortex) and an outer surface (epidermis). Between the outer surface and the inner core, there are radial pathways, which probably serve as conduits for water/moisture exchange between the core of the fibre and the environment.

4.5.1 Energy dispersive spectroscopy (EDS) analysis

EDS analysis was carried out to determine the stereochemistry elemental composition of the raw, treated and cellulose nanocrystals of the BPFs. The EDX spectra indicate that the fibre samples were composed of mainly Carbon and Oxygen and some traces of sulphur and Calcium. Theoretically, expected Stoichiometric mass percent of Carbon and Oxygen are well above 80 % and 20 % respectively. Table 4.16 depicts the Stoichiometric mass of elements of Baobab pod fibres.

Table 4.16: Stoichiometric mass of elements of Baobab fibres

Element	Raw Baobab (wt %)	Treated Baobab fibres (wt %)	Cellulose nanocrystals (wt %)
C	69.43	67.47	59.16
O	29.73	31.72	39.04
Mg	0.08	-	0.19
S	0.06	0.12	0.28
K	0.57	-	-
Ca	0.12	0.7	1.32

4.5.2 SEM for raw baobab pod fibres

The SEM/EDS shows the enlarge view of the inner region of an untreated BPFs. Baobab fibre is a bundle of fibre made up of several elementary fibre having its own lumen located at the inner region.. The middle lamella shown at a higher magnification in Figure 4.8 (a) sticks the elementary fibres together and they comprises of lignin and hemicellulose. Figure 4.8 (b) shows cracks and voids in the fibres.

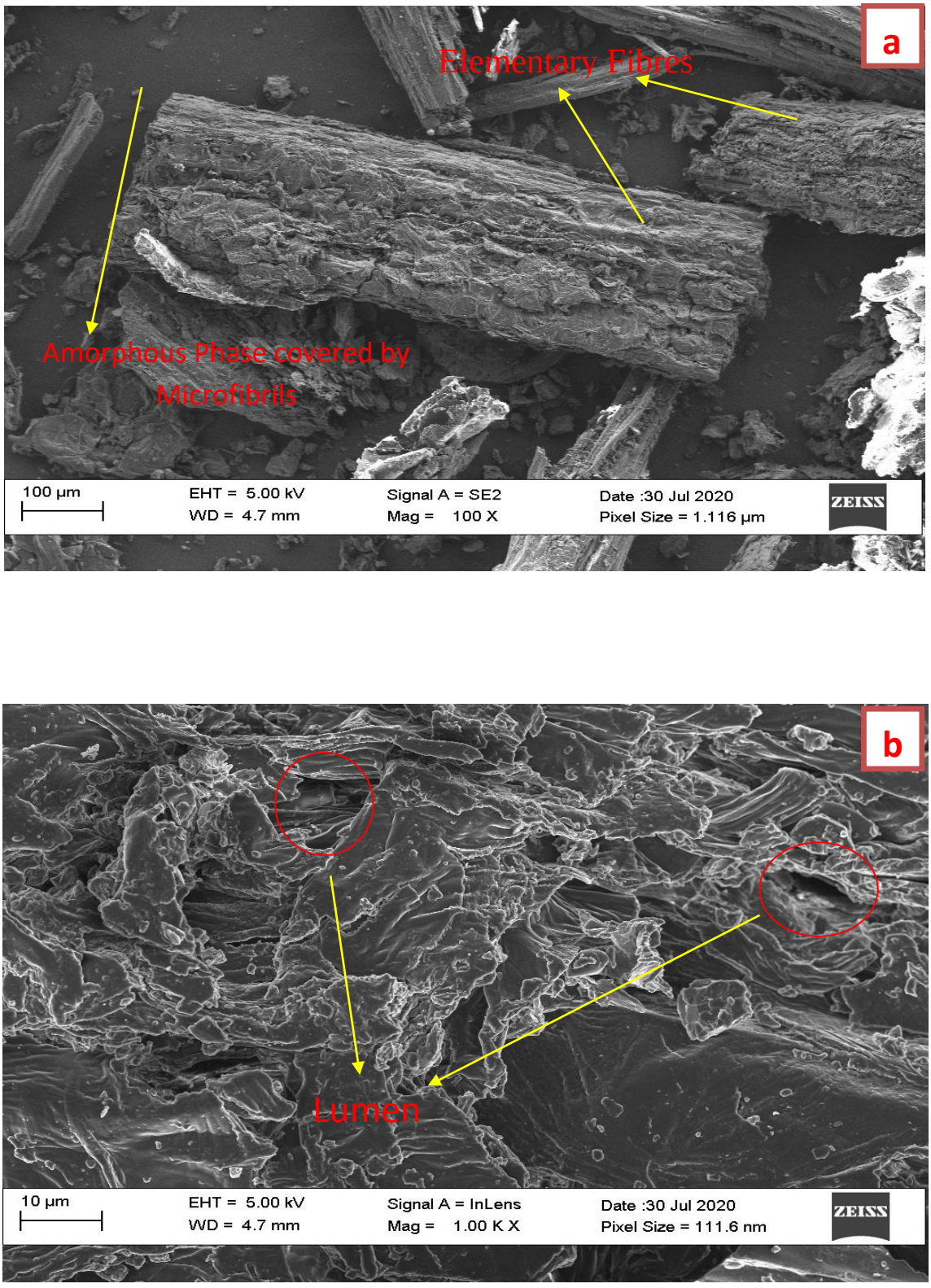

Figure 4.8: SEM Spectrum for Raw BPFs

The cross-sectional structure of BPF is similar to the reported structure of several natural fibres like, Rafia (Fadele, 2017), coir fibres (Tran *et al.*, 2015) and sisal fibre (Ernestina *et*

al., 2013). The surface morphology of the raw Baobab Fibre and microfibrils cellulose consisted of an amorphous phase of lignin and hemicelluloses covering the cellulose microfibrils. Scanning electron micrographs of the raw fibres shows the presence of longitudinal cracks on the surface of the fibres. Such type of cracks has been reported to affect the fracture behaviour of natural fibres (Chiga carasco *et al*., 2011).

4.5.3 SEM for alkali treated BPFs

The chemical treatment leads to significant changes in the fibre surface morphology. The surfaces of alkali treated BPFs appear to be much cleaner than those of raw fibres as shown in Figures. 4.9 (a and b). This indicates that Sodium Hydroxide removed oil, wax and other impurities from the surfaces of the fibres. The use of chemical treatment on natural fibres results in the removal of non-cellulose components and also resulted in changes in both thermal properties and surface chemistry of natural fibres. The removal of these materials is expected to promote strong bonding between the fibre and the polymer matrix when used in composite manufacture (Kabir *et al*, 2012).

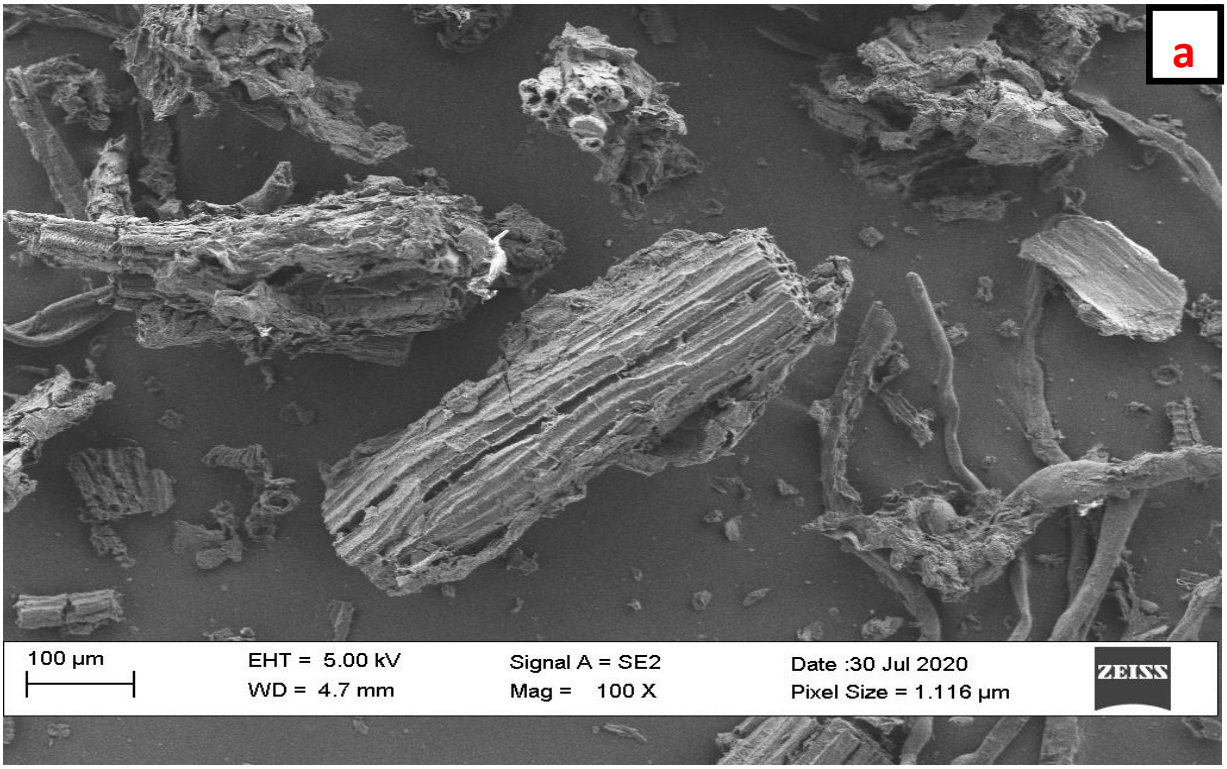

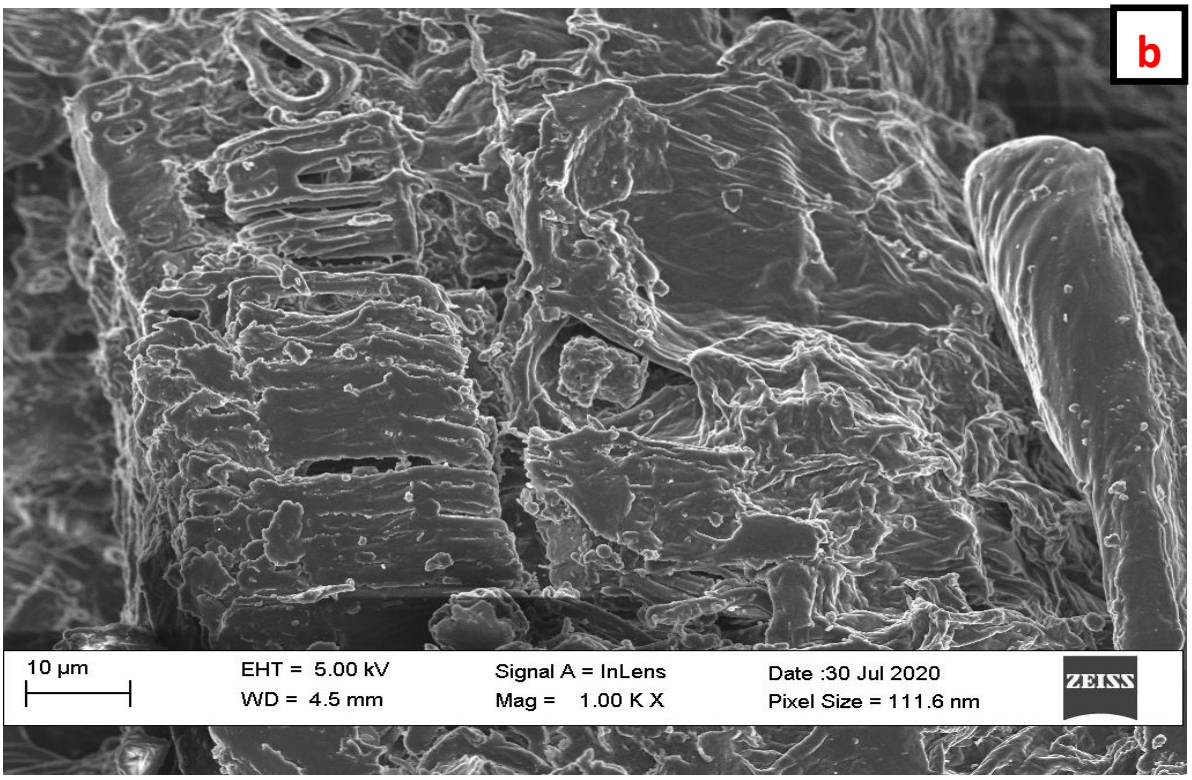

Figure 4.9: SEM Spectrum for treated BPFs

The lignin and hemicelluloses dissolved in the chemical solutions during treatment, leading to fibrillation of the cellulose microfibers as shown in Figure 4.9 (b). The crystalline cellulose microfibrils networks were arranged in a disorderly manner.

4.5.4 SEM of baobab fibres nanocellulose

SEM was employed to analyze the structure of nanocrystals of the cellulose formed. The SEM images in Figure 4.10 indicate changes in morphology of the BPFs. The nanocrystals have tiny rod like shapes and some spherical in shape.

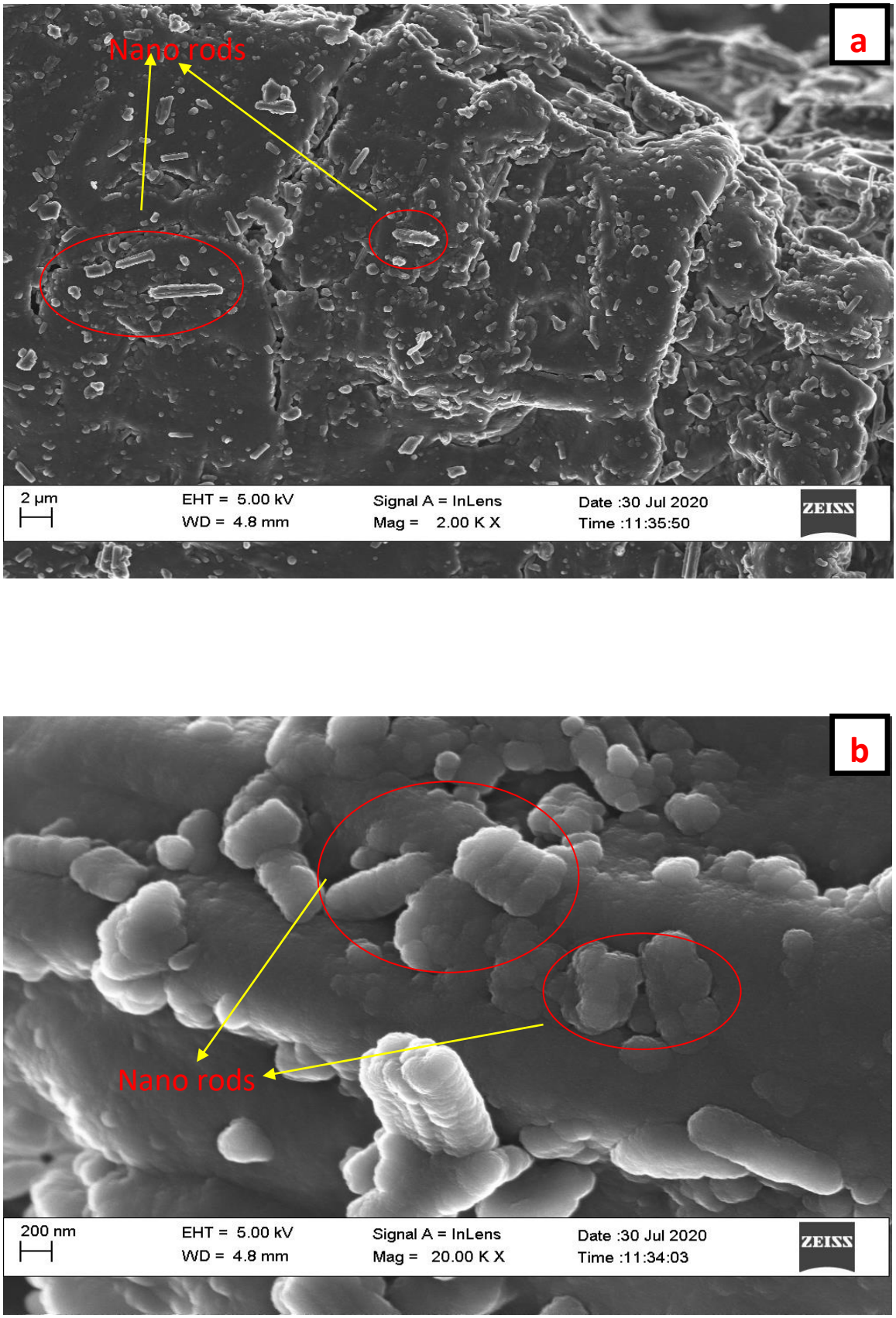

Figure 4.10: SEM Spectrum for Baobab fibre CNC

4.6 XRD Analysis of Raw, Treated and CNC

The XRD of raw Baobab pod fibres showed in Figure 4.11 shows peaks which are peculiar to natural fibres. Investigation of the crystalline structure of the Raw, Treated and CNC of the Fibre was done using X-ray Diffraction Analysis. The XRD patterns of the samples were recorded in the diffraction angle range 5.000° to 79.9850°. The sharp and strong diffraction peaks in the XRD patterns of the CNC confirm the high crystalline nature of the fibre. The spectrum also shows that the peak intensity increases as the samples are being modified.

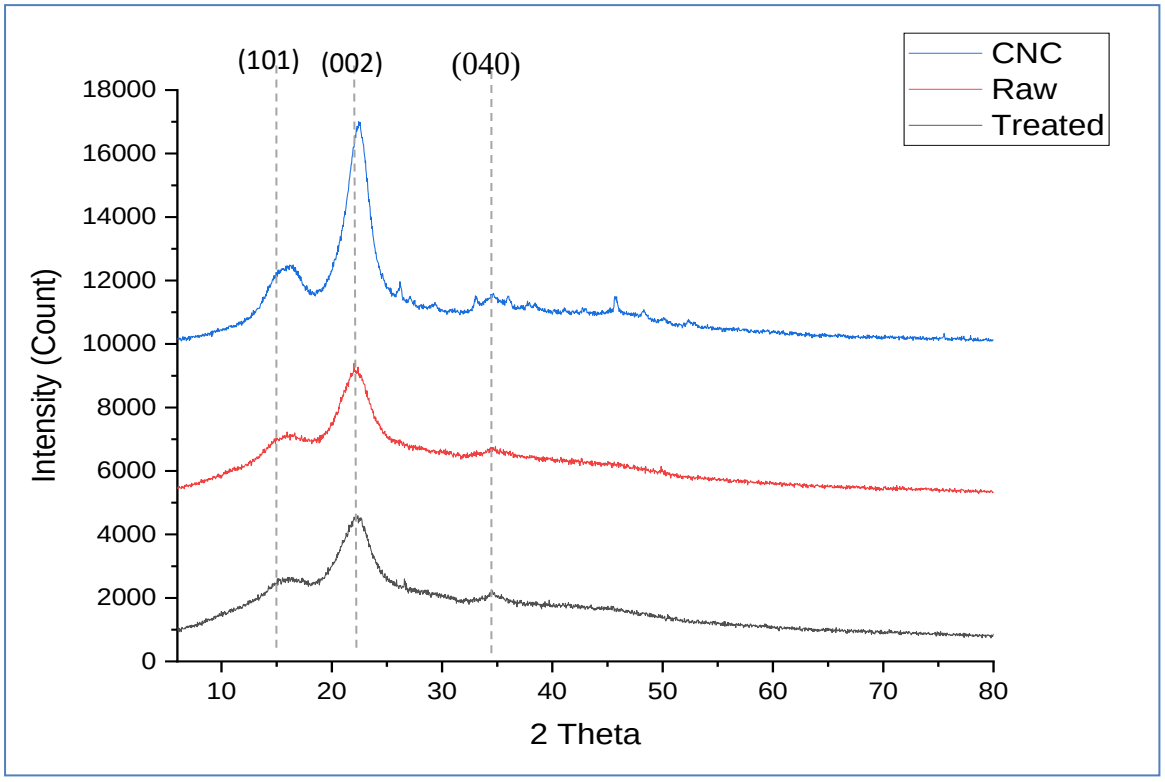

Figure 4.11: XRD Patterns of Raw, Treated and CNC of BPFs

The CNC exhibited a typical cellulose I pattern at a sharp peak of 2θ =22°. The diffraction peak at 22° corresponds to the 002 crystallographic plane of the cellulose I lattice. The crystallinity index (CrI) was calculated according to the Segal empirical method. Table 4.17 shows the crystallinity index for raw, treated and CNC.

Table 4.17: Crystallinity index of Raw, Treated and CNC BPFs

Fibre	I (002)	I_{am}	CrI (%)
Raw	2750	500	81
Treated	2400	400	83
CNC	5600	300	95

The Crystallinity index for the raw BPFs which is initially at 81% is higher than that reported by Elenga *et al*. (2009) of Wrighitia tinctoria seed fibres (49.2 %), ramie and (58 %). The percentage increased significantly after NaOH treatment and acid hydrolysis to about 95%. This increase shows the improvement in the cellulose structure of the fibre which in turn contributed to enhancing its tensile strength.

Crystallite size is also supportive of the description of crystallinity of the cellulose. From Equation (3.15), the crystal size of the isolated Baobab nano cellulose was found to be 3.003 nm as shown in Appendix E. Almost similar results were found with the cellulose jackfruit peel and brown seaweed as shown in Table 4.18.

Table 4.18: Comparison of crystallinity index and crystallite size with other CNCs

Cellulose nanocrystals (CNC)	CI (%)	CS (nm)	Reference
Baobab Fibres	95	3.03	This study
Jack fruit peel	83.42	2.80	Trilokesh and Kiran, 2019
Brown Seaweed	78.7	2.80	He *et al*., 2018
Popular wood chips	50	-	Ju *et al.*, 2015
Eucalyptus globulus	55.3	-	Carillo *et al*., 2018
Ni-Al_2O_3	-	41.50	Yerima *et al*., 2021

4.7 TGA/DTA Analysis of Raw, Treated and CNC

Thermal analysis of the untreated (raw), treated and Cellulose Nanocrystals of the Baobab pod fibres are carried out to further comprehend the thermal properties. The results are

presented in Figures 4.12 and 4.13. It showed that the thermal behaviour exhibited by the fibre is in line with those that are used in the production of polymeric composites. The curve for the Raw Fibre shows an endemic peak within the range of 110 ˚C to 140 ˚C, this can be attributed to evaporation of water. Exothermic peaks were observed at higher temperatures, which can be attributed to decomposition of hemicellulose and cellulose (Martins *et al.*, 2008). The plot showed that there was an overall increase in the amount of heat generated, Tg value, degradation temperature of hemicellulose and cellulose for the alkali treated and Cellulose Nanocrystals of Baobab Fibres. The TGA profile for the CNC presents the same thermal behaviour in agreement with reported studies (Kargarzade *et al.*, 2012). The weight loss below 140–180 ˚C could be attributed to water evaporation; similarly, two degradation stages were evident around 230 and 350 ˚C.

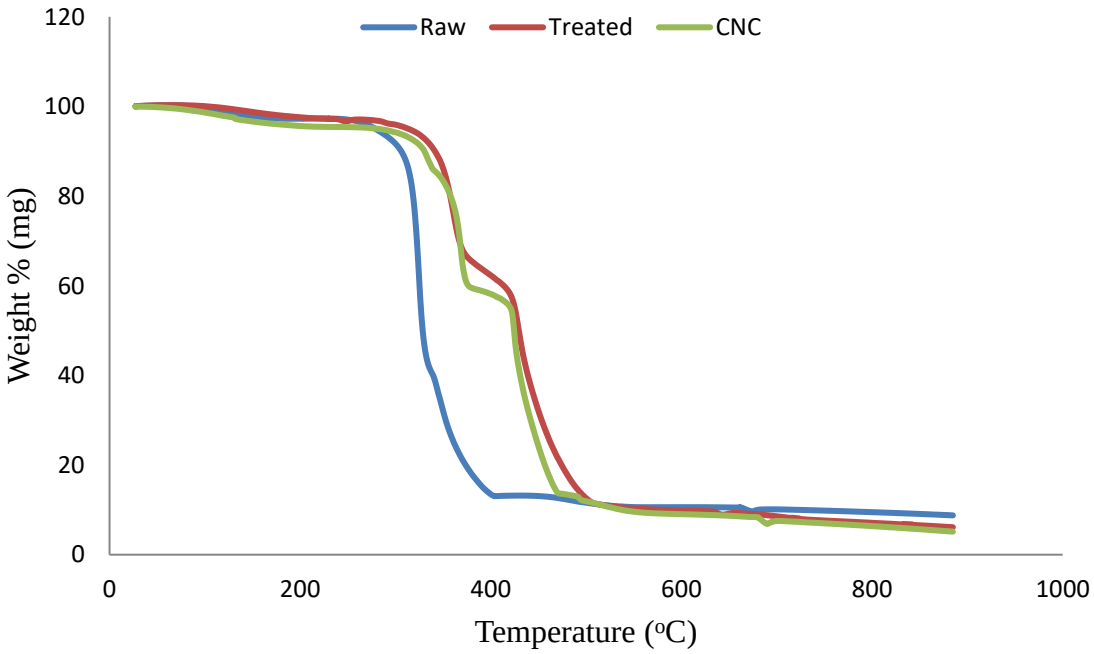

Figure 4.12: TGA for Raw, Treated and CNC BPFs

The point of maximum rate of thermal degradation (T_{max}) is found as the DTA peak associated with the steeper region of mass loss on the TGA curve. The results indicated that

the alkali treated fibre has a comparatively higher resistance to thermal degradation than the raw and the CNC has a higher resistance to thermal degradation than the treated fibre.

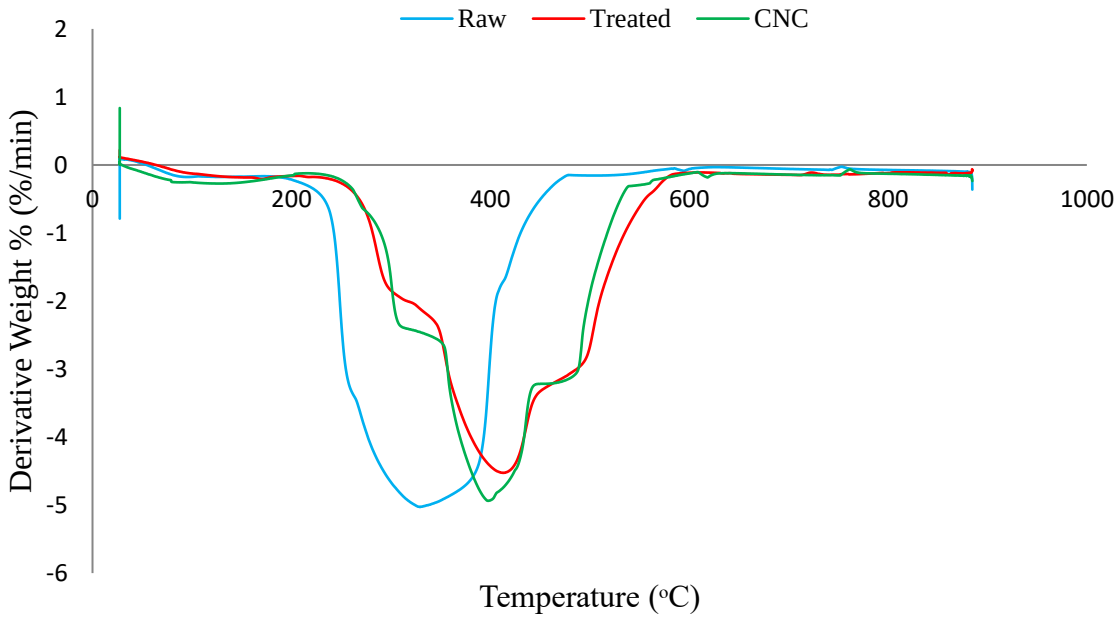

Figure 4.13: DTA for Raw, Treated and CNC BPFs

4.8 Characterization of Baobab CNC/LDPE Reinforced Polymer Composites

4.8.1 Effect of CNC loading on density of reinforced composites

Density is the mass per unit volume of a material. Density is especially relevant because plastic is sold on a cost per pound basis and a lower density means more material per pound or varied part weight. Figure 4.14 shows density of reinforced composite at varying cellulose loading. It can be seen from the results that the densities of the reinforced composites are higher than that of the virgin LDPE

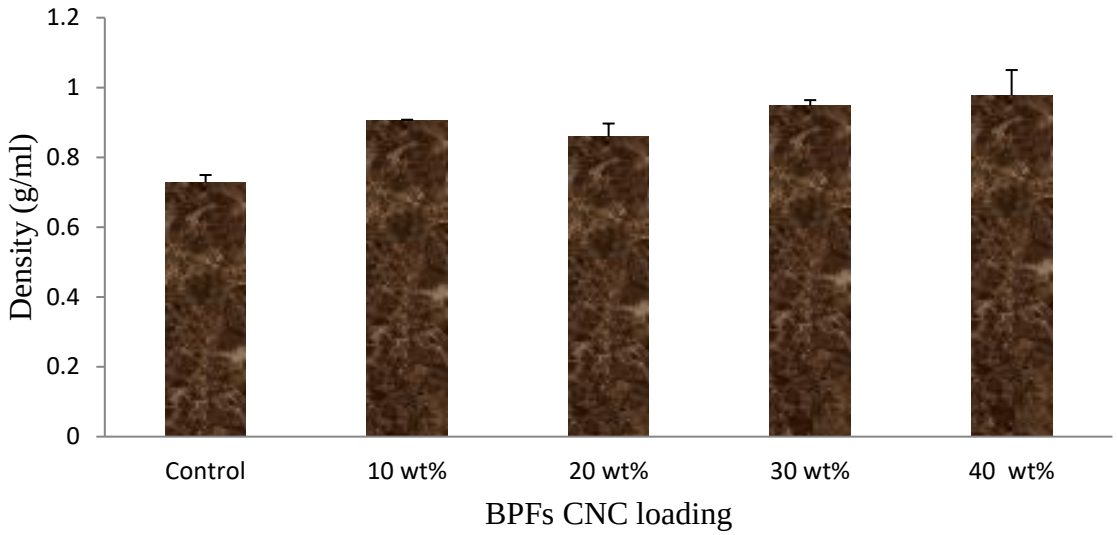

Figure 4.14: Density of Reinforced Composites at varying CNC loading

4.8.2 Water absorption properties of reinforced composites

This test method for rate of water absorption has two chief functions: first, as a guide to the proportion of water absorbed by a material and consequently, in those cases where the relationships between moisture and electrical or mechanical properties, dimensions, or appearance have been determined, as a guide to the effects of exposure to water or humid conditions on such properties and secondly, as a control test on the uniformity of a composite. Figure 4.15 shows the results of water absorption properties on varying CNC loading. The water absorption capacity of the fibres increased with increasing cellulose nanocrystals loading. Natural fibres are hydrophilic in nature and have that natural capacity to absorb water content which can make them to swell and deteriorate at a faster rate.

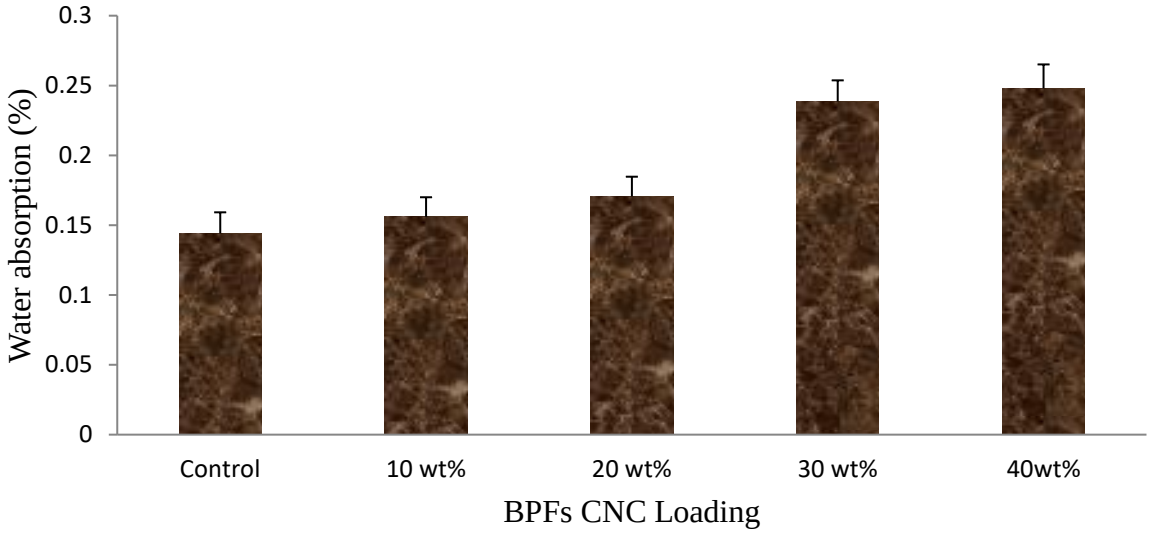

Figure 4.15: Water absorption properties of composites at varying CNC loading

4.8.3 Tensile properties of reinforced composites

Tensile strength is one of the most important properties of nanocellulose reinforced composites because it indicates the resistance of material to break under tension. Figure 4.16 shows the maximum tensile strength for the composites was 86 MPa for 30 wt % which is much higher than that of the virgin (unreinforced) composite which has 61 MPa.

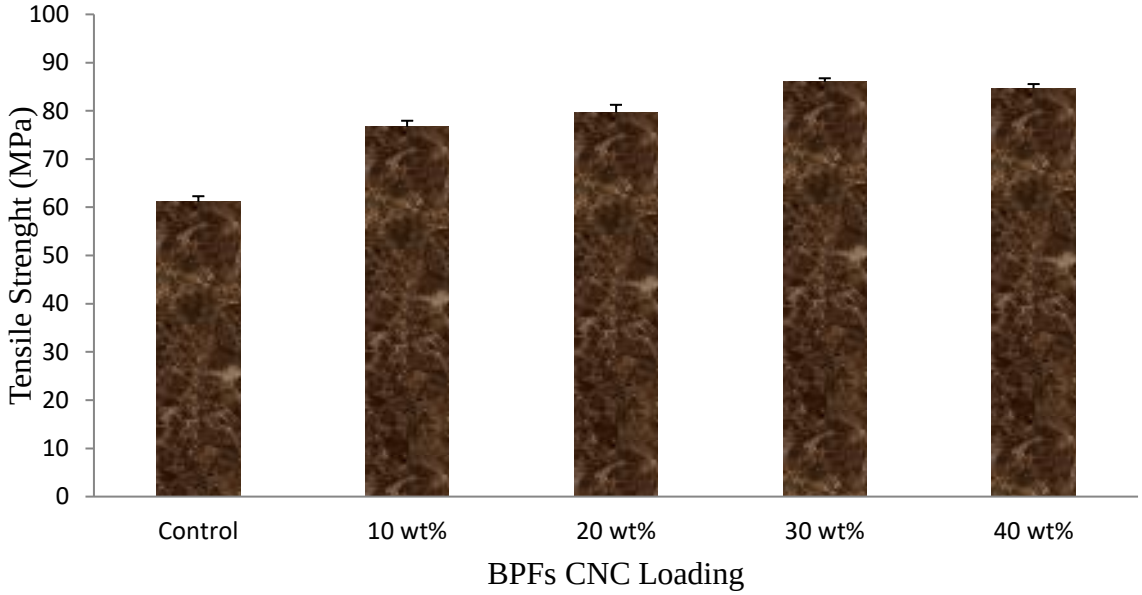

Figure 4.16: Tensile Strength of composites at varying CNC loading.

The maximum tensile strength obtained at 30 wt% might be due to proper binding between the fibre Nanocrystals and matrix of the LDPE all other reinforced composites had tensile strength higher than that of the unreinforced LDPE.

4.8.4 The effect of flexural strength on properties of reinforced composite

The flexural strength of the reinforced LDPE/CNC composites is higher than that control unreinforced LDPE as shown in Figure 4.17. This is a clear indication that flexural strength was increased with CNC reinforcement. The highest flexural strength was obtained at 30 w % which is 17.36 MPa. The overlap in error bar between 20 wt %, 30 wt % and 40 wt % does not show much significant difference between the results.

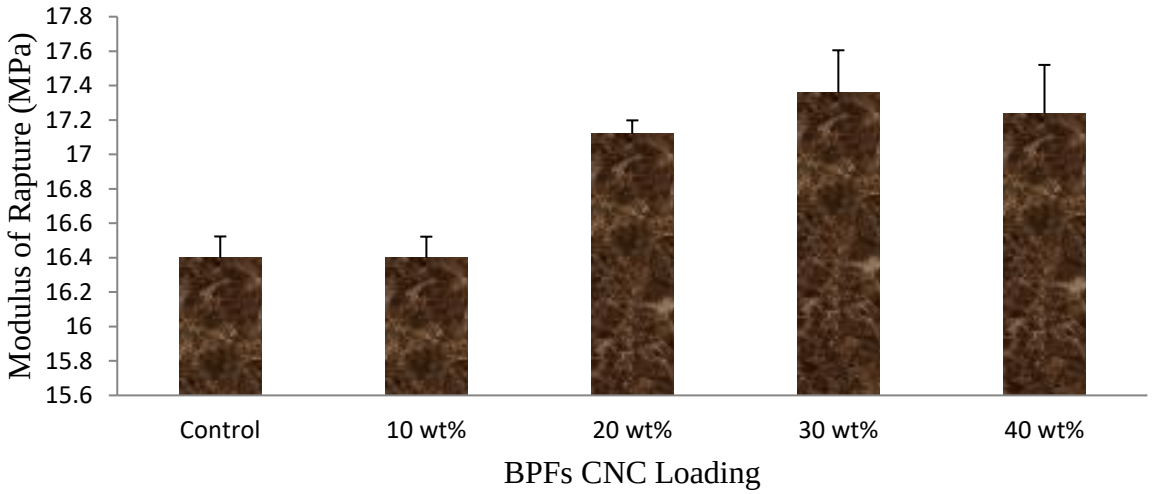

Figure 4.17: Flexural Strength of Composite at varying CNC loading

All samples have modulus of rapture above 16.4 MPa while that of the unreinforced sample stood at 16.4 MPa this shows that the unreinforced LDPE has the tendency to rapture faster than that of the CNC reinforced composites.

4.8.5 Hardness properties of CNC reinforced LDPE composites

From Figure 4.18 it was observed that the addition of the Cellulose Nanocrystals to polyethylene increases the hardness property, this indicated that hardness of the composite

material formed is directly proportional to the increase in CNC addition at the point where there is high proportion of CNC reinforcement loading with respect to the LDPE. The lowest hardness strength of 26.7 HV was obtained at 10 wt% of Baobab fibre loading while the highest was recorded at 45.3 HV for 40 wt %

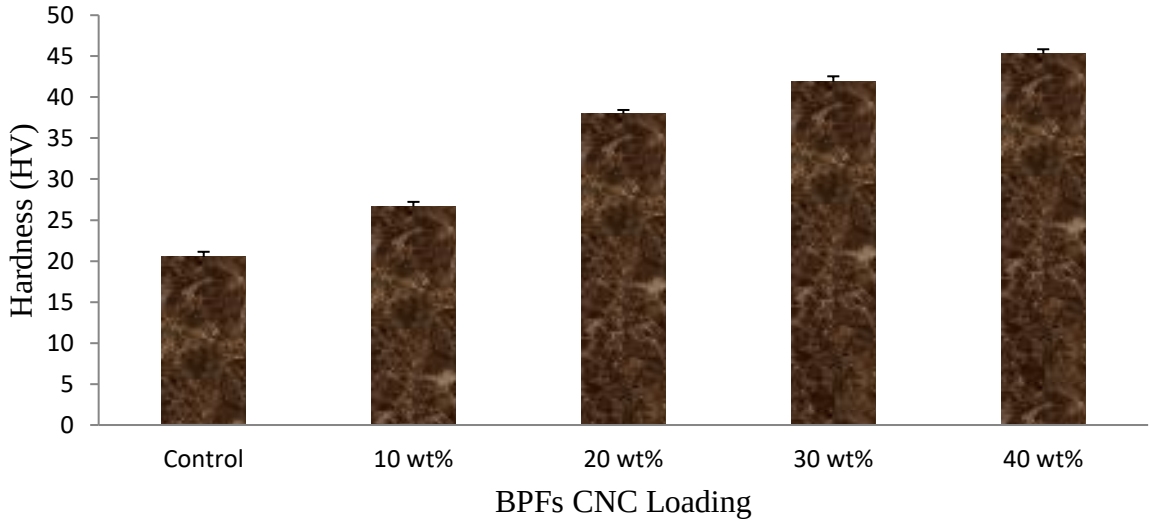

Figure 4.18: Hardness of Composites at varying CNC loading

4.8.5 The effect of impact strength on properties on reinforced composite

The impact strength of the reinforced BPFs CNC composites decreased with increased loading as can be seen from Figure 4.19. The impact properties decrease due to poor interfacial adhesion between the matrix and the fibre. The fibre loading increases the brittleness of the composite. The error bar overlapped between 10 wt %, 20 wt% and 30 wt% fibre loading shows that there was no significant change in impact strength between the two composites.

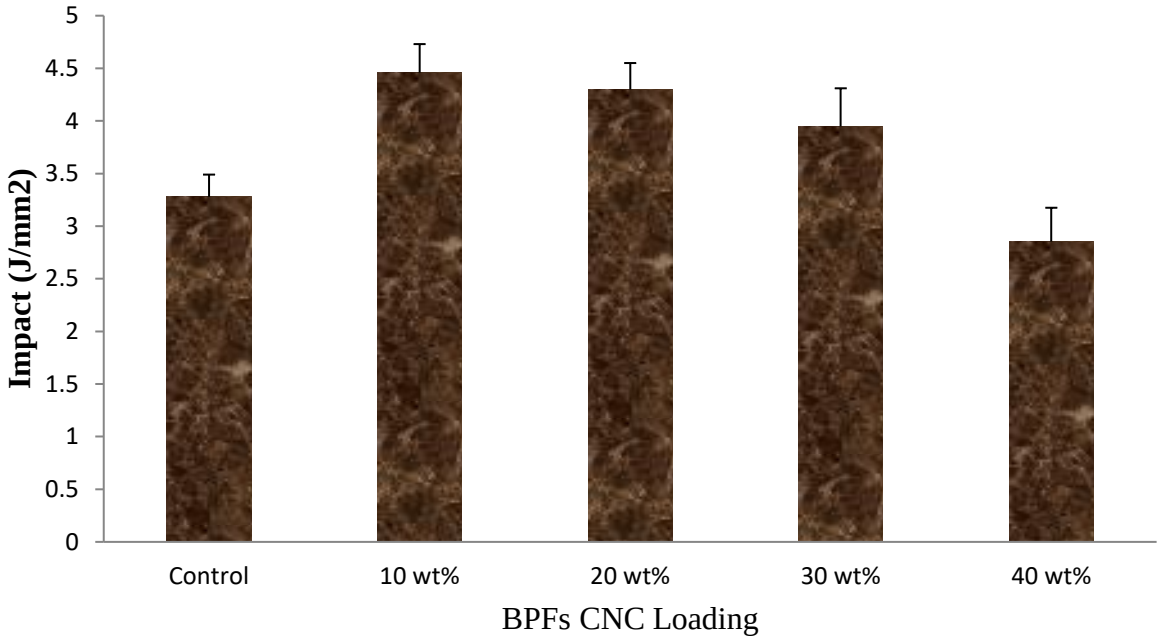

Figure 4.19: Impact Strength of Composite at CNC loading

Tensile strength and water absorption are important properties to be determined when using natural fibre as a reinforcing material. For this study, the composite that exhibits best of those properties is sample 3 (30 wt% Baobab CNC and 70 wt% LDPE). It has very low water absorption of 0.1707 % and the highest tensile strength of 86.05 MPa. The hydrophobic nature of the reinforcing material (LDPE) will not allow water absorption into the matrix and thereby restraining water sensitivity. The tremendous increase in the tensile property of the CNC may be attributed to proper homogeneous mixing of the CNC and the matrix at the CNC-LDPE interface after the fibre was chemically treated and hydrolyzed.

4.9 TGA Analysis of Composites

Figure 4.16 shows the TGA/DTA curves obtained for the Baobab pod fibre nanocellulose reinforced composites. In the first degradation stage (25 to 150 ˚C), it is observed that the loss of mass increased with increasing fibre nanocellulose content.

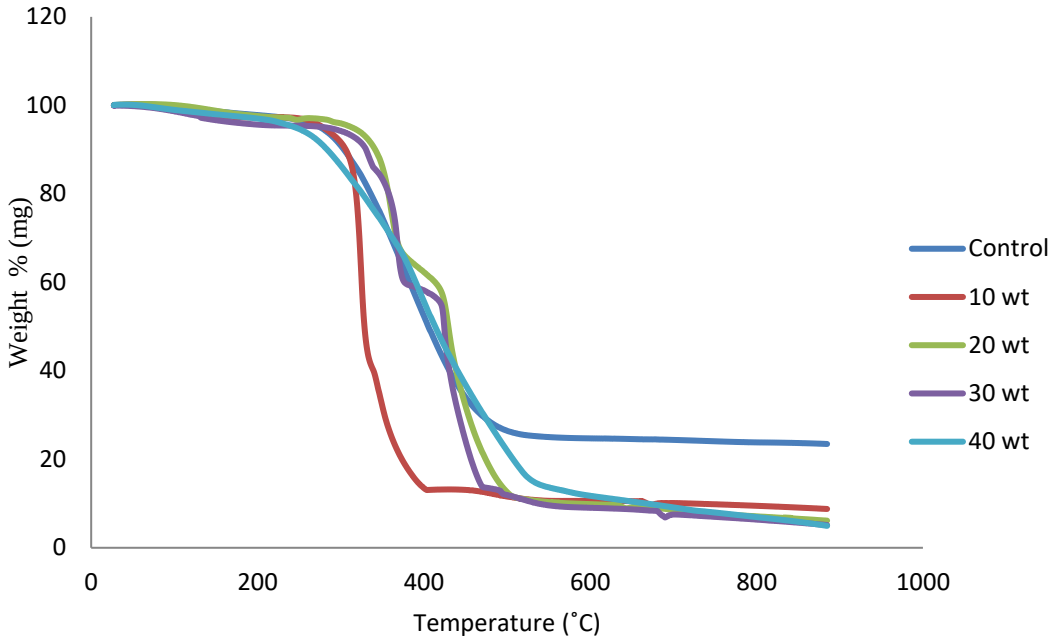

Figure 4.20: Effect of CNC loading on mass loss of composites

Table 4.20 presents the main TGA parameters obtained for the investigated composites and The onset of thermal degradation (T_{onset}) was obtained by the estimated point of deviation from the initial slope, almost a horizontal line in the TGA curves of Figure 4.19. A minimum detected thermal degradation (T_{min}) is proposed as the intercept between the initial, almost horizontal, slope and the steeper slope clearly related to the subsequent interval of thermal degradation of the material structure (Monteiro *et al*., 2012). Figure 21 depicts the DTA curves f or composites

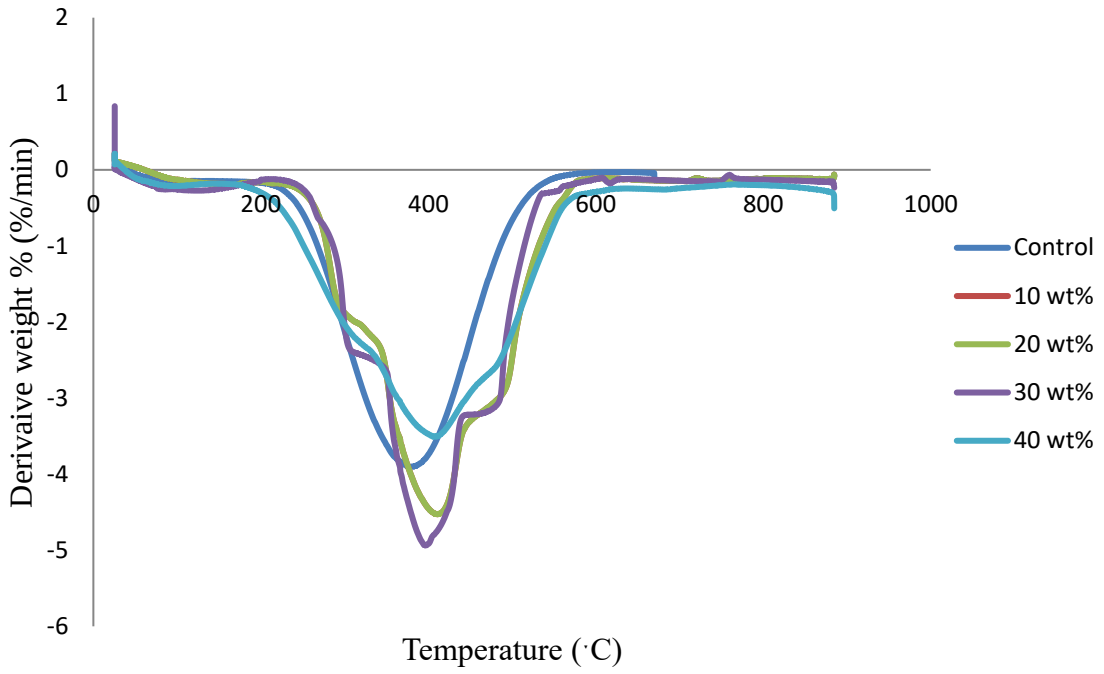

Figure 4.21: DTA curves of composites

Table 4.19 presents the degradation temperatures and mass loss for the Baobab CNC/LDPE reinforced composites.

Table 4.19: Degradation temperatures and mass loss of composites

Sample	T_{onset} (˚C)	T_{min} (◦C)	T_{max} (˚C)	Mass Loss (%)	Residue at
Control	216	268	355	9.8	2.17 (700 ˚C)
10 wt%	218	267	307	1.65	2.35 (700 ˚C)
20 wt%	237	302	355	2.45	9.10 (900 ˚C)
30 wt%	235	299	353	3.49	7.60 (900 ˚C)
40 wt%	230	293	322	4.17	3.19 (900 ˚C)

Based on the values of T_{onset} in Table 4.20, it is possible to assume, in principle, that a safe maximum working temperature for the composite would be 200 ˚C, which is comparable to those of other natural fibre LDPE composites. However, within the possible statistical variation of T_{onset} the working temperature might eventually be safely raised to 220 ˚C as an

upper limit. Figure 4.20 shows the comparison of the maximum working temperatures for Baobab and other works.

Table 4.20: Comparison of maximum working temperatures of Baobab CNC reinforced LPDE composites with other composites

Sample	Maximum working temperatures (˚C)	Reference
LPDE & Baobab	220	This study
Epoxy & kenaf fibre	200	Chan *et al*., 2013
Sisal & interlamina	180	Mwaikambo *et al*., 2002
Raffia & HDPE	210	Fadele, 2017
Wiskers & PE	232	Azizisamir *et al.*, 2015

CHAPTER FIVE

5.0 CONCLUSION AND RECOMMENDATIONS

5.1 Conclusions

In this research work, reinforced polymer composites were developed from low-density polyethylene and cellulose nanocrystals extracted from Baobab pod fibres using the two roll mill and compression moulding techniques. The physical, mechanical and thermal properties related to the raw fibres, treated fibres, cellulose nanocrystals and composites were investigated. This study also went a step forward by optimising the alkaline treatment process of BPFs using response surface methodology (RSM).

Based on the experimental results and analysis of the data it is concluded that, NaOH treatment of Baobab pod fibres enhances the physical and mechanical properties of the fibres to a large extent. The higher the concentration of the sodium hydroxide used for the treatment, the lower the tensile strength and the young modulus. The optimal conditions were found when the fibres were soaked in 6.953 % NaOH concentration at 99.763 ˚C for 359.963 min in terms of tensile strength and Young modulus. The SEM analysis revealed that NaOH treatment and Acid hydrolysis modified the fibre morphology. The crystallinity index of the Baobab pod fibres increase significantly with NaOH treatment. Further increase of 95 % was recorded after the acid hydrolysis TGA/DTA results showed that chemical treatment and acid hydrolysis improved thermal stability of the Baobab pod fibres. The fibre content in the polymer is associated with a thermal stabilization of the composites. The fibre interaction with macromolecular chains affects the polymer glass transition of temperature, which is decreased, and then causes a total amorphous structure to be formed at lower temperature. This allowed thermal softening to be displaced to higher temperatures. Composites produced from nanocrystals have better surface area and mechanical properties when compared to that produced from micro materials, thereby making them suitable materials to meet the emerging

demands arising from scientific and technological advances. Micro hardness, water absorption capacity, density, charpy impact and flexural strength of LDPE composites increase as the CNC content of the composites is increased. In contrast, the tensile strength of the composites decreased when compared with unreinforced LDPE.

5.2 Recommendations for Future Work

For future research work, the following recommendations are suggested:

Future studies can be directed toward finding the CNC capability to reinforce other plastics such as high density polyethylene (HDPE) and polyethylene terephthalate (PET). An alkaline treatment (Mercerization) was used in this study to modify the surface chemistry of the fibre. Other treatments such as acetylation, silane and sodium chlorite may also be considered. Acid hydrolysis was used in the production of cellulose nanocrystals from the treated fibres. Other processes such as mechanical attrition may also be considered. Morphological examination of fractured charpy impact sample should be carried out in future researches in order to observe and analyze the fibre pull out from the matrix.

5.3 Contribution to Knowledge

The research serves as means of obtaining data on raw Baobab pod fibres which is very rear. Reinforced composite materials produced from the fibre can be an alternative material for petroleum based synthetic polymers because of its low density, good tensile strength, renewability and biodegradability. More so, alternative use of Baobab pod fibres will also leads to development in the field of agriculture as it can bring more income to the farmers and will also help in the field of solid waste management and control.

1

REFERENCES

Abhishek, D. & PremKumar B. (2015). Study of characteristics of Natural fibre reinforced (NFRP) Composite – A Review. *International Journal for Scientific Research and Development* (3), 2321 - 0613

Adesina, O. T., Jamiru, T., Sadiku, E. R., Ogunbiyi, O. F. & Beneke, L.W. (2019). Mechanical evaluation of hybrid Natural-fibre reinforced Polymeric Composites for automotive bumper beam; a review. *International Journal of Advanced Manufacturing T echnology* 103; Pp: 1781-1797

Akampumuza, O., Wambua, P., Ahmed, A., Li, W. & Qin, X. H. (2017). Review of the Applications of Biocomposites in the Automotive Industry. *Polymer Compos*ite, 38, 2553–2569.

Aliotta, L., Vannozzi, A., Panariello, L., Gigante, V., Coltelli, M.B., Lazzeri K. (2020). A Sustainable Micro and Nano Additives for Controlling the Migration of a Biobased Plasticizer from PLA-Based Flexible Films. *Journal of Polymers*, 12, 13-66.

Al-Oqla, F.M. Sapuan, S. Anwer, T. Jawaid, M. Hoque, E. & Sapuan, S.M. (2015). Natural fibre reinforced conductive polymer composites as functional materials: A review. *Synthetic Material*, 206, 42-54

Alves, C. Silva, A. J. Reis, L. G. Freitas, M. Rodrigues, L. B. & Alves, D. E. (2010). Eco design of Automotive Components Making Use of Natural Jute Fibre Composites. *Journal of Clean Production*. 18, 313–327.

Anteneh G., Tamene A. D., Pieter, D. W. & Hans, D. B. (2021). An Overview of the Characterization of Natural Cellulosic Fibre. *Article in Key Engineering Materials* DOI: 10.4028/www.scientific.net/KEM.881.107. ISSN: 1662-9795, Vol. 881, pp 107-116

ASTM D 570-98 ASTM D570 – 98 – (2014) Standard Test Method for Water Absorption of Plastics. *ASTM International* U.S.A.

Arun, K. S., Rakesh, B., Amit, A. & Ruta, R. (2020). A study of advancement in application opportunities of Aluminium metal matrix composites. *Materials today proceedings* (10) 2214-2215

Azizisamir, M. A. S., Alloin, F. & Dufresne, A. (2005). Review of recent research into cellulosic whiskers, their properties and their application in nanocomposite field. *Journal of biomacromolecules* 6:612–626.

Balla, V. K. Kate, K.H. Satyavolu, J. Singh, P. & Tadimeti, J. G. D. (2019). Additive manufacturing of natural fibre reinforced polymer composites: Processing and prospects. *Composite Particulate B.Eng*. 174, 106956.

Bledzki, A. K. & Gassan, J. (1999). Composites reinforced with cellulose based fibres. *Program in Polymer* Science, 24, 221–274.

Bouasker, M. Belayachi, N. Hoxha, D. & Al-Mukhtar, M. (2014). Physical Characterization of Natural Straw Fibres as Aggregates for Construction Materials Applications. *CompositeMaterials* 7 (4), 3034–3048. https://doi.org/10.3390/ma7043034.

Brigante, D. (2014). New Composite Materials: Selection, Design and Application. *Springer International Publication Switz*.1–179, doi: 10.1007/978-3-319-01637-5.

Chan, C. H. Chia, C. H. Zakaria, S. Ahmad, I. & Dufresne, A. (2013). Production and characterisation of cellulose and nano- crystalline cellulose from kenaf core wood. *Journal of BioResources*. 8, 785–794

Chandar, J.V., Shanmugan, S. Murugan, P., Mutharasu, D. & Sudesh, K. (2016). Structural Analysis of ZnO Nanoparticles Reinforced P (3HB-co-15 mol% 3HHx) Bioplastic Composite. *Journal of Polymer and Environment*, 25, 1251–1261

Chawla, N. & Shen, Y. L. (2001). Mechanical behavior of particle reinforced metal matrix composites. *Advance Enineering Material*. 3, 357–370

Chen, H. Cui, Y. Liu, X. Zhang, M. Hao, S. & Yin, Y. (2019). Study on depositing SiO_2 nanoparticles on the surface of jute fibre via hydrothermal method and its reinforced polypropylene composites. *Journal of Vinyl Additive Technology*. 26, 43–54

Chen, L., Yang, W. J. & Yang, C. Z. (1997). Preparation of nanoscale iron and Fe_3O_4 powders in a polymer matrix. *Journal of Materials Science*. 32(13):3571-3575.

Chermoshentseva, A. S. Pokrovskiy, A.M. & Bokhoeva, L. A (2016). The behavior of delaminations in composite materials—Experimental results'. *IOP Conerence series in Material Science Engineering*. 116, 012005

Costa, U.O., Nascimento, L.F.C., Garcia, J.M., Monteiro, S.N., Luz, F.S., Pinheiro, W.A., Filho, F.C.G (2019). Effect of Graphene Oxide Coating on Natural Fibre Composite for Multilayered Ballistic. *Armor. Polymers*,11,13-56

Damfeu, J. C., Meukam, P. & Jannot, Y (2016). Modeling and measuring of the thermal properties of insulating vegetable fibres by the asymmetrical hot plate method and the radial flux method: Kapok, coconut, groundnut shell fibres and rattan. *Thermochimical Acta* , 630, 64–77.

De Caluwe, E., Katerina, H. & Patrick, V.M. (2010). Adansonia digitata L. – A Review of Traditional uses. Phytochemistry and pharmacology. *Afrika Focus* – 23,11-51

Dipen K.R., Pradip M., Durgesh, P. & Emanoil, L. (2019). Fibre-Reinforced Polymer Composites: Manufacturing, Properties, and Applications. *MDPI Polymers*. (11), 1667; doi:10.3390/polym11101667

Dresselhaus, M. S., Dresselhaus, G., Saito, R. & Jorio, A. (2005). Raman spectroscopy of carbon nanotubes. *Physics Report - Review Section of Physics Letters*. 409(2):47-99.

Fadele, O.E. (2017). Development and Characterization of Raffia Palm Fibre Reinforced Polymer Matrix Composites. *Master's Thesis, university of Saskatchewan*. 10-13

Farid, K. M. Péter, G. H. & Tibor, A. (2020). Potential Natural Fibre Polymeric Nanobiocomposites: A Review'. *Simonyi Károly Faculty of Engineering, University of Sopron, Sopron, 9400 Gyor, Hungary*. doi:10.3390/polym12051072. 2-3

FAO (1988). Traditional food plants. *Food and Agriculture Organisation of the United Nations;Rome*, 24: 63-67.

Faruk, O. Bledzki, A. K. Fink, H. P & Sain, M. (2012). Biocomposites reinforced with natural fibres. *2000-2010. Program in polymer science*, 37, 1552–1596.

Fischer, H. (2003). Polymer nanocomposites: from fundamental research to specific applications. *Materials Science and Engineering*. 23(6-8):763-772.

Frank, S. J. V., Harik, V. M., Odegard, G. M., Brenner, D. W & Gates, T. S. (2003). The stress–strain behavior of polymer–nanotube composites from molecular dynamics simulation. *Composites Science and Technology*. 63(11):1655-1661.

Groover, M. P. (2010). Fundamentals of Modern Manufacturing: Materials, Processes, and Systems. *John Wiley Sons, Incoporated Danvers, Massachusetts, USA*, 4, 1025.

Harrigan, W. C. (1998). Commercial processing of metal matrix composites. *Material Science and Engineering*, 244, 75–79.

Harshai, P., Vjay, S. & Pramod, R. (2019). Characterization of natural fibre reinforced polymeric composites for automotive application - a review. *An article on technical textiles.*www.researchgate.net/publication/33199170

Hazrol, M. D., Spuan, S. M, Zuhri, M. Y. M. & Ilyas, R. A. (2019). Eletrical properties of sugar palm nanocellulose fibre reinforced sugar palm starch biopolymer composite. *In proceeding Semina Enau Kebangsaan* pp 2 - 11

Himmelsbach, D. S. & Akin, D. E. (1998), Near-infrared Fourier-transform Raman spectroscopy of flax (Linum usitatissimum L.) stems. *Journal of Agriculture, Food and Chemical*. 46, 991–998.

Ho, M. Wang, H. Lee, J. H. Ho, C. Lau, K. Leng, J.& Hui, D. (2012). Critical Factors on Manufacturing Processes of Natural Fibre Composites. *Composite Part B Engineering* 43, 3549–3562

Idowu, D. I., Tamba, J. & Gbenga, E. (2016). Mechanical properties of sisal fibre-reinforced polymer composites: a review. *Composite Interfaces*. Vol.23, Issue.No.1, pp. 15–36.

Ishikawa, A, Okano, T. & Sugiyama, J. (1997). Fine structure and tensile properties of ramies in the crystalline form of cellulose I, II, III and IV'. *Polymers* 38(2): 463 – 8.

Igboeli, L.C., Addy, E. & Salami, L. I. (1997). Effects of some processing techniques on the antinutrient contents of Baobab seeds (*Adansonia digitata*). *Bio resource Technol*ogy 59: 29-31.

Iwata, T. Doi, & Y. (1998). Morphology and enzymatic degradation of poly (L-lactic acid) single crystals. *Macromolecules.* 31, 2461-2467.

Jacobs, M., Thomas, S., & Varughese, K.T., (2004). Mechanical properties of sisal/oil palm hybrid fibre reinforced natural rubber composites. *Composite Science Technology*. 64 (7), 955 - 965

Jenkins, B. M., Baxter, L. L., Miles Jr, T. R. & Miles, T. R. (2008). Combustion properties of biomass Fuel. *Process Technology* .54:17–46. 2008.

Jeyapragash, R. Srinivasan, V. & Sathiyamurthy, S. (2020). Mechanical properties of Natural Fibre/Particulate reinforced epoxy composites – A review of the litrature. *Material Today Processing*. 22, 1223 - 1227

Joerg, G. & Mathias, G. (2018). Selected natural ingredients derived from native species (UNCTAD).

Joseph, K., Mattoso, L. H. C., Toledo, R. D., Thomas, S., de Carvalho, L. H., Pothen, L. Kala. S., & James, B. (2000). Natural polymers and agrofibres composites. *Embrapa, USP-IQSC, UNESP, Brazil. 35, 234-257.*

Kabir, M. M., Wang, H., Lau, K. T. & Cardona, F. (2012). Chemical treatments on plant-based natural fibre reinforced polymer composites: An overview. *Composite Part B Engineering.* 43, 2883–2892.

Kambli, N. D., Mageshwaran, V., Patil, P. G., Saxena, S. and Deshmukh, R. R. (2017). Synthesis and characterization of microcrystalline cellulose powder from corn husk fibres using bio-chemical route. *Journal of Cellulose Technology*, 24, 5355–5369.

Krishan, K. C. (2012). Composite materials. *Science and Engineering, Third edition*. DOI 10.1007/978-0-387-74365-3. 3, 73 – 74.

Kojima, Y. Usuki, A. Kawasumi, M. Okada, A. Fukushima, Y. Karauchi, T. & Kamigaito, O. (1993). Mechanical properties of nylon-6-clay hybrid. *Journal of Materials Research*. 8(5):1185-1189.

Lavanya, K. Santhi, R. & Annapurani, S. (2017). Green Synthesis of Silver Nanoparticles from the Leaf Extract of Volkameria inermis. *International Journal of Pharmaceutical and Clinical Research*. 9(8): 610-616. doi:10.25258/ijpcr.v9i08.9587

Layth, M. Ansari, M. N., Grace, P., Mohammad, J. & SaifulIslam, M. (2015). A Review on Natural Fibre Reinforced Polymer Composite and Its Applications. *Hindawi Publishing Corporation International Journal of Polymer Science, Article ID 243947*, http://dx.doi.org/10.1155/2015/243947

Leja, K. (2010). Polymer Biodegradation and Biodegradable. *Polish Journal of Environmental Studies*, 255 - 266.

Low, I. M. (2006). Ceramic-Marix Composites; Microstructure, properties and applications. *Woodhead publishing*. UK. ISBN; 1855739429. 234 -236

Martins, M. A. Pessoa, J. D. C. Gonçalves, P. S. Souza, F. I. & Mattoso, L. H. C. (2008). Thermal and mechanical properties of the acai fibre/natural rubber composites. *Journal of Material Science,* 43, 6531–6538

Matthews, F. L. & Rawlings, R. D. (1999) Composite Materials: Engineering and Science. *Woodhead Publishing, Cambridge*. 13, 630–641

Mallick, P. (2007). Fibre-Reinforced Composites. *Dekker Mechanical Engineering; CRC Press: Boca Raton, FL, USA*, Volume 20072757, ISBN 978-0-8493-4205-9.

Mehdi, J. Yelda, D., Razer, O. & Christina, O (2015). Different preparation methods and properties of nanostructured cellulose from various natural resource and residue – a review. *Springer Science Business Media Dordrecht*. DOI 10.1007/s10570-015-0551-0, 22, 935–969

Mehmet, S. Yoldas, S. Kutlay, S. & Cenk, D. (2014). Determination of properties of Althaea officinalis L. (Marshmallow) fibres as a potential plant fibre in polymeric composite materials. *Journal of composites, Elsevier publications*, 57. Pp: 180 – 186

Michael, A.& Philippe, D. (2000). Polymer-layered silicate nanocomposites: preparation, properties and uses of a new class of materials. *Material Science Engineering* 28(1):1–63

Miyashiro, D. Hamano, R. & Umemura, K. A. (2020). Review of Applications Using Mixed Materials of Cellulose, Nanocellulose and Carbon Nanotubes. *Nanomaterials* , 10, 186

Modibbo, U.U., Aliyu, B. A. & Nkafamiya I.I. (2009). The effect of mercerization media on the physical properties of local plant bast fibres. *International Journal of Physical Sciences.* 4 (11); 698-704.

Mohammed, L. Ansari, M. N. M. Pua, G. Jawaid, M. & Islam, M. S. (2015). A Review on Natural Fibre Reinforced Polymer Composite and Its Applications. *International Journal of Polymer*. doi:10.1155/2015/243947.

Mohammed Z. (2021). A Review on Natural Fibre Bio-Composites, Surface Modifications and Applications. Journal of Molecules 26, 404. https://doi.org/10.3390/molecules 26, 20 - 40

Mohanty, A. K., Misra, M. & Hinrichsen, G. (2000). Biofibres, biodegradable polymers and biocomposites: an overview. *Macromol Material Engineering* 276–277:1–24

Mwaikambo, L. Y. & Ansell, M. P. (2002). Chemical modification of hemp, sisal, jute, and kapok fibres by alkalization. *Journal of Applied Polymer Science*. 2222–2234, doi:10.1002/app.10460.

Namita, R. (2015). Methods of preparation of nanoparticles – a review. *International Journal of Advances in Engineering & Technology*. ISSN: 22311963

Narayan, R. (2006). Biobased and Biodegradable Polymer Materials: Principles, Concepts and Technology Exemplars. *In Proceedings of the World Polymer Congress and 41st International Symposium on Macromolecules, MACRO, Rio de Janeiro, Brazil*, 16–21.

Narin, K., Mehmet, A. & Ersen, B. (2019). Surface Modification effects on the mechanical properties of woven jute fabric reinforced laminated composites. *Journal of natural fibres*. doi.org:10.1080/15440478.2018.1431995.

Nguyen, T.A. Han, B. Sharma, S. Longbiao, L. & Bhat, K. S. (2020). Fibre-reinforced nanocomposites: An introduction. In Fibre-Reinforced Nanocomposites: Fundamentals and Applications. *Elsevier BV: Amsterdam, The Netherlands*, 3–6

Niddles, H. L., (2001). Textile fibres, dyes, finishes and process. *Special publishers Distributors.67, 89-90.*

Nissen, D. and Stutz, H. (1985). Advanced Composite Matrices CCM Annual Workshop, Centre for Composite Materials. *University of Delaware, Newark*. Del. 19, 7-16.

Nkafamiya, I. I, Osemeahon, S. A, Dahiru, D. & Umaru, H. A. (2007). Studies on the chemical composition and physicochemical properties of the seeds of Baobab (Adasonia digitata). *African Journal of Biotechnology* Vol. 6 (6), pp. 756-759

Oboh, J.O. Okafor, J.O. Kovo, A.S. Abdurrahman, A.S & Okele A.I. (2018). Isolation of Cellulosic Nanoparticles from coir Fibre for the preparation of Natural rubber composites. *Journal of polymer and composites*. Volume 6(1). ISSN:2321-2810

Odian, G. (2004). Principles of Polymerization. *4th edition, John Wiley & Sons, New Jersey*. 12, 567-678

Ogawa, M. K. & Uroda, K. (1997). Preparation of inorganic composites through intercalation of organoammoniumions into layered silicates. *Bulletin of the Chemical Society of Japan.* 1997; 70(11):2593-2618.

Omid Nabinejada, D. Sujana, M. E. Rahmana & Ian J. (2017). Effect of filler load on the curing behavior and mechanical and thermal performance of wood flour filled thermoset composites. *Journal of Cleaner Production*. 164 pp. 1145-1156 DOI: 10.1016/j.jclepro.2017.07.036

Omotesho, K.F., Sola-Ojo, F.E., Adenuga, A.H. & Garba, S.O. (2013). Awareness and usage of the Baobab in Rural Communities in Kwara State, Nigeria. *Ethiopian Journal of Environmental Studies and Management* 6(4). http://dx.doi.org/10.4314/ejesm.v6i4.10

Omrani, E., Menezes, P. L, and P. K. Rohatgi (2016). State of the Art on Tribological Behavior of Polymer Matrix Composites Reinforced with Natural Fibres in the Green Materials World. *Engineering Science and Technology, an International Journal*,19 (2):717-36.

Osman, M.A. (2004). Chemical and Nutrient Analysis of Baobab (Adansoniadigitata) Fruit and Seed Protein Solubility. *Plant Foods for Human Nutrition,* 59, 29-33.

Paulo, P. Hugo, C., Hafiz, S. and Marco, L. (2018). Natural Fibre Composites and Their Applications: A Review. *Journal of composite science 2*, 66; doi:10.3390/jcs2040066.

Peijs, T., Van, M., S.K. Garkhail, G.T. Pott, A. Stamboulis, & C.A. Baillie (1998). Natural-Fibre-Mat-Reinforced Thermoplastics Based on Upgraded Flax Fibres for Improved

Moisture Resistance. In Proceedings of *European Conference on Composite Materials*, Naples, Vol. 2, 119.

Peets, P., Leito, I., Pelt, J. & Vahur, S. (2017). Identification and classification of textile fibres using ATR-FT-IR spectroscopy with chemometric methods. *Spectrochim Acta Molecular Biomolecular Spectroscopy*.; 15(173):175–81

Pickering, K.L. Efendy, M.A. & Le, T.M. (2016). A review of recent developments in natural fibre composites and their mechanical performance. *Composites. Part A. Applies Science Manufacturing.* 2016, 83, 98–112

Pilleriin, P., Karl, K., Signe, V. & Ivo, L. (2019). Reflectance FT-IR spectroscopy as a viable option for textile fibre identification. *Heritage science research article*. https://doi.org/10.1186/s40494-019-0337-z

Pott, R. J. Pilot. & Hazendonk, J. M. (1997). Upgraded Flax Fibre as Reinforcement in Polymer Composites. *In Proceedings of 5th European Conference on Advanced Materials and Processes and Applications*. *Vol. 2*, 107-123.

Pranamuda, H. Tokiwa, Y. & Tanaka, H (1997). Polylactide degradation by an Amycolatopsis sp. *Applied Environmental Microbiology*. 63, 1637-1640.

Praveenkumar, J., Sunderraj, N., Chandan, H. R., Srivathsa, M. & Madhu, P. (2018). Natural fibres and composites and its engineering applications: an overview. *International Journal of Industrial Electronics and Electrical Engineering.* 6, 2347-6982.

Rahman, M.M. Mallik, A.K., & Khan M.A (2007). Influences of Various Surface Pretreatments on the Mechanical and Degradable Properties of Photografted Oil Palm Fibres. *J. Appl. Polym. Sci.* 105, 3077–3086

Ramamoorthy, S. K., Skrifvas, M. & Persson A. (2014). A review of natural fibres used in Biocomposites; plant, animals and regenerated cellulose fibres. *polymer Revision*. 55 (1), 107 -162

Ramesh, M., Atreya, T. S., Aswin, U. S., Eashwar, H. & Deepa, C. (2014). Processing and Mechanical Property Evaluation of Banana Fibre Reinforced Polymer Composites. *Procedia Engineering*. 97:563-72.

Randbaran, E., Dayang, L., Zahari, R., Sultan, M.T.H. & Mazlan, N. (2020). Advantages and Disadvantages of Using Composite Laminates in the Industries. *Lupine Publishers, Morden approaches on material sciences.* DOI: 10.32474/MAMS.2020.03.000158. 349-350

Rohan, T., Tushar, B. & Mahesha, G.T. (2018). Review of natural fibre composites. *IOP Conference Series Material Science Eng*ineering, 314, 12 – 20.

Rong, M. Z., Zhang, M. Q., Liu, Y., Yang, G. C. & Zeng, H. M.(2001). The Effect of Fibre Treatment on the Mechanical Properties of Unidirectional Sisal-Reinforced Epoxy Composites. *Composites Science and technology*, 61(10):1437-47.

Russo, P.,Vitiello, L., Sbardella, F., Santos, J. I., Tirillò, J., Bracciale, M. P., Rivilla, I., Sarasini, F. (2020). Effect of Carbon Nanostructures and Fatty Acid Treatment on the Mechanical and Thermal Performances of Flax/Polypropylene Composites. Polymers. 12, 4-38

Saba, O. S. (2014). Manufacture and Characterization of Fibre Reinforced Epoxy for Application in Cowling Panels of Recreational Aircraft. *MSc. Thesis; University of Saskatchewan, Saskatoon, Canada.*116.

Sanjay, M.R., Arpitha1, G.R., Laxmana Naik, K. Gopalakrishna, & B. Yogesha (2016). Applications of natural fibres and its composites: An overview. Natural Resources, 7, 108-114 *Published online in journal of Science Resources.* http://www.scirp.org/journal/nr http://dx.doi.org/10.4236/nr.73011

Satyamurthy, P., Jain, P., Balasubramanya, R. H. & Vigneshwaran, N. (2011). Preparation and characterization of cellulose nanowhiskers from cotton fibres by controlled microbial hydrolysis. *Carbohydrate Polymers* 83:122–129

Saurab, C. & Inderdeep, S. (2016). Novel Aloe Vera fibre reinforced biodegradable composites— Development and characterization. *Journal of Reinforced Plastics and Composites.* Vol. 35(19) 1411–1423

Schmidt, D., Shah, D. & Giannelis, E. P. (2002). New advances in polymer/layered silicate nanocomposites. *Current Opinion in Solid State & Materials Science*. 6(3):205-212

Schwartz M (1997). Composite Materials. *Prentice Hall PTR, Upper Saddle River, New Jessy*, USA, Vol.1, pp 4-5

Shehu, U. & Isa, M. T. (2017). Effects of NaOH modification on the mechanical properties Of Baobab pod fibre reinforced LDPE composites. *Nigerian Journal of Technology* (NIJOTECH), 36, 87 – 95.

Shivani Pandya (2015). Nanocomposites and its application-Review. *parul university publications.* DOI: 10.13140/RG.2.1.2798.9840. 23: 3-4

Sidibe. M., & Williams, J. T. (2002). Baobab - *Adansonia digitata*. Fruits for the future. *International Center for Under Utilised Crops*, Southampton, UK, pp 96.

Sgriccia, N. Hawley, M.C. & Misra, M.(2008). Characterization of Natural Fibre Surfaces and Natural Fibre Composites. *Composites Part Applied Science Manuf*acturing 39, 1632–1637

Sreekala, M.S., Kumaran, M.G. & Thomas, S. (2001). Stress relaxation behaviour in oil palm fibres. *Material Letters*, vol. 50, no 4, pp. 263-273

Srinivas, K. Naidu, A.L. & RajuBahubalendruni, M.A. (2017). Review on Chemical and Mechanical Properties of Natural Fibre Reinforced Polymer Composites. *International Journal of Performance of Eng*ineering, 13, 189–200.

Staiger, M. P. & Turker, N. (2008). Natural fibre composites in structural applications. *Cambridge UK wood head publishing*, pp 269-300

Subramanian, K., Kumar, P.S., Jeyapal, P. & Venkatesh, N. (2005). Characterization of lignocellulosic seed fibre from Wrightia tinctoria plants for textile applications an exploratory investigation. *European Polymer Journal*. 41(4): 853–61.

Tan, B., Ching, Y., Poh, S., Abdullah, L. & Gan, S. (2015). A Review of Natural Fibre Reinforced Poly (Vinyl Alcohol) Based Composites: Application and Opportunity. *Polymers (Basel)* 7, 2205–2222.

Tsuji, H. & Miyauchi, S. (2001). Effects of crystallinity on enzymatic hydrolysis of poly(l-lactide) without free amorphous region. *Polymer Degradation Stability*, 71, 415-424.

Ubi, P. A. & Abdulrahman, S. A. (2015), Effect of Sodium Hydroxide Treatment on the Mechanical Properties of Crushed and Uncrushed Luffa Cylindrical Fibre Reinforced LDPE Composites. *International journal of chemical, Nuclear, Material and Metallurgical Engineering*. 9, (1), 203-208.

Venter, F. & Venter, J.(1996). Baobab in Making the Most of Indigenous Trees. *Briza publications, Pretoria, South Africa*.26-27. Wikipedia, Retrieved 29th June, 2020

Voevodin, A. A & Zabinski, J. S. (2005). Nanocomposite and nanostructured tribological materials for space applications. *Composites Science and Technology*. 65(5):741-748

William, D., Callister, J. & Rethwisch, D. G. (2014). Materials Science and Engineering: An Introduction. *John Wiley Sons Inc* 9, 266–267.

Wu, H., Fahy, W., Kim, S., Kim, H., Zhao, N., Pilato, L., Kafi, A., Bateman, S. & Koo, J. (2020). *Recent developments in polymers/polymer nanocomposites for additive manufacturing. Program Material Science*, 100638.

Yakubu A., Gabriel A. & Folahan A (2017). Synthesis and Characterization of Cellulose Nanoparticles and Its Derivatives using a Combination of Spectro-Analytical Techniques. *International Journal of Nanotechnology in Medicine & Engineering*. ISSN 2474-8811: 66-67

Yoldas, S., Mehmet, S., Kutlay, S. & Cenk, D. (2013). Extraction and properties of ferula communis (chakshir) fibres as novel reinforcement for composite materials. *Journal of composites, Elsevier publications* 44; Pp: 517- 523

Yusriah, L., Sapuan, S. M., Zainudin, E. S. & Mariatti, M. (2014). Characterization of Physical, Mechanical, Thermal and Morphological Properties of Agro-Waste Betel Nut (Areca Catechu) Husk Fibre. *Journal of Cleaner Production* 72, 174–180. https://doi.org/10.1016/j.jclepro.2014.02.025.

Zahra, D., Abdan, K., Jawaid, M., Mohd, A. K, Mohammad, B., Masoud, D., Francisco, C., & Ishak, M. (2017). Mechanical and Thermal Properties of Natural Fibre Based Hybrid Composites: A Review. *Pertanika Journal of Science & Technology*. 25 (4): 1103 - 1122

Zhu, K. & Schmauder, S. (2003). Prediction of the failure properties of short fibre reinforced composites with metal and polymer matrix. *Composite Material Science*. 28, pp. 743748.

Zwawi M.A. (2021). A Review on Natural Fibre Bio-Composites, Surface Modifications and Applications. *Journal of Molecules*, 26, 404. https://doi.org/10.3390/ molecules 26, 20 -44

APPENDIX A

Physical properties of Baobab pod fibres

Table A1: Diameter and length measurement

Description	Diameter (mm)	Length (mm)
1	0.23	65
2	0.31	63
3	0.22	60
4	0.19	14
5	0.11	89
6	0.21	34
7	0.18	57
8	0.22	39
9	0.13	47
10	0.24	58
11	0,27	39
12	0.24	40

Mean Average = $\frac{606}{12}$

= 50.42mm

Mean Average = $\frac{2.28}{12}$

= 0.19mm

APPENDIX B

Methods for determining chemical composition of fibre

ADF Method – Method 5

Apparatus:

1. Analytical Balance – capable of weighing 0.1 mg.

2. Oven – capable of maintaining a temperature of 102 ± 2°C.

3. Digestion instrument – capable of performing the digestion at 100 ± 0.5°C and maintaining a pressure of 10 – 25 psi. The instrument must be capable of creating a similar flow around each sample to ensure uniformity of extraction (ANKOM200 with 65 rpm agitation, ANKOM Technology).

4. Filter Bags – constructed from chemically inert and heat resistant filter media, capable of being heat sealed closed and able to retain 25-micron particles while permitting solution penetration (F57 and F58, ANKOM Technology).

5. Heat sealer – sufficient for sealing the filter bags closed to ensure complete closure (1915, ANKOM Technology).

6. Desiccant Pouch – collapsible sealable pouch with inside that enables the removal of air from around the filter bags (Moisture Stop weigh pouch, ANKOM Technology)

. 7. Marking pen – solvent and acid resistant (F08, ANKOM Technology).

Reagent:

Acid Detergent Solution – Add 20 g cetyl trimethylammonium bromide (CTAB) to 1L 1.00 N H2SO4 previously standardized (premixed chemical solution available from ANKOM). Agitate and heat to aid solution.

NDF

Apparatus:

1. Analytical Balance – capable of weighing 0.1 mg.

2. Oven – capable of maintaining a temperature of 102 ± 2°C.

3. Digestion instrument – capable of performing the digestion at 100 ± 0.5°C and maintaining a pressure of 10 – 25 psi. The instrument must be capable of creating a similar flow around each sample to ensure uniformity of extraction (ANKOM200 with 65 rpm agitation, ANKOM Technology).

4. Filter Bags – constructed from chemically inert and heat resistant filter media, capable of being heat sealed closed and able to retain 25-micron particles while permitting solution penetration (F57 and F58, ANKOM Technology).

5. Heat sealer – sufficient for sealing the filter bags closed to ensure complete closure (1915, ANKOM Technology).

6. Desiccant Pouch – collapsible sealable pouch with inside that enables the removal of air from around the filter bags (Moisture Stop weigh pouch, ANKOM Technology).

7. Marking pen – solvent and acid resistant (F08, ANKOM Technology).

Reagents:

Neutral Detergent Solution—Add 30g Sodium dodecyl sulfate (USP), 18.61g Ethylene diaminetetraacetic disodium salt (dehydrate), 6.81g Sodium borate, 4.56g Sodium phosphate dibasic (anhydrous), and 10.0ml Triethylene glycol to 1L distilled H2O (premixed chemical solution available from ANKOM Technology). Check that pH is from 6.9 to 7.1. Agitate and heat to aid solution.

ADL

Reagents:

Sulfuric acid (72% by weight) – ANKOM Technology FSA72 or dilute reagent grade H_2SO_4 to a specific gravity of 1634 g/L at 20°C (24.00N) by adding 1200 g H_2SO_4 to 350 ml H_2O in a 1 L MCA volumetric flask with cooling. Standardize this solution to 1634 g/L at 20°C specific gravity by removing solution and adding H_2O or H_2SO_4 as required.

Apparatus:

a) Filtration device – ANKOM Technology – F57 Filter Bags

b) Impulse bag sealer – ANKOM Technology – 1915 Heat Sealer

c) Desiccator – ANKOM Technology – Desiccant/Moisture Stop pouch – X45

d) 2L & 3L Beaker

APPENDIX C

FTIR spectrum of raw/treated/CNC Baobab pod fibres

FTIR of Baobab Pod Fibre

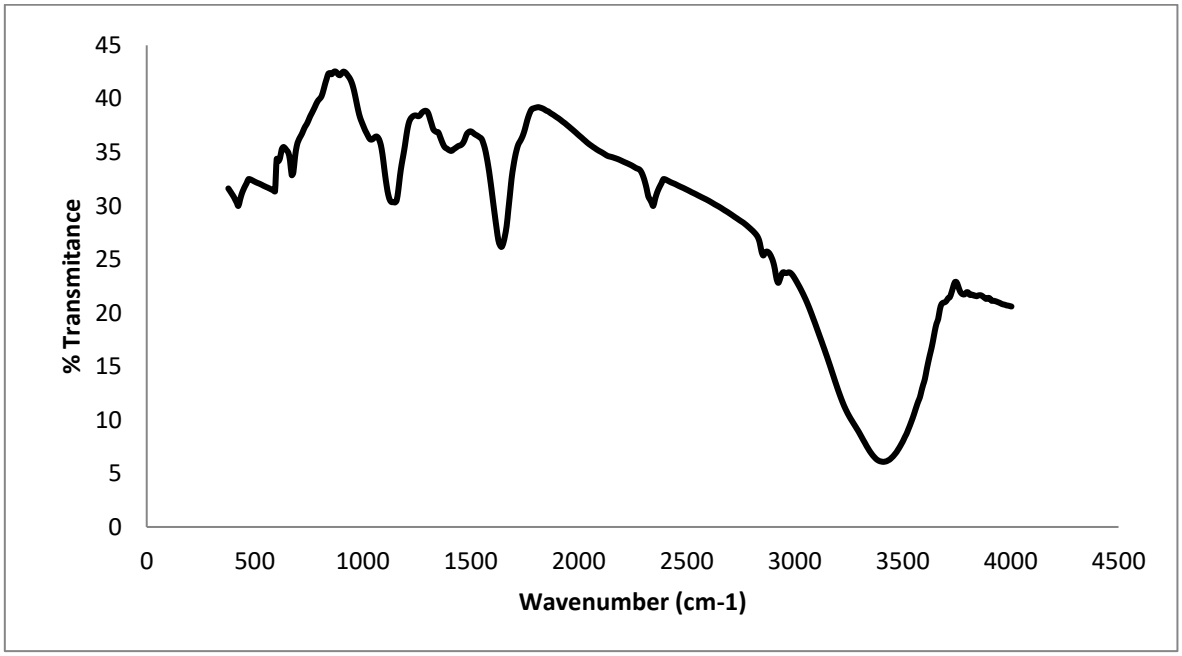

Figure A1: FTIR spectrum of raw Baobab fibres

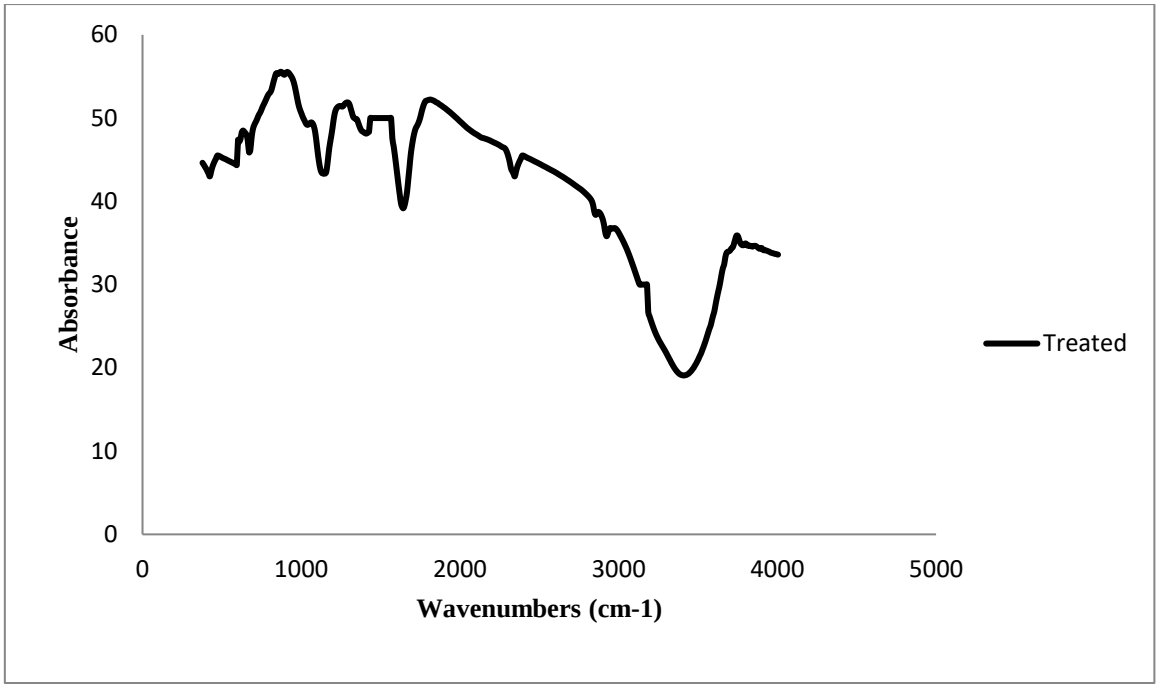

Figure A2: FTIR spectrum of treated Baobab fibres

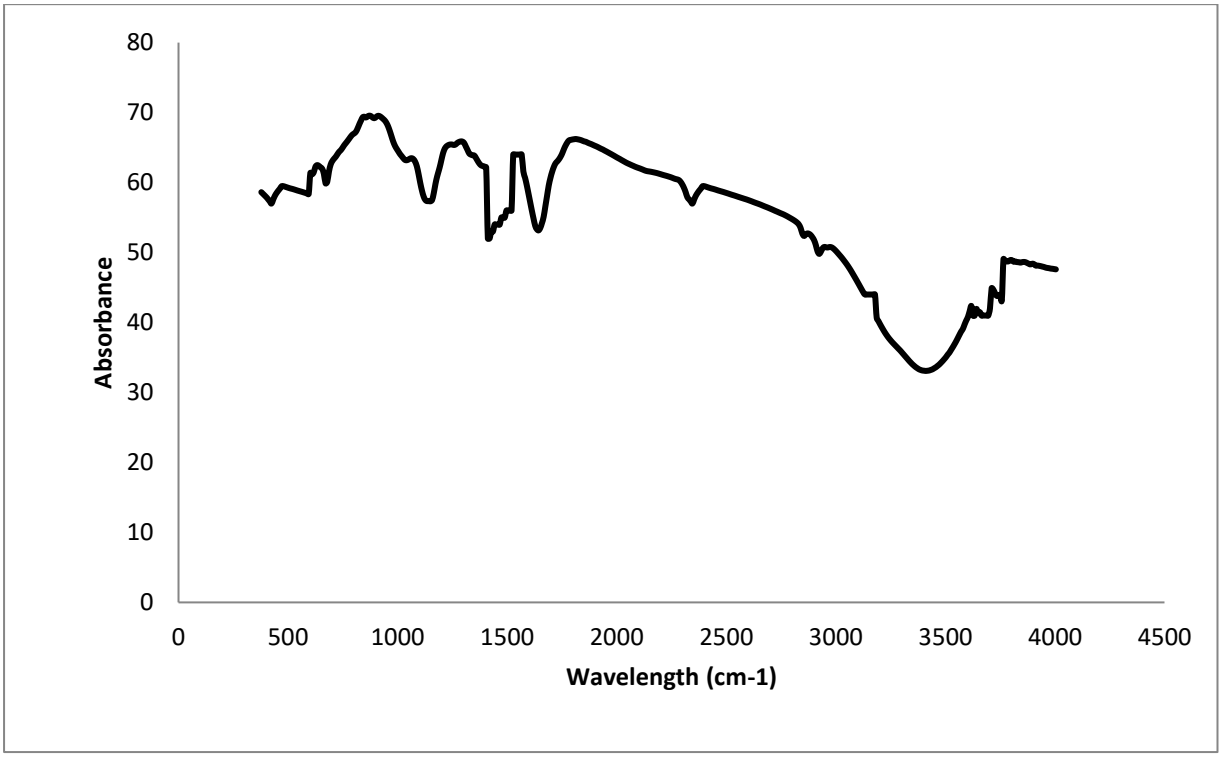

Figure A3: FTIR spectrum of Baobab fibres nanocellulose

APPENDIX D

XRD spectrum of raw/treated/CNC Baobab pod fibres

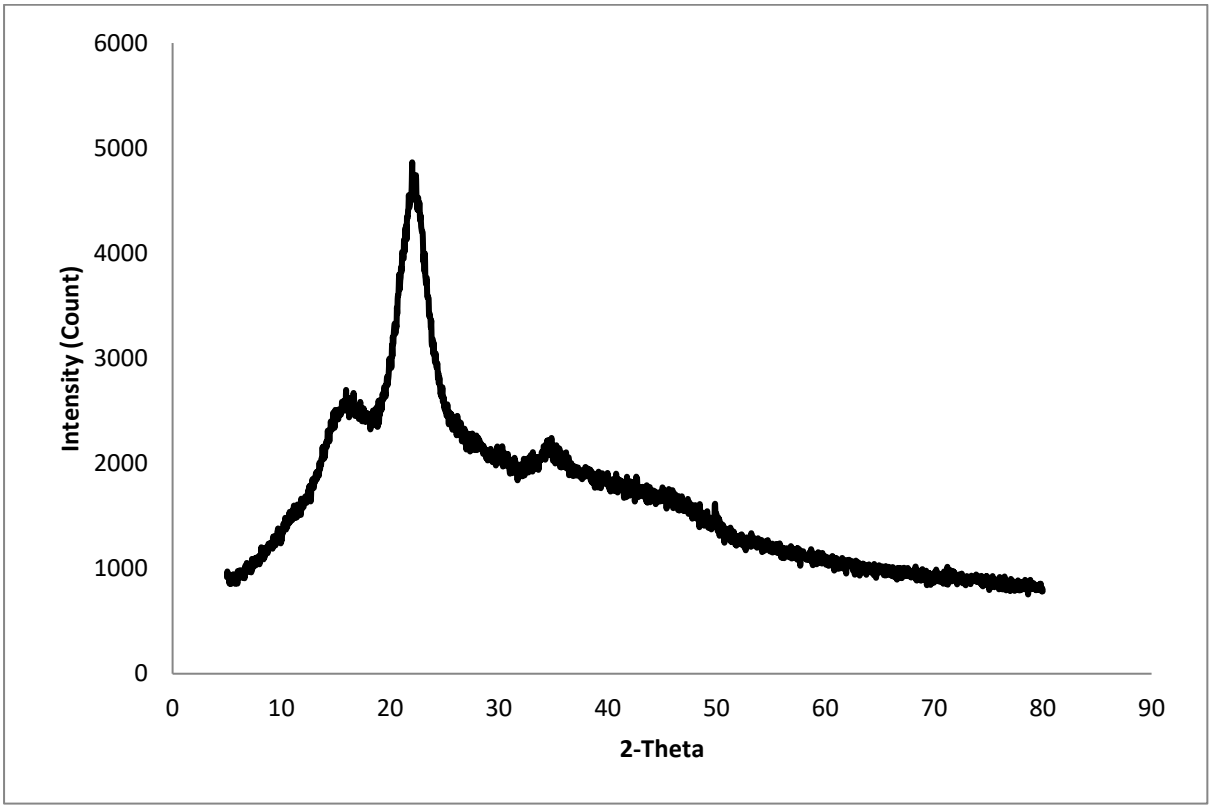

Figure A4: XRD Spectrum of raw Baobab fibres

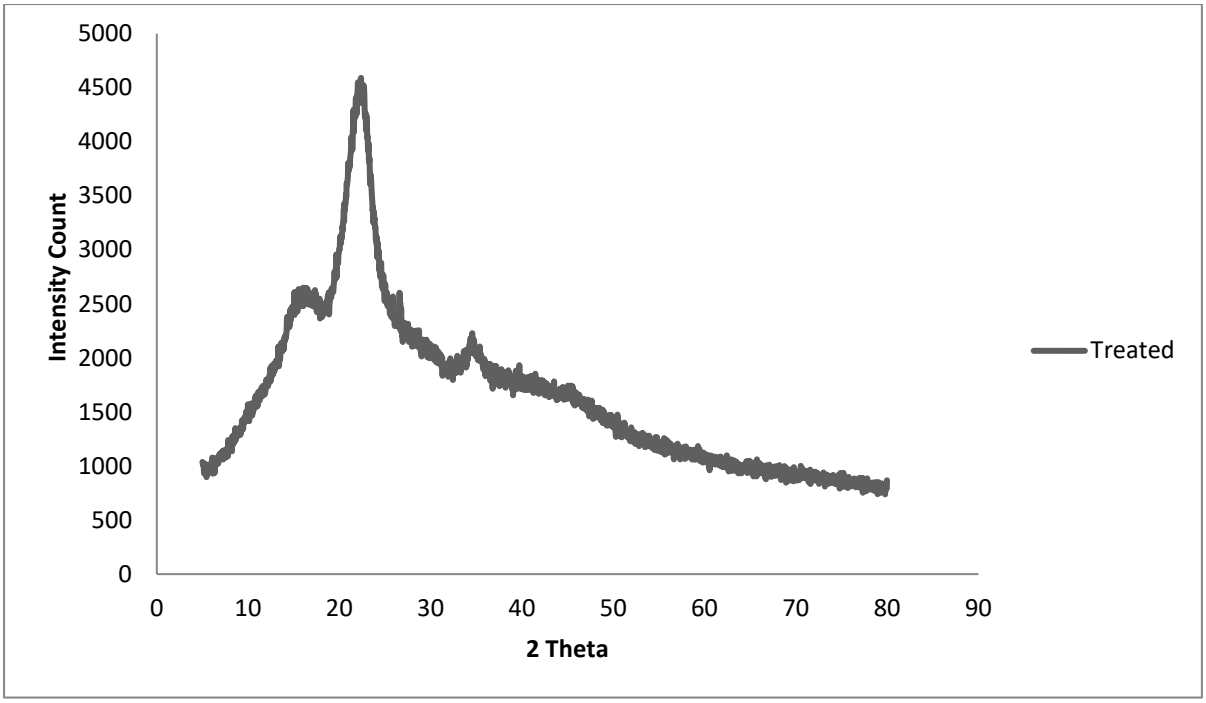

Figure A5: XRD spectrum of treated Baobab fibres

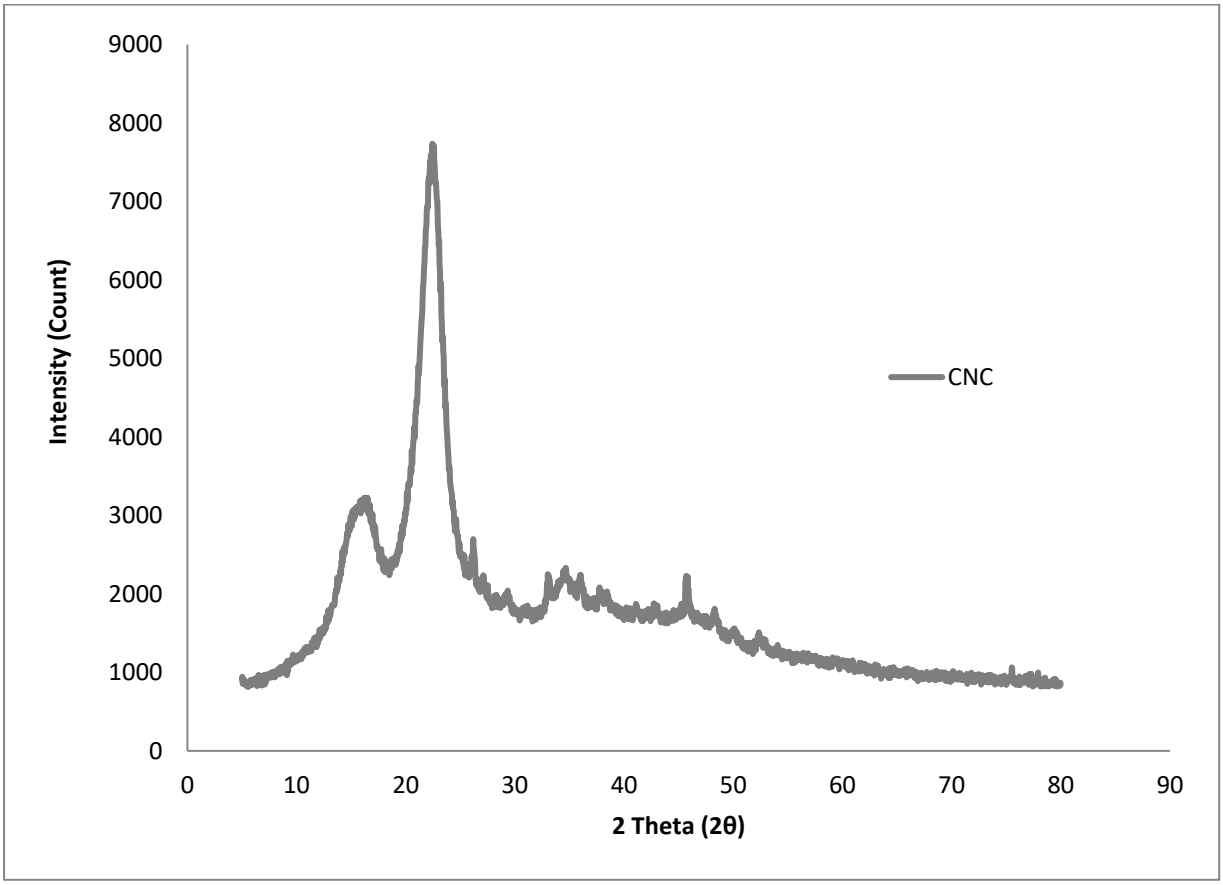

Figure A6: XRD spectrum of Baobab Fibre nanocellulose

APPENDIX E

The average crystallite particle size was determined from the XRD patterns of the CNC using Scherer equation

$$D = \frac{k\,\lambda}{\beta cos\theta}$$

Where

D = the particle size diameter

β = the full width at half maximum was determined from XRD using Origin and MS Excel, value was obtained to be =4.9˚

λ = the wave length of X-ray = 15.118 nm

θ = the diffraction angle (peak position) = $(\frac{22}{2}) = 11^{\circ}$

K = the Scherer constant = 0.94

$$D = \frac{0.94 \times 15.1180}{4.9\ cos11}$$

$$= \frac{14.49292}{4.9\ cos11}$$

$$= \frac{14.49292}{4.9\ (0.9851)}$$

$$= \frac{14.49292}{4.82699}$$

= 3.003 nm

APPENDIX F

TGA spectrum of raw/treated/CNC Baobab pod fibres

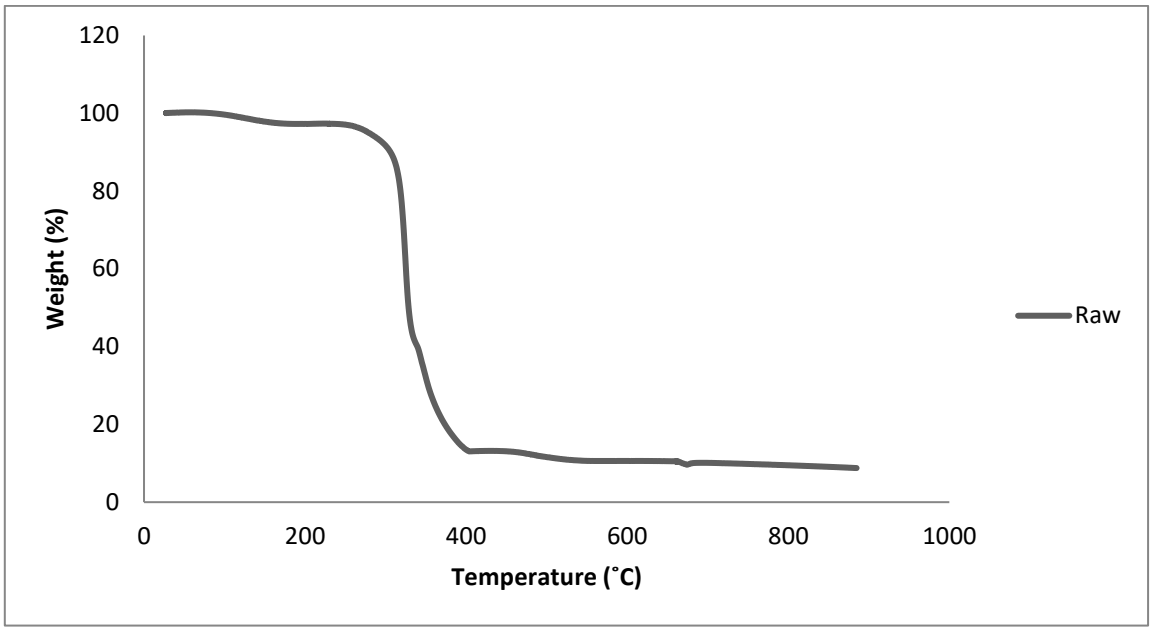

Figure A7: TGA spectrum of raw Baobab fibre

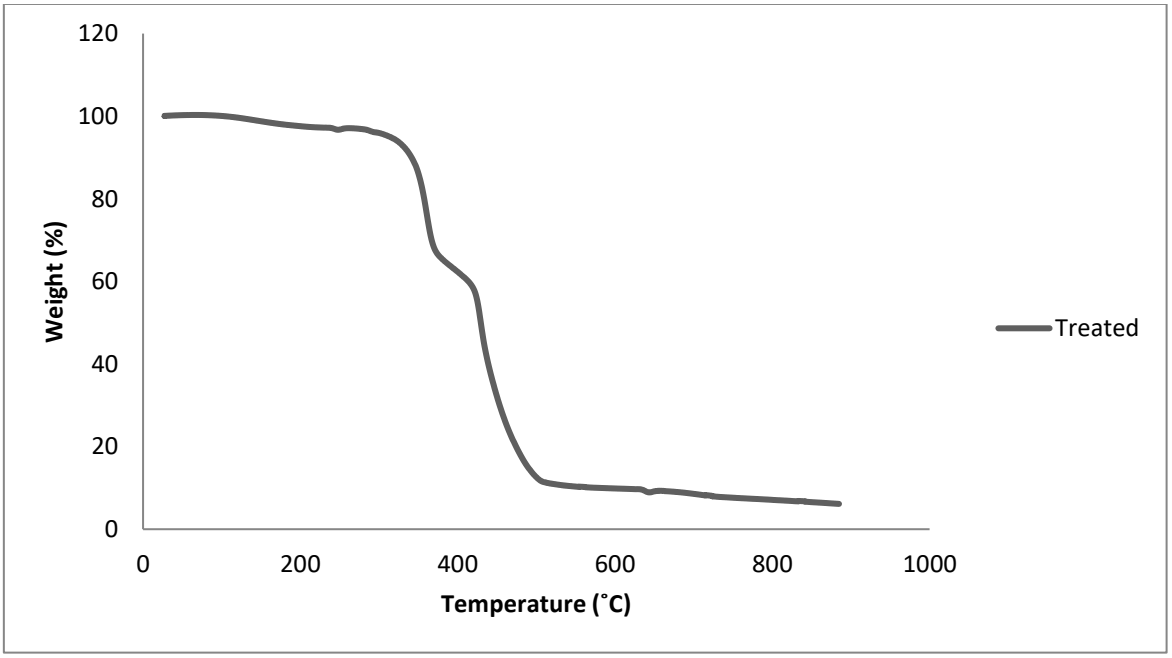

Figure A8: TGA spectrum of treated Baobab fibre

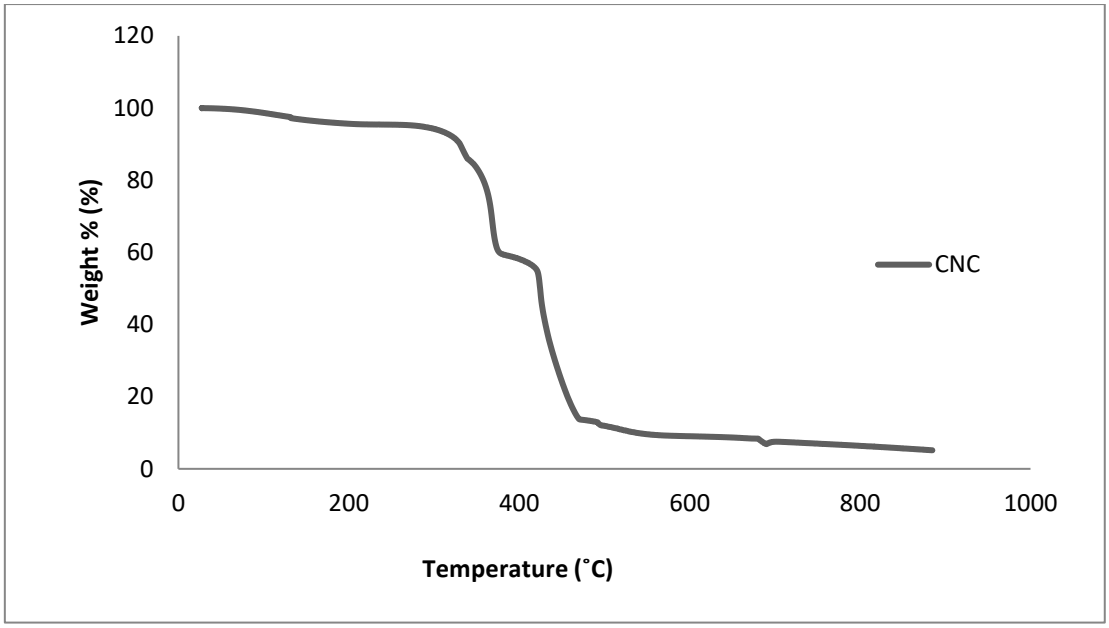

Figure A9: TGA Spectrum of Baobab fibre nanocellulose

APPENDIX G

Methods for determining density/water absorption of Baobab fibre

Effect of Density and Water Absorption on BPFs reinforced Composites

Table A2: Density properties of BPFs reinforced Composites

Parameters	**Control**	**Sample A**	**Sample B**	**Sample C**	**Sample D**
Volume (ml)	1.9	1.2	1.5	1.2	1.3
Initial Weight (g)	1.4561	1.085	1.2891	1.137	1.2718
Density (g/ml)	0.7281	0.9042	0.8594	0.9475	0.9783

Table A3: Water absorption properties of BPFs reinforced Composites

Parameters	Control	Sample A	Sample B	Sample C	Sample D
Volume (ml)	1.9	1.2	1.5	1.2	1.3
Initial Weight (g)	1.4561	1.085	1.2891	1.137	1.2718
Final weight (g/)	1.4582	1.0872	1.2913	1.1454	0.9783
Weight Difference (g)	0.0021	0.0023	0.0012	0.0084	0.0057
Water Absorption (%)	0.1442	0.212	0.1707	0.7387	0.4481

APPENDIX H

Graph tables for mechanical properties of composites

Table A4: Tensile Test Graph Table for Control Sample

Elastic Modulus	10.95MPa	Upper Yield	0.00MPa
Yield Strenght	2.22MPa	Break Strength	0.11MPa
Break Elongation	141.36%	Elongation after fractyre	141.36%
Total Elongation	79.56%	Yield Elongation	2.16%
Yield Ratio	31.75%	Rp0.2	6.44MPa
Rp0.5	6.44MPa	Rt0.1	0.00MPa
Rt0.2	0.00MPa	Rt0.5	0.22MPa
Rp0.05	6.44MPa	MaxLoad	0.25kN
Max Elong	80.58mm	Lower Yield	0.00MPa
Tensile Strength	61.65MPa	Reduction of Area	100.00%
Non Proport Elongation	77.40%	Rp0.01	6.44MPa

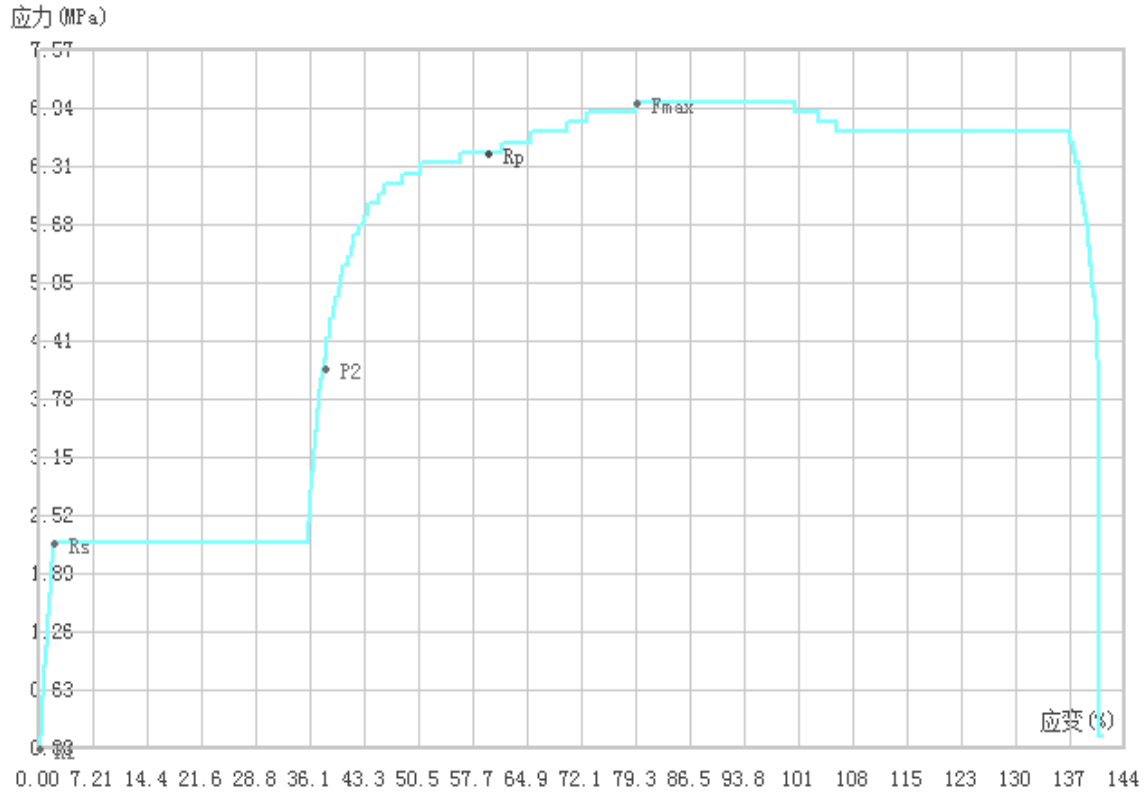

Figure A10: Tensile Test Graph Table for Control Sample

Table A5: Tensile Test Graph Table for Sample A

Elastic Modulus	80.18MPa	Upper Yield	0.00MPa
Yield Strenght	56.44MPa	Break Strength	71.33MPa
Break Elongation	75.39%	Elongation after fractyre	75.39%
Total Elongation	75.36%	Yield Elongation	72.54%
Yield Ratio	79.13%	Rp0.2	42.89MPa
Rp0.5	42.22MPa	Rt0.1	0.78MPa
Rt0.2	0.22MPa	Rt0.5	0.00MPa
Rp0.05	42.78MPa	MaxLoad	2.57kN
Max Elong	42.97mm	Lower Yield	0.00MPa
Tensile Strength	71.72MPa	Reduction of Area	100.00%
Non Proport Elongation	2.81%	Rp0.01	42.78MPa

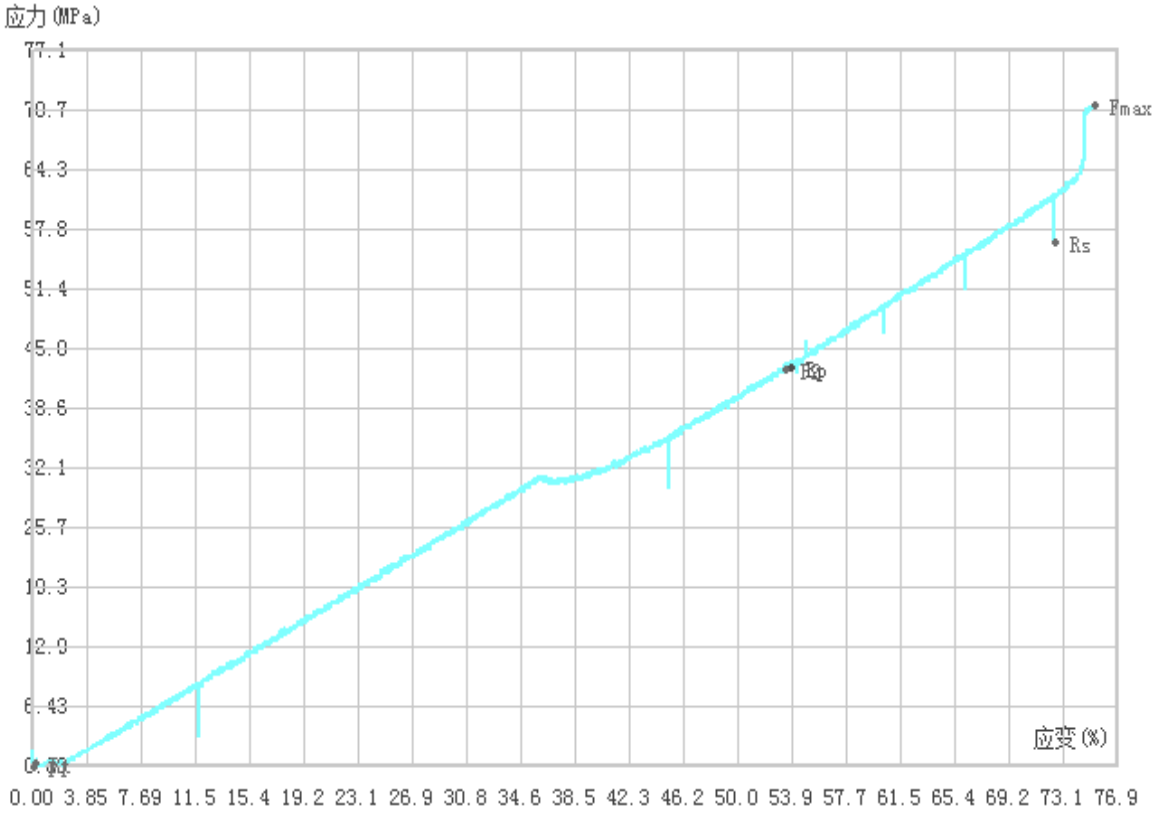

Figure A11: Tensile Test Graph Table for Sample A

Table A6: Tensile Test Graph Table for Sample B

Elastic Modulus	166.87MPa	Upper Yield	0.00MPa
Yield Strength	71.33MPa	Break Strength	95.11MPa
Break Elongation	66.19%	Elongation after fracture	66.19%
Total Elongation	65.18%	Yield Elongation	42.49%
Yield Ratio	71.41%	Rp0.2	71.89MPa
Rp0.5	73.11MPa	Rt0.1	3.67MPa
Rt0.2	3.67MPa	Rt0.5	4.22MPa
Rp0.05	69.44MPa	MaxLoad	3.60kN
Max Elong	37.73mm	Lower Yield	0.00MPa
Tensile Strength	79.72MPa	Reduction of Area	100.00%
Non Proport Elongation	22.69%	Rp0.01	68.11MPa

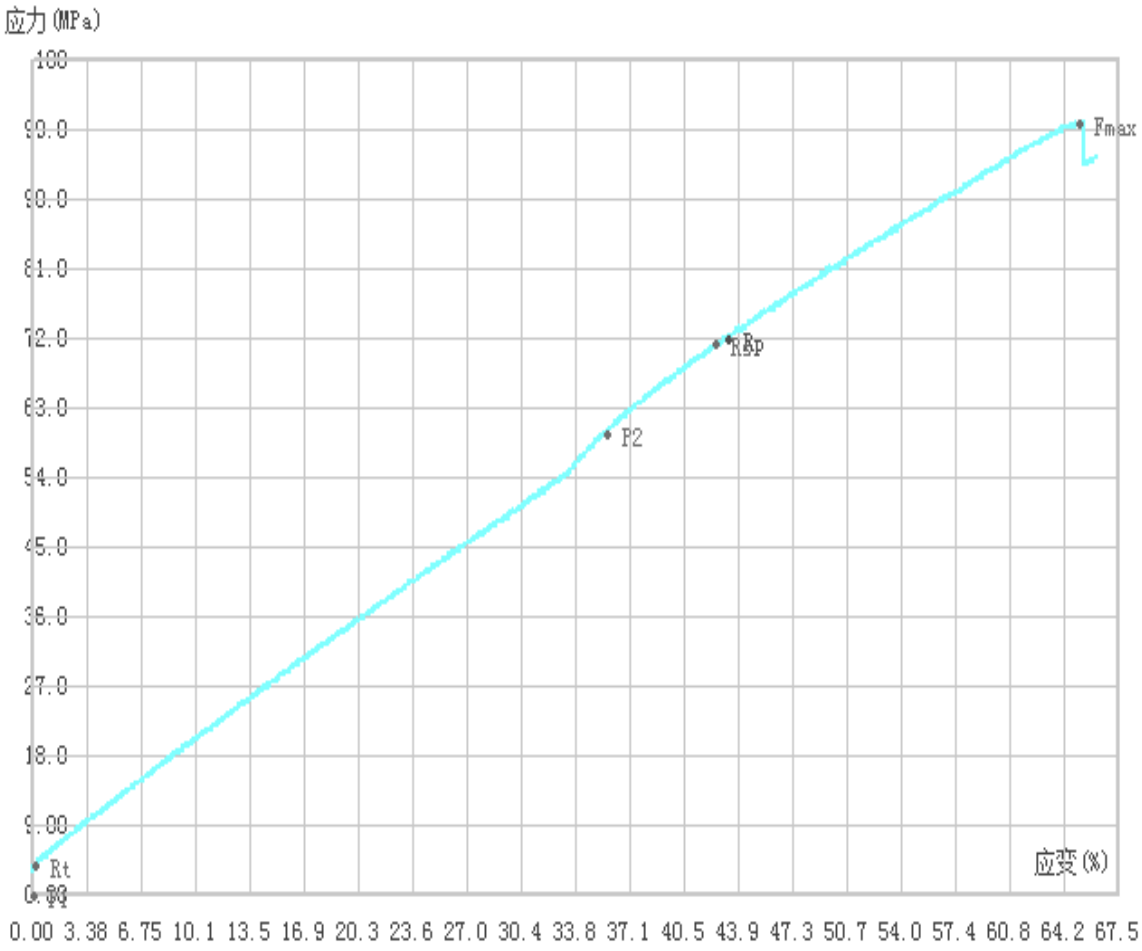

Figure A12: Tensile Test Graph for Sample B

Table A7: Tensile Test Graph Table for Sample C

Elastic Modulus	3.51MPa	Upper Yield	0.00MPa
Yield Strenght	18.78MPa	Break Strength	18.11MPa
Break Elongation	1.#J%	Elongation after fractyre	1.#J%
Total Elongation	1.#J%	Yield Elongation	1.#J%
Yield Ratio	90.86%	Rp0.2	9.44MPa
Rp0.5	9.44MPa	Rt0.1	0.00MPa
Rt0.2	0.00MPa	Rt0.5	0.00MPa
Rp0.05	9.44MPa	MaxLoad	0.74kN
Max Elong	31.36mm	Lower Yield	0.00MPa
Tensile Strength	86.01MPa	Reduction of Area	100.00%
Non Proport Elongation	1.#J%	Rp0.01	9.44MPa

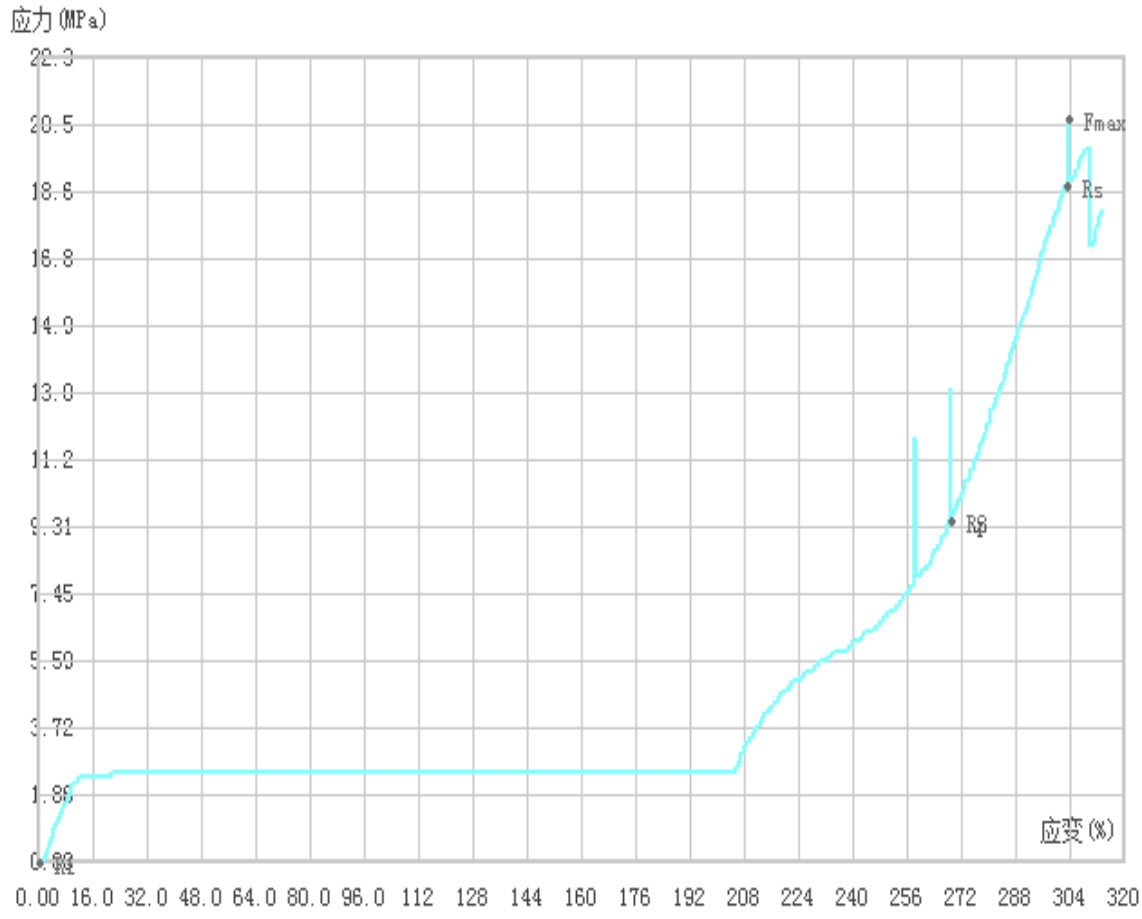

Figure A13: Tensile Test Graph for Sample C

Table A8: Tensile Test Graph Table for Sample D

Elastic Modulus	10.46MPa	Upper Yield	0.00MPa
Yield Strength	2.33MPa	Break Strength	0.67MPa
Break Elongation	63.25%	Elongation after fractyre	63.26%
Total Elongation	54.22%	Yield Elongation	1.62%
Yield Ratio	36.21%	Rp0.2	6.00MPa
Rp0.5	6.00MPa	Rt0.1	0.00MPa
Rt0.2	0.00MPa	Rt0.5	0.33MPa
Rp0.05	6.00MPa	Max Load	0.23kN
Max Elongation	35.42mm	Lower Yield	0.00MPa
Tensile Strength	84.72MPa	Reduction of Area	100.00%
Non Proport Elongation	52.60%	Rp0.01	6.11MPa

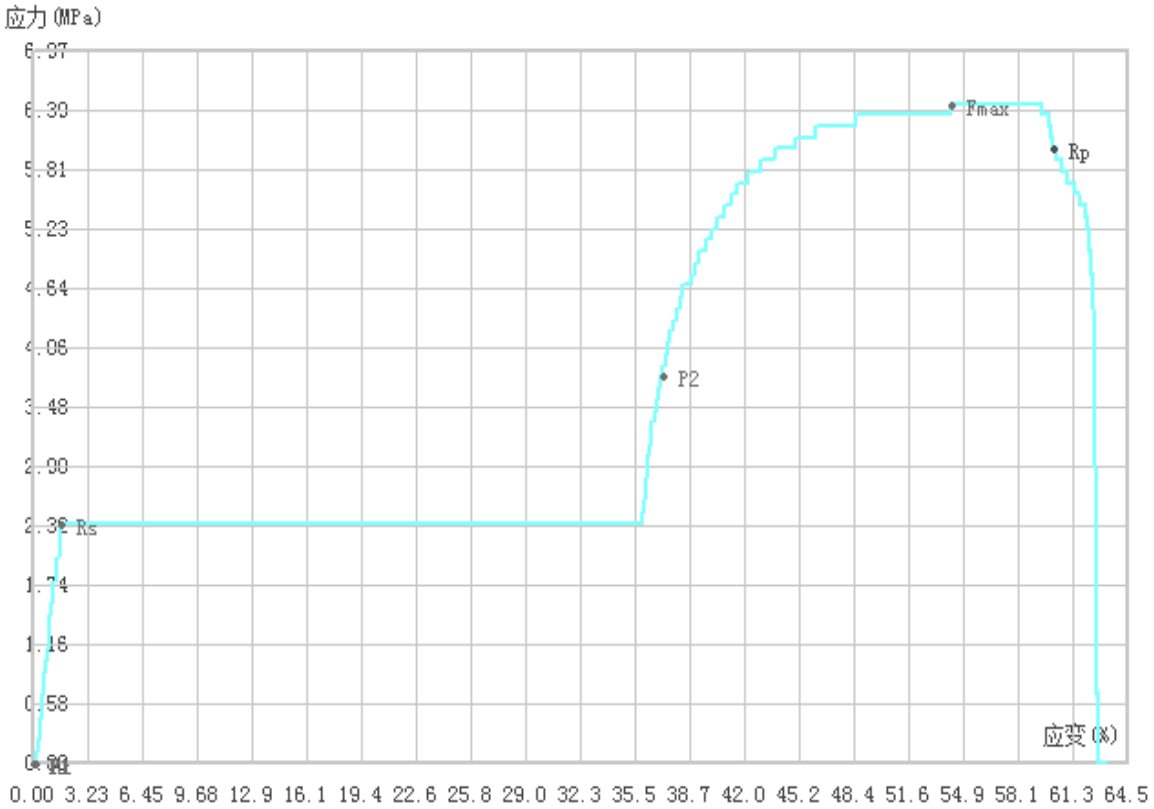

Figure A14: Tensile Test Graph for Sample D